Copyright Undertaking

This thesis is protected by copyright, with all rights reserved.

By reading and using the thesis, the reader understands and agrees to the following terms:

1. The reader will abide by the rules and legal ordinances governing copyright regarding the use of the thesis.

2. The reader will use the thesis for the purpose of research or private study only and not for distribution or further reproduction or any other purpose.

3. The reader agrees to indemnify and hold the University harmless from and against any loss, damage, cost, liability or expenses arising from copyright infringement or unauthorized usage.

The Hong Kong Polytechnic University

School of Optometry

Early Functional Changes in Human Diabetic Retina

–

A Multifocal Electroretinogram Study

Jenny Chun-Yee Lung

A thesis submitted in partial fulfillment of the requirements for the Degree of Doctor of Philosophy

September 2013

Certificate of Originality

I hereby declare that this thesis is my own work and that, to the best of my knowledge and belief, it reproduces no material previously published or written, nor material that has been accepted for the award of any other degree or diploma, except where due acknowledgement has been made in the text

_____ (signed)

LUNG Jenny Chun-Yee (Name of student)

<u>Abstract</u>

Diabetes mellitus (DM) is a set of metabolic disorders leading to chronic hyperglycemia. It has become one of the most concerning health problems around the world. DM can damage the ocular capillary circulation which develops into diabetic retinopathy (DR).

DR is the most common cause of new incidence of blindness among the working population due to its sight-threatening complications. The current clinical screening tests involve the fundus camera and ophthalmoscopy. These two tests form an effective and accurate means of detecting DR; however, DR can only be confirmed when obvious retinal vascular defects or damage exist. Studying early retinal changes before there are visible signs of retinopathy can help to prevent the visual functional loss resulting from DR. This helps in relieving the heavy economic burden to society produced by DR.

Multifocal electroretinogram (mfERG) is a functional test which can reflect subtle retinal changes before any visible retinopathy. By modifying the mfERG paradigm, retinal activity from different origins can be measured. The modified mfERG is likely to be a more suitable technique to investigate the underlying mechanism of DR at an early stage. In this study, modified mfERG paradigms (Global flash multifocal electroretinogram [MOFO mfERG] and "Long-duration" multifocal electroretinogram) were applied in human eyes with type II DM to study any early retinal changes. Comparisons were made with two other common clinical morphological and functional assessments (Humphrey perimetry and Stratus circumpapillary retinal nerve fiber layer (RNFL) thickness measurement) so as to study their correlations and their diagnostic sensitivity.

Objectives

1) To ascertain the characteristics of the response triggered by the global flash multifocal electroretinogram (MOFO mfERG) under various combinations of global and focal flash luminance, and to determine the optimal conditions for this measurement in healthy subjects

2) To investigate early functional changes of local retinal defects in type II diabetic patients using the global flash multifocal electroretinogram (MOFO mfERG)

3) To investigate the correlations of the global flash multifocal electroretinogram (MOFO mfERG) with two common clinical visual assessments – Humphrey perimetry and Stratus circumpapillary retinal nerve fiber layer (RNFL) thickness measurement in type II diabetic patients

4) To investigate the characteristics of the multifocal on- and off-responses in the human diabetic retina by a "long-duration" multifocal electroretinogram paradigm. This was to evaluate any changes in the antagonistic interaction in the middle and inner retina in the early stage of Type II DM

Methods

Experiment 1: The global flash electroretinogram (MOFO mfERG) measurement was applied in this experiment with a visual stimulation consisting of a 103-hexagon pattern. The stimulation was displayed with four video frames (multifocal flashes, followed by a dark frame, a global flash and then another dark frame). The focal and global flash intensities were varied independently at

four levels (50, 100, 200 and 400 cd/m^2). Ten healthy young adult subjects were recruited and underwent MOFO mfERG measurements with sixteen combinations of focal and global flash luminance. The mfERG responses were grouped into central and peripheral regions for analysis.

Experiment 2: The MOFO mfERG measurement was carried at high (98%) and low (46%) contrast conditions. A 103-hexagon pattern was used as the stimulus. The focal and global luminance at the high contrast condition was kept at the optimal ratio found in Experiment 1. Thirty-eight type II diabetic patients and fourteen age-matched controls were recruited. Nine of the diabetics were free from retinopathy, while the remainder had mild to moderate non-proliferative diabetic retinopathy (NPDR). The mfERG responses were grouped into 35 regions for comparison according to the DR classification at those locations. The diagnostic values of the MOFO mfERG parameters on DR were also evaluated by constructing the receiver-operating-characteristic (ROC) curve.

Experiment 3: Three visual assessments were carried out: the MOFO mfERG measurement with 103-hexagon stimulus pattern at high (98%) and low (46%) contrast conditions, Humphrey perimetry and Stratus circumpapillary retinal nerve fiber layer (RNFL) thickness. Forty-two type II diabetic patients and fourteen age-matched controls were recruited for comparison. Ten of the diabetics were free from diabetic retinopathy, while the remainder had mild to moderate NPDR. Correlations between local values of mfERG responses, perimetric sensitivity and RNFL thickness were evaluated by mapping the localized responses for the three subject groups. This helped in evaluating the early functional and morphological changes at the early stage of DR.

Experiment 4: A "long-duration" mfERG paradigm was used to evaluate the multifocal on- and off-responses in the human diabetic retina. In this paradigm, the stimulus pattern contained eight successive multifocal flashes, and followed by eight successive dark frames. The mfERG stimulus was a 61-hexagon pattern with measurement carried out under two chromatic conditions --- white and blue conditions. Twenty type II diabetic patients with no or mild NPDR and twenty-one age-matched healthy controls were recruited. The mfERG responses were grouped into rings for analysis. Changes of the mfERG responses under the two chromatic conditions were used to investigate any changes in antagonistic interaction within the retina at the early stage of DR.

Results

Experiment 1: The MOFO mfERG paradigm gave rise to two main components in the resultant waveform: the direct component (DC) and induced component (IC). The DC amplitude increased with the focal flash intensity with global flash held constant. The global flash and focal flash luminance (g/f ratio) was an important parameter in determining the optimal DC and IC responses; the IC amplitude reached the peak value when the g/f ratio was at about 2:1. Further increasing the global flash luminance did not enhance the IC amplitude. Keeping this ratio at 1:1 with the focal flash luminance set between 100 cd/m^2 and 200 cd/m^2 was recommended for subsequent experiments.

Experiment 2: The MOFO mfERG paradigm helped in investigating the middle and inner retinal responses in terms of DC and IC respectively. Local reduction of the DC and IC amplitudes were found in diabetic patients with and without DR. With increasing severity of retinopathy, a further reduction of the mfERG

amplitudes was found. The reductions in the DC and IC responses provided crucial evidence that the middle and inner retina are impaired at an early stage in diabetic patients. Under the MOFO mfERG paradigm, the amplitude of the high contrast DC was useful in screening for localized functional deterioration, even before the appearance of visible DR signs.

Experiment 3: The MOFO mfERG was superior to the automated Humphrey perimetry and the Stratus circumpapillary RNFL thickness measurement in type II diabetic patients, in showing differences between the diabetic group and the controls. The MOFO mfERG parameters demonstrated a better correlation with the functional perimetric assessment than the RNFL thickness measurement. All the MOFO mfERG amplitudes (except IC amplitude at high contrast) correlated significantly with the perimetric sensitivity (Pearson's r ranged from 0.23 to 0.36, $p<0.01$) than did the mfERG implicit time at both high and low contrast conditions across all subject groups. No consistent correlation was found between the mfERG parameters and the RNFL thickness for any subject group.

Experiment 4: The "long-duration" mfERG paradigm helped in minimizing the overlap between the on- and off-pathway activities of the retinal responses. The resultant mfERG waveform includes two main parts. The first part is predominantly from the on-pathway activity containing a negative trough (N1), a positive peak (P1) and then a trough (N2). Beyond N2, there is a plateau followed by a second peak (P2). The diabetic group showed significantly greater N2 amplitude than the controls under white stimulation in retinal regions Rings 2 and 4 ($p<0.05$). The blue stimulation generally triggered greater mfERG amplitudes in P1, N2 and P2 ($p<0.05$) than did the white stimulation for both

diabetic and control groups. When the stimulus changed from white to blue, the diabetic group showed a smaller percentage change than the controls in the peripheral retinal region (Ring 5) (p<0.02).

Conclusion

The MOFO mfERG indicated that the middle and inner retinal function has deteriorated before the existence of clinically visible DR lesions. Such functional impairment would be expected to continue with the existence of observable vascular lesions. The MOFO mfERG measurement correlated better with the functional perimetric sensitivity than the morphological RNFL changes. However, the deterioration of local luminance sensitivity (as measured using perimetry) could not fully explain the functional loss found by mfERG. The "long-duration" mfERG paradigm, under two different chromatic stimulation conditions, demonstrated an imbalance of lateral antagonism which is proposed to be at or near the middle retinal layer.

<u>Publications arising from the thesis</u>

Lung JC, Chan HH. (2010). Effects of luminance combinations on the characteristics of the global flash multifocal electroretinogram (mfERG). Graefes Archive for Clinical and Experimental Ophthalmology, 248:1117-25.

Lung JC, Swann PG, Chan HH. (2012). Early local functional changes in the human diabetic retina: a global flash multifocal electroretinogram study. Graefes Archive for Clinical and Experimental Ophthalmology, 250: 1745-54.

Lung JC, Swann PG, Wong DS, Chan HH. (2012). Global flash multifocal electroretinogram: early detection of local functional changes and its correlations with optical coherence tomography and visual field tests in diabetic eyes. Documenta Ophthalmologica, 125: 123-35.

Lung JC, Swann PG, Wong DS, Chan HH. The multifocal on- and off-responses in the human diabetic retina. (Manuscript prepared for submission).

<u>Conference presentations</u>

<u>Oral presentations</u>

Lung JC, Tang GY, Chu PH, Ng YF, Chan HH. (July 6-10, 2009). Global flash mfERG in the early detection of the local functional changes of diabetic retinopathy lesions. 47th International Society for Clinical Electrophysiology of Vision (ISCEV) Symposium, Padova, Abano Terme, Italy

(Published in Doc Ophthalmol 2009: 119; 17-92)

Lung JC, Swann PG, Chan HH. (Sept 18-23, 2011). The on- and off-responses in human diabetic eye − a multifocal electroretinogram study. 49th International Society for Clinical Electrophysiology of Vision (ISCEV) Symposium, Lac-Beauport, Quebec, Canada.

(Published in Doc Ophthalmol 2011: 123; 3-50)

Poster presentations

Lung JC, Chu PH, Ng YF, Chan HH. (July 10-15, 2008). Characteristics of global flash multifocal electroretinogram (mfERG) under different combinations of global and focal flash luminance. 46th International Society for Clinical Electrophysiology of Vision (ISCEV) Symposium, Morgantown, WV, USA.

(Published in Doc Ophthalmol 2008: 117; 3-10)

Lung JC, Swann PG, Chan HH. (May 2-6, 2010). Global flash multifocal electroretinogram (MOFO mfERG): Early detection of local functional changes and its correlations with optical coherence tomography and visual field test in diabetic patients. The Association for Research in Vision and Ophthalmology (ARVO) Annual meeting 2010, Fort Lauderdale, FL, USA.

Lung JC, Lam AK, Chan HH. (March 5-6, 2011). The early inner retinal changes (GCC) in type II diabetic patients with and without non-proliferative diabetic retinopathy (NPDR). 6th International Symposium on Healthy Aging "A New Golden Age" by The University of Hong Kong Li Ka Shing Faculty of Medicine Research Centre of Heart, Brain, Hormone and Healthy Aging, Sheraton Hong Kong Hotel and Towers, Tsim Sha Tsui, Hong Kong.

Lung JC, Chan HH. (July 15-18, 2011). The antagonistic interaction of cones in the human eye - a pilot study. Asia-Pacific Conference on Vision (APCV), The University of Hong Kong, Hong Kong.

(Published in i-Perception 2011: 2: 302)

Lung JC, Wong DS, Chan HH. (Sept 18-23, 2011). The age-related changes of the on- and off-responses in human eye - a multifocal electroretinogram study. 49th International Society for Clinical Electrophysiology of Vision (ISCEV) Symposium, Lac-Beauport, Quebec, Canada.

(Published in Doc Ophthalmol 2011: 123; 3-50)

<u>Acknowledgements</u>

NEOC, the ISCEV and ARVO international meetings, with their peer-support and sharing, my study life has been fruitful and memorable.

Last but not least, I would be grateful to the endless love from my family over the years. With their continuous caring and support, I can maintain a healthy condition, devote myself to the study and finish it finally.

Table of Contents

Contents			Pages
Declaration of originality			II
Abstract			III
Publications from the thesis			IX
Acknowledgements			XII
Table of contents			XIV
Lists of figures, tables and abbreviations			XXIII

Lists of figures, tables and abbreviations

List of figures

shows $\pm$ 1 standard deviation

Figure 6.5a The central IC implicit time at various g/f ratios. Each coloured line represents the DC amplitude under different focal flash intensities. The error bar shows $\pm$ 1 standard deviation

Figure 6.5b The peripheral IC implicit time at various g/f ratios. Each coloured line represents the DC amplitude under different focal flash intensities. The error bar shows $\pm$ 1 standard deviation

Figure 6.6 Waveform of the MOFO responses contain two main components: the direct component (DC) and the induced component (IC). Note that the implicit time of the DC is measured from the onset of the multifocal stimulus to the response peak of the DC, while the implicit time of the IC is measured from the onset of the global flash (26.6 ms) to the response peak of the IC

Figure 6.7 The multifocal stimuli pattern was mapped with the automated mosaic fundus photo (each circle indicates the fundus photo taken at a particular gaze position. There are in total nine gaze positions, one central gaze position and eight peripheral gaze positions, to form a mosaic fundus photo). Both were divided into 35 regions as in previous studies (about two to three hexagons were grouped as one region in the mfERG topography as indicated by the dark polygons). This figure illustrates the regional mfERG waveform of a diabetic patient with DR lesions at different locations. Those regional mfERG samples with DR (in red lines) are compared with the averaged regional samples from the control group (in blue lines)

Figure 6.8 Comparison of the DC amplitude z-scores (DCA_z) for groups 0 to 4 at high (98%) and low (46%) contrast levels. *: $p<0.05$ when compared with group 0; †: $p<0.05$ when compared with group 1. Boxplot: centre line- the mean; the edges of the box - $\pm$ 1 standard deviation; the edges of the vertical bars -

indicates parameters that achieved statistically significance level with p<0.05)

(Error bar: indicates ± 1 standard deviation)

Table 7.4 Summary of Pearson's correlation (r) between plasma glucose level (mmol/L) with each mean visual assessment parameters (VF mean deviation [dB], RNFL mean thickness [um] and the averaged MOFO mfERG parameters [z-scores])

(*: Significance level with $p < 0.05$)

List of abbreviations

Abbreviations	
AAO	American Academy of Ophthalmology
AGEs	Advance glycosylation end products
ANOVA	Analysis of variance
AR	Aldose-reductase
AUC	Area-under-the-curve
CRT monitor	Cathode-ray tube monitor
CS	Contrast sensitivity
DC	Direct component
DM	Diabetes mellitus
DR	Diabetic retinopathy
DTL electrode	Dawson-Trick-Litzkow electrode
EOG	Electro-oculogram
ERG	Full-field elelctroretinogram
ETDRS	Early Treatment Diabetic Retinopathy Study
FFA	Fundus fluorescein angiogram
GEE	Generalized estimating equation
HbA1c	Glycated haemoglobin
HK	Hong Kong
IC	Induced component
IDDM	Insulin-dependent diabetes mellitus
IFG	Impaired fasting glycaemia
IGT	Impaired glucose tolerance
IRMA	Intraretinal microvascular abnormalities

ISCEV	International Society for Clinical Electrophysiology of Vision
MD	Mean deviation
mfERG	Multifocal electroretinogram
mfOP	Multifocal oscillatory potential
MOFO	Global flash multifocal electroretinogram
MW	Middle wavelength
NIDDM	Non-insulin-dependent diabetes mellitus
NMDA	N-methyl-D-aspartic-acid
NPDR	Non-proliferative diabetic retinopathy
OCT	Optical coherence tomography
OGTT	Oral glucose tolerance test
OP	Oscillatory potential
PDR	Proliferative diabetic retinopathy
PERG	Pattern electroretingram
PhNR	Photopic negative response
PKC	Protein kinase C
RNFL	Retinal nerve fiber layer
ROC curve	Receiver-operating-characteristic curve
RPE	Retinal pigment epithelium
SD	Standard deviation
sfmfERG	Slow-flash multifocal electroretinogram
SW	Short-wavelength
SWAP	Short-wavelength automated perimetry
TD	Total deviation

VA	Visual acuity
VEGF	Vascular endothelial growth factor
VF	Visual field
WHO	World Health Organization
WWP	White-on-white perimetry

Part I

Introduction & Literature Review

Chapter 1: Diabetes mellitus (DM) and diabetic retinopathy (DR)

1.1 Background information of diabetes mellitus

Diabetic mellitus (DM) is a clinically and genetically heterogeneous group of systemic disorders. This systemic disease is caused by a deficiency of insulin secretion, and a cellular resistance to the action of insulin, these result in chronic high level of blood glucose - hyperglycemia (LeRoith et al. 2004). DM may present with characteristic symptoms such as thirst, polyuria, blurred vision and weight loss (Alberti & Zimmet 1998).

DM increases the risk of stroke, renal failure and lower limb amputations. It can cause severe visual impairment and blindness (Alberti & Zimmet 1998). According to World Health Organization (WHO) statistics in 2008, about 1.3 million persons died from DM worldwide which is noted to be one of the leading fatal causes among the non-communicable disease categories (WHO 2010).

1.1.1   Metabolism and endocrine problems

Deficiency of a hormone called insulin is the main cause of diabetes. This hormone is a chemical messenger produced by the pancreas. It has effects on many distant parts of the body through its release into the bloodstream. However, if there is a complete failure of insulin production or a combination of partial failure of insulin production with a reduced body response to the insulin (insulin resistance), a problem of blood glucose regulation will result and give rise to different types of DM (which will be discussed below) (Alberti & Zimmet 1998; Clark 2004).

1.1.2 Clinical diagnostic tests

Measurement of the venous plasma glucose level (fasting plasma glucose level or a 2-hour postprandial plasma glucose level) is the common clinical test for diagnosis of DM (Alberti & Zimmet 1998; Holt 2004). In 2009, an expert group from WHO concluded that glycated haemoglobin (HbA1c), which reflects the average plasma glucose over the previous 8-12 weeks, should be accepted as the official means to represent the plasma glucose level (WHO 2011). A patient who fails in one of the above plasma glucose assessments and who reports the classic diabetic symptoms meets the clinical diagnosis of DM. For an asymptomatic patient, a supplementary oral glucose tolerance test (OGTT) is required. The WHO recommends that a 75g OGTT should be performed under this situation (Alberti & Zimmet 1998; Holt 2004).

1.1.3 Definition of DM

The current WHO diagnostic criteria for diabetes is a patient with fasting plasma glucose equal to or above 7.0 mmol/L (126 mg/dl) or a 2-hour postprandial plasma glucose equal to or above 11.1 mmol/L (200 mg/dl) (Alberti & Zimmet 1998). In 2009, the WHO recommended that a cut-off point for the diagnosis of DM, an HbA1c value equal to or above 6.5% indicates a possibility of DM (WHO 2011). The WHO also provides a conversion table between the values of the capillary plasma and the venous plasma glucose concentration for easier comparison (Table 1.1).

Values for diagnosis of diabetes mellitus and other categories of hyperglycaemia

| | Glucose concentration, mmol l^{-1} (mg dl^{-1}) | | Plasma* |
| | Whole blood | | |
	Venous	Capillary	Venous
Diabetes Mellitus:			
Fasting *or*	≥ 6.1 (≥ 110)	≥ 6.1 (≥ 110)	≥ 7.0 (≥ 126)
2–h post glucose load	≥ 10.0 (≥ 180)	≥ 11.1 (≥ 200)	≥ 11.1 (≥ 200)
Impaired Glucose Tolerance (IGT):			
Fasting (if measured) *and*	< 6.1 (< 110) and	< 6.1 (< 110) and	< 7.0 (< 126) and
2–h post glucose load	≥ 6.7 (≥ 120)	≥ 7.8 (≥ 140)	≥ 7.8 (≥ 140)
Impaired Fasting Glycaemia (IFG):			
Fasting	≥ 5.6 (≥ 100) and	≥ 5.6 (≥ 100) and	≥ 6.1 (≥ 110) and
	< 6.1 (< 110)	< 6.1 (< 110)	< 7.0 (< 126)
and (if measured)			
2-h post glucose load	< 6.7 (< 120)	< 7.8 (< 140)	< 7.8 (< 140)

* Corresponding values for capillary plasma are: for Diabetes Mellitus, fasting ≥ 7.0 (≥ 126), 2–h ≥ 12.2 (≥ 220); for Impaired Glucose Tolerance, fasting < 7.0 (< 126) and 2–h ≥ 8.9 (≥ 160) and < 12.2 (< 220); and for Impaired Fasting Glycaemia ≥ 6.1 (≥ 110) and < 7.0 (< 126) and if measured, 2–h < 8.9 (< 160).
For epidemiological or population screening purposes, the fasting or 2–h value after 75 g oral glucose may be used alone. For clinical purposes, the diagnosis of diabetes should always be confirmed by repeating the test on another day unless there is unequivocal hyperglycaemia with acute metabolic decompensation or obvious symptoms.
Glucose concentrations should not be determined on serum unless red cells are immediately removed, otherwise glycolysis will result in an unpredictable under–estimation of the true concentrations. It should be stressed that glucose preservatives do not totally prevent glycolysis. If whole blood is used, the sample should be kept at 0–4 °C or centrifuged immediately, or assayed immediately.

Table 1.1. Conversion table between the capillary plasma values and the venous plasma glucose concentration provided by WHO (Adopted from Alberti & Zimmet 1998)

1.2 Classification of DM

According to the WHO Expert Committee on Diabetes in early 80s, two forms of DM, insulin-dependent DM (IDDM) and non-insulin-dependent DM (NIDDM), were classified. Considering the modifications recommended by the American Diabetes Association, a new classification with four main categories was launched by the WHO in 1999 as follows (Alberti & Zimmet 1998):

1.2.1 Type I DM

Type I DM, previously known as IDDM or juvenile-onset DM, is caused by pancreatic beta-cell destruction. It is usually immune mediated, and represents about 10% of all of diabetic cases (Holt 2004). It results in loss of insulin secretion and absolute insulin deficiency (LeRoith et al. 2004).These patients are

prone to ketoacidosis (Alberti & Zimmet 1998) and the majority of these patients are diagnosed as children or as adolescents (LeRoith et al. 2004).

1.2.2 Type II DM

Type II DM, previously known as NIDDM, is caused by a combination of genetic and non-genetic factors. It is more common and makes up to about 90% of the global diabetic population (LeRoith et al. 2004). The incidence of this form of DM increases with age, with most cases diagnosed after the age of 40 years (Holt 2004). The common non-genetic factors are ageing, obesity and lifestyle including diet. Both genetic and non-genetic factors will result in impaired insulin action due to insulin resistance and insulin deficiency caused by partial dysfunction of pancreatic beta-cells (Holt 2004; LeRoith et al. 2004). However, this type of DM is frequently not diagnosed for many years because the hyperglycemia is often not severe enough to cause obvious symptoms in the early stages (Alberti & Zimmet 1998).

1.2.3 Other types of DM

Causes of these types of DM include known genetic defects affecting beta-cell function or insulin action, diseases of the exocrine pancreas, drug-induced pancreatic changes etc. They account for about 1-2% of the diabetic cases (LeRoith et al. 2004).

1.2.4 Gestational diabetes

Gestational diabetes is carbohydrate intolerance resulting in hyperglycemia with variable severity (Alberti & Zimmet 1998; LeRoith et al. 2004) caused by insulin resistance and/or insulin deficiency associated with the onset or recognition of

DM occurring during pregnancy. It is found in about 3% to 5% of all pregnancies. Women with gestational diabetes are at high risk for development of type II DM after pregnancy (LeRoith et al. 2004).

The WHO diagnostic criteria also recognize two further categories: impaired fasting glycaemia (IFG) and impaired glucose tolerance (IGT); while the latter can only be diagnosed following a 75g OGTT (Holt 2004). IFG and IGT, which are not interchangeable, represent the abnormal glucose regulation in the fasting state and in the post-prandial state respectively (Alberti & Zimmet 1998). IFG and IGT are not distinct clinical entities, but rather risk factors for future development of DM and cardiovascular disease (pre-diabetes) (Holt 2004).

1.3 Pathogenesis of diabetic vascular abnormalities

Hyperglycemia results from reduced insulin secretion or insulin resistance. Both small blood vessels (microvascular) and large blood vessels (macrovascular) can be affected. Macrovascular complications are caused by deposits of lipids and other substances on the wall of large arteries leading to the narrowing of vessel lumen. The reduction of blood flow results from the atherosclerosis (Tuch et al. 2000).

Hyperglycemia also causes an abnormal increase in blood flow and vascular permeability in smaller vessels. As a consequence, capillary leakage which is a microvascular complication exists in the retina and renal systems. This process is reversible in the early stage but the abnormalities of the extracellular matrix contribute to an irreversible increase in vascular permeability. Together with the decrease in production of trophic factors for endothelial and neuronal cells,

microvascular cell loss, apoptosis and progressive capillary occlusion occurs over time (LeRoith et al. 2004).

There are four major hypotheses for the pathogenesis seen in microvascular systems: 1) The activation of the polyol pathway - The aldose-reductase (AR) of the glucose metabolism in polyol pathway of all cells is activated and is overstimulated by lack of insulin (Camera et al. 2007); 2) The activation of the protein kinase C isoform - Long-standing high blood glucose level increases the diacylglycerol production. This activates the production of protein kinase C (PKC) isoform which can lead to endothelial dysfunction (LeRoith et al. 2004; Camera et al. 2007); 3) The activation of non-enzymatic glycosylation - Non-enzymatic glycosylation protein occurs during hyperglycemia and results in advance glycosylation end products (AGEs) (LeRoith et al. 2004). This will create an oxidative stress and lead to vascular disorders in diabetic patients (Van Bijsterveld 2000; Yokoi et al. 2005); 4) The activation of hexosamine pathway – this will elevate N-acetyl-glucosamine levels (Hanover 2001) which will induce insulin-resistance and hinders insulin-induced vasodilation (Hanover 2001; Veldman & Vervoort 2002; Wallis et al. 2005).

1.4 Vascular abnormalities in retina – Diabetic retinopathy (DR)

There are five basic pathologic processes at the retinal capillary level in development of DR. Due to the loss of capillary pericytes, microaneurysms are formed. With the increased formation of microaneurysms and the breakdown of endothelial tight junctions in retinal capillaries, there is excessive vascular permeability leading to formation of hard exudates. This is followed by capillary closure and formation of acellular capillaries, intraretinal haemorrahge and

7

dilated retinal veins/ venous beading are formed. Increasing vascular non-perfusion will also further trigger the formation of intraretinal microvascular abnormalities (IRMA). When the abnormal new blood vessels grow from the retinal layers towards the vitreous, DR is in the proliferative stage. These abnormal fibrovascular projections can contract, leading to a larger scale of haemorrhage and to retinal detachment with severe visual loss (LeRoith et al. 2004).

1.5 Prevalence of DM and DR

DM has become one of the most concerning health problems, and it has come to create a heavy economic burden in both developing and developed countries, due to a dramatic increase in patient numbers.

1.5.1   DM population worldwide

According to the statistical data from the World Health Organization (WHO), the prevalence of DM in 2004 was 220.5 million worldwide; and 44.7 million of these were from the South-East Asia (WHO 2008). The global prevalence of diabetes in 2008 was estimated to be 10% in adults aged 25 years or above (WHO 2010). The total number of people with diabetes was projected to rise from 171 millions in 2000 to 366 millions in 2030 (Wild et al. 2004).

1.5.2   DM population in Hong Kong and its expected statistics

In Hong Kong (HK), according to the report from the Hong Kong Society for Endocrinology, nearly 10% of the population suffers from DM (Diabetes Division, Hong Kong Society for Endocrinology, Metabolism and Reproduction 2000). The prevalence of diabetes in the working population has doubled over

the past 10 years (Tam et al. 2005). The prevalence of young-onset type II DM (<40 years old) is increasing with a different causes and natures. The occurrence of DM ranged from 2% in people with age less than 35 years to more than 20% in those older than 65 years. The increasing number of diabetic patients with increasing age was suggested to be caused by diet, obesity and physical inactivity (Diabetes Division, Hong Kong Society for Endocrinology, Metabolism and Reproduction 2000).

1.5.3   DR population worldwide and in HK

DR is an important cause of blindness due to long-term accumulated damage to the retinal microvascular circulation. This ocular complication exists in both types I and II diabetic patients. For the two types of patients who survive over 20 years with DM, nearly all type I patients and more than 77% of those with type II DM develop DR at different stages (Klein et al. 1984; Klein et al. 1984).

WHO reported that DR is the 5th leading cause of blindness and had estimated that DR is responsible for 48% of the 37 million cases of blindness throughout the world (Resnikoff et al. 2004). By the meta-analysis of 25 studies (from 1980-2008) with 22,896 diabetic individuals, it was estimated that there would be 92.6 million (35.4%) diabetic adults with any type of DR, 17.2 million (7.2%) with proliferative DR, 28.6 million (11.7%) with vision-threatening DR and 20.6 million (7.4%) with diabetic macular oedema (Yau et al. 2012).

Among patients with type II diabetes, 40% have evidence of DR with 8% in a vision-threatening state (pre-proliferative or proliferative DR or macular oedema) at any time (Kempen et al. 2004). Of those without retinopathy, it has been

suggested that the risk of incidence of new retinopathy is between 5% and 10% per year (Wong & Hyman 2008). Local HK studies reported a prevalence of DR of 15-23% among DM patients (Siu et al. 1998; Wang et al. 1998).

Concerning the type of DM, type I patients are more likely to have proliferative DR whereas those with type II DM patients are prone to have macular oedema (Van Bijsterveld 2000). The diagnosis of DR is often delayed, and hyperglycemia has been reported to be present for more than 20 years before the diagnosis is confirmed (Liu et al. 2002).

Among diabetic patients, the majority will have type II DM, and these patients will form the basis of this study.

Chapter 2: Current management and care for DM patients

2.1 Current clinical assessments for DR screening

Retinal photography or dilated pupil fundus examination using ophthalmoscopy are the methods currently used to screen out the retinal anomalies in diabetes (Garg & Davis 2009). Dilated pupil fundus examination by direct ophthalmoscope, slit-lamp biomicroscopy and binocular indirect ophthalmoscopy are three common ways to detect vascular anomalies. Biomicroscopic examination of the fundus is highly sensitive for DR screening (Khalaf et al. 2007). However, these tests must be performed by skillful and experienced professionals.

Mydriatic fundus photodocumentation is recommended as an effective and accurate method for DR screening (Carmichael et al. 2005). It provides an easy way of recording and comparison of the disease progression. Its sensitivity and specificity in screening the presence of DR has been reported to be comparable to the ophthalmological examination with direct and indirect ophthalmoscopy (Carmichael et al. 2005; Garg & Davis 2009). The 'gold standard' was taking seven 30 degree stereoscopic colour photos as suggested by the Early Treatment Diabetic Retinopathy Study (ETDRS) (Early Treatment Diabetic Retinopathy Study Research Group 1991). Different modified methods of fundus photography with comparable accuracy to the gold standard have been suggested (Scanlon et al. 2003; Williams et al. 2004; Garg & Davis 2009; Vujosevic et al. 2009). Fundus photodocumentation has been used to detect the capillary occlusion as an early clinical feature of DR that leads to retinal non-perfusion and subsequent damage; this early form of non-perfusion is potentially reversible (Bloomgarden 2008).

Fundus fluorescein angiogram (FFA) is naturally the most effective means of detecting microaneurysms. A significant correlation has been found between the microaneurysm counted by FFA and colour fundus photographs of individual patients (Hellstedt et al. 1996). Although in the past it has been reported that about twice as many microaneurysms detected on the FFA as on the colour photographs (Friberg et al. 1987; Hellstedt et al. 1996) both the microaneurysm counts obtained from FFA and colour fundus photographs were also demonstrated to predict and correlate well with the progression of early DR (Hellstedt et al. 1996). With the improvement in the resolving power of modern fundus cameras, the accuracy of retinopathy detection by fundus photography can reach a very high level. In the absence of DR detected by colour photography, the result of FFA is usually found to be negative. Even if it is positive, the angiograms will usually show only one or two microaneurysms (The Diabetes Control and Complications Trial Research Group 1987). The microaneurysms in FFA and red dots in colour photographs reflect the level of DR. About half of the red dots in photographs do not represent open aneurysms in FFA. It has been proposed that in fact the "missing" microaneurysms are small intraretinal haemorrhage, or that the aneurysms are occluded by material containing erythrocytes and are thus visible in photography but not in FFA (Hellstedt et al. 1996). Due to the invasiveness and cost of angiogram, colour fundus photography has been preferred in the study of early DR (Hellstedt et al. 1996).

In 2002, Shiba and co-authors suggested a simpler photographic method. A nine-field of retinal view was taken, which displayed more than 90 degrees vertically and horizontally. This field covers more than 95% of the fundus area photographed by the standard ETDRS method (Shiba et al. 2002) and has

comparable accuracy to ophthalmoscopy performed by experienced professionals. This photographic method will be applied in this study.

2.2 Clinical grading system of DR

The ETDRS Research Group launched a severity grading scale of DR in the 1990s. This scale provides a standard set of definitions and photographs of various types of retinal lesions describing the severity of diabetic retinopathy (Wilkinson et al. 2003). It consists of different levels of severity including mild and moderate NPDR, moderately severe and severe NPDR, non-high-risk and high-risk and advanced proliferative DR (PDR) (Early Treatment Diabetic Retinopathy Study Research Group 1991). Although it is recognized as the gold standard, its complexity makes it difficult to apply in clinical practice.

In 2001, the AAO launched a project to develop a new clinical severity scale of DR (Wilkinson et al. 2003). The AAO scale simplified the sub-levels of the ETDRS classification and grouped them into a five-stage classification for DR severity, including three low-risk stages (No DR, mild NPDR and moderate NPDR), a severe NPDR stage, followed by a proliferative stage. The existence of microaneurysms is the sign of mild NPDR in the AAO scale, while microaneurysms must be individually graded in the ETDRS scale before proceeding to the NPDR levels.

In 2012, the United Kingdom National Screening Committee further simplified the grading system, based on the essence of ophthalmological referral and the follow-up intervals, in order to ease the screening program. DM patients without retinopathy are graded as R0 and those with non-referrable retinopathy are R1.

Those with potentially sight-threatening non-proliferative and proliferative DR, are graded as R2 and R3 respectively with referral required. Apart from this simplification, the system is more or less similar to the AAO grading (Taylor 2012; Heng et al. 2013).

2.3 Current clinical management of DR patients

There is no active ophthalmological treatment for DM patients at the early stage of non-proliferative DR except for regular dilated fundus examination and glycemic control. Ophthalmic treatment is only applied for late-stage DR with sight-threatening retinopathy signs. For many years, the most common ophthalmic treatment has been destructive laser photocoagulation. By ablating the ischemic retinal area or the retinal region with vascular leakage, angiogenic growth factor(s) and vascular leakage are reduced. However, peripheral visual field constrictions with poor dark adaptation, and occasional subretinal fibrosis and vitreous haemorrhage sometimes occur as side-effects after this treatment (Yam & Kwok 2007; Bandello et al. 2013; Heng et al. 2013).

Other surgical interventions include vitrectomy and intravitreal injections of anti-VEGF substances. The aims are to remove the VEGF and to reduce the abnormal neovascularization formation at the late stage of DR (Yam & Kwok 2007; Bandello et al. 2013; Heng et al. 2013). Currently, there is no active medical treatment for the earlier stage of the disease in order to postpone the occurrence of the irreversible retinopathy or to reduce any progression of DR.

2.4 Quality of life and socio-economic burden of DR patients

DR and its treatment affect many aspects of the quality of life of patients who suffer from the condition. DR leads to reduction of both central visual acuity and contrast sensitivity which directly affect the patient's daily life in terms of reading, facial recognition, reading street signs, dialing a telephone and locating objects in a room (Warrian et al. 2010). For DR patients with retinal laser photocoagulation, peripheral vision will also be reduced (Warrian et al. 2010). DR may produce negative emotional reactions due to anxiety about the future, and restriction of physical activities which are not proportional to the actual loss of visual capacity (Woodcock et al. 2004).

Among 136 categories of diseases and injury cases as classified by the WHO, DM ranked the 12th in the leading causes of death among all ages in 2004 (WHO 2008). DM accounts for 3.5% of cases of death among non-communicable diseases (WHO 2012). It was also estimated that the ranking of DM will rise from 19th in 2004 to 10th by 2030, in terms of the leading causes of social burden of diseases over the world (WHO 2008). As DM patients require at least two to three times more health-care resources than people without DM (WHO 2009), diabetes care may account for up to 15% of national healthcare budgets (Zhang et al. 2010). Among diabetic patients, there is a higher rate of visual impairment than in the general population (Schmier et al. 2009). The average health care costs increase with the severity of DR (Schmier et al. 2009; Heintz et al. 2010). Total health care payments were 35% higher in patients with proliferative DR than in those with non-proliferative DR (Schmier et al. 2009; Heintz et al. 2010). These findings suggest that delaying DR progression markedly assists in lowering of health care expenditures (Schmier et al. 2009; Heintz et al. 2010).

<u>Chapter 3: Pathogenesis of DR</u>

The persistent high blood glucose level in DM creates oxidative stress, which causes deterioration of the vascular system and of the neuroretinal components in the ocular system and consequently leads to diabetic retinopathy. Two hypothesized mechanisms have been proposed. However, which pathway as the first step of the DR development is still controversial in human as previous experiments are mainly based on animal studies. The two hypothesized pathways of DR are:

3.1 Vascular pathway

The continuous high blood glucose level activates abnormal pathways for metabolizing glucose which result in accumulation of abnormal byproducts in the ocular vascular system, and osmotic and oxidative stress. The capillary basement membrane thickens, the endothelial cells and pericytes of the blood vessels are damaged (Van Bijsterveld 2000; LeRoith et al. 2004). The damaged capillaries leak contents intraretinally and form hard exudates (confluents of lipids and lipoproteins). The non-perfusion of capillaries contribute to an early clinically visible manifestation of DR－ microaneurysms (Khan & Chakrabarti 2007). This is a landmark of non-proliferative diabetic retinopathy (NPDR).

During the disease progression, the endothelial cells multiply on the inner wall of the blood vessels to repair the damage; this blocks the leakage from the capillaries (Khan & Chakrabarti 2007) but the retardation of the axoplasmic flow at the margin of the microvascular infarct forms a swollen area at the retinal nerve fiber layer － cotton wool spots (Van Bijsterveld 2000; LeRoith et al. 2004).

With further blockage of large blood vessels, and as more non-perfused capillaries are formed, the endothelial cells of blood vessels will have proliferative response changes to form branches of intraretinal microvascular abnormalities (IRMA). Non-perfusing capillaries may extend up to the major veins causing irregularities of the vein wall and venous beading or segmentation will occur (Van Bijsterveld 2000; LeRoith et al. 2004).

The increase of the non-perfused capillary and higher vitreous concentrations of the vasoproliferative growth factors will cause IRMA to break through the internal limiting membrane on to the retinal surface. These new vessels may grow rapidly. This is the mark of proliferative diabetic retinopathy (PDR) which results in new vessels elsewhere, even on the optic disc (Van Bijsterveld 2000; LeRoith et al. 2004).

Due to the effect of the proliferating endothelial cells on the posterior hyaloid surface, the configuration of the vitreous collagen may be changed and lead to localized vitreous contraction. This may give rise to pre-retinal haemorrhage, vitreous traction and tractional retinal detachment (Van Bijsterveld 2000; LeRoith et al. 2004).

3.2 Neuronal pathway

Glial reactivity and altered glial glutamate metabolism have been shown to be early pathological changes in the rat model of diabetic retinopathy developed by Lieth and co-workers (Lieth et al. 1998). These elevated levels of retinal glutamate are toxic to the retina.

In human retina, glial cells include the Müller cells, astrocytes and microglial cells. They play an important role in the homeostatic regulation of the retina, and control critical processes such as uptake of glucose from the circulation and transfer of energy to neural cells in the retina (Lopes de Faria et al. 2002). The glial cells also induce the formation of the tight endothelial junctions and thus confer barrier properties to the retinal blood vessels (Mizutani et al. 1998). They help to maintain the endothelial lining of retinal microvessels in the blood-retinal barrier so as to maintain normal neuronal and vascular functions in the retina. The glia aid in maintaining low synaptic levels of neurotransmitters. The major excitatory neurotransmitter in the retina is glutamate, which is an amino acid toxic to retinal neurons at high levels (Lieth et al. 1998). Glial cells are activated during certain injury states.

In the diabetic condition, there are several aspects that lead to the neural degeneration in the retina. First, there are changes in the glutamate metabolism of diabetic rats (Barber et al. 1998). Glutamate accumulation in the retina may cause glutamate toxicity which will in turn lead to neuronal apoptosis.

Secondly, the rate of apoptosis increases in DM. The retinal cells involved in the apoptosis are ganglion cells, glial cells (Müller cells and retinal astrocytes) and other neurons (Barber et al. 1998). With the loss of Müller cells, the compromised blood-retinal barrier triggers the activation of Müller cells to increase immunoreactivity to the intermediary filament glial fibrillary acid protein. This process may be involved in retinal capillary occlusion in diabetic patients (Van Bijsterveld 2000).

Finally, the progressive dysfunction of capillaries leads to ischemia which causes neuronal death from the inner retinal layers down to the outer plexiform layer. Diabetic retinopathy is the final result of these vascular and neuroretinal degenerations, it is an irreversible outcome even after good glycemic control is re-instituted. It is probably caused by the oxidative stress built up in the diabetic condition which creates a phenomenon called metabolic memory (Kowluru & Chan 2007).

Chapter 4: The influence of DM on the visual system

4.1 Morphological aspects

4.1.1 Cornea

Decreased corneal sensitivity is a common finding in patients with DM (Aiello et al. 1998; Yam & Kwok 2007; Scott et al. 2010). Moreover, due to the thickening of the corneal basement membrane, decreased hemidesmosome frequency and decreased penetration of anchoring fibrils (Scott et al. 2010), there is poor adhesion of the corneal basement membrane which leads to impaired epithelial barrier function and recurrent corneal erosion after trauma.

4.1.2 Crystalline lens

Accumulation of the sugar alcohol sorbitol leads to the influx of water molecules to the fibers of the lens. Swelling of the crystalline lens, which is reversible, leads to fluctuation of refractive error in diabetic patients (Scott et al. 2010).

Diabetic patients are also at risk of early cataract formation compared to those in non-diabetic groups. The accumulation of crystalline, a long-lived protein, in the lens has been suggested to have a role in lens protein insolubilization. The formation of crystalline fragments scatters lights and is the starting point for cataractogenesis (Sharma & Santhoshkumar 2009). The ultrasonic and biochemical evaluation of the human diabetic lens has revealed that the diabetic changes mainly influence the lens of early-onset (type I) rather than late-onset (type II) diabetic patients. No significant differences have been found in terms of lens thickness, ultrasound attenuation coefficient and lens protein amount between the type II diabetic patients to age-matched controls (Raitelaitiene et al. 2005). The biometric findings in late-onset diabetes are in marked contrast to the

large overall effect of diabetes reported in early-onset diabetes (Sparrow et al.
1992). By means of Scheimpflug photography and densitograms, very little
effect was found in type II DM on different zones of the lens. These findings
suggest that type I and II DM have different underlying pathophysiologic
mechanisms (Wiemer et al. 2008).

4.1.3 Retinal nerve fiber layer (RNFL) thickness

Oshitari and co-workers (Oshitari et al. 2009) found that type II DM patients
with DR had significantly thinner retinal nerve fiber layer than did the eyes of
control patients. However, no significant thinning was found between DM
patients without DR and the controls. Lopes de Faria and co-workers (Lopes de
Faria et al. 2002) also stated that significant nerve fiber loss in the superior retina
occurred before the existence of DR in type I DM. Similar findings by optical
coherence tomography (OCT) had been reported by Sugimoto and co-workers
(Sugimoto et al. 2005). It has been proposed that the loss of the neuroglial cells
in hyperglycemia increases neural apoptosis. However, the discrepancy of the
findings between studies would be probably due to the limitation of the OCT
operation principles. The OCT measures the retinal nerve fiber layer, and not
only the ganglion cell axons, which also includes the Müller cell processes,
astrocytes and the intraretinal fluid accumulation. This may cause inconsistent
RNFL findings in studies of DM and result in over-estimation of the RNFL
(Sugimoto et al. 2005; Takahashi & Chihara 2008) .

4.1.4 Macular thickness

Optical coherence tomography (OCT) has been applied to investigate structural changes at the macula in diabetic patients without clinically significant macular oedema. Thickening of the macular region in diabetic patients without retinopathy was reported by Sugimoto et al. (Sugimoto et al. 2005) and Cho et al. (Cho et al. 2010). Macular thickening laws found to increase with the severity of DR (Cho et al. 2010). The thickening was proposed to be caused by the low resistance to oedema of the macular region (Sugimoto et al. 2005). On the other hand, Bressler et al. (Bressler et al. 2008) and Browning et al. (Browning et al. 2008) reported no significant difference in macular thickness of diabetic patients with no or minimal retinopathy and their control subjects.

There are other studies reporting pericentral macular thinning at the early stage of disease (Biallosterski et al. 2007; Nilsson et al. 2007; Van Dijk et al. 2009; DeBuc & Somfai 2010; Van Dijk et al. 2010). These investigators reported retinal thinning which was attributed to selective loss of the inner retinal layers, including the ganglion cell layer, followed by the axonal loss, which then led to the reduction of the retinal nerve fiber layer thickness. Thus, early DR was proposed to include a neurodegenerative component even before the onset of vascular lesions (Van Dijk et al. 2009; DeBuc & Somfai 2010; Van Dijk et al. 2010). Oshitari et al. and Browning et al. suggested that neuronal abnormalities gave rise to retinal thinning in diabetic eyes without retinopathy. With the increase of retinopathy severity, the nerve fiber layer thinning was overwhelmed by the intraretinal fluid accumulation of the other retinal layers (Browning et al. 2008; Oshitari et al. 2009). Further, Verma et al. reported that thinning also existed in the photoreceptor level of diabetic patients without retinopathy (Verma

et al. 2009). Hence, there are great variations among the structural measurement in the diabetic retina in the early stages of the disease.

4.1.5 Retinal Pigment Epithelium (RPE)

Incomplete removal of photoreceptor outer segment disks with subsequent incomplete release of degraded material initially leads to the increased accumulation of outer segment-derived material in the outer retina and subretinal space. Over time, the accumulated material will thicken the outer retina and result in autofluorescence (Schmitz-Valckenberg et al. 2008; Spaide 2008).

Hyperglycemia has been shown to lead to oxidative damage of the retinal mitochondria. It causes apoptosis of the retinal pericytes and endothelial cells. In the diabetic retina, an increased level of fundus autofluorescence has been demonstrated (Kowluru & Abbas 2003; Elner et al. 2008). It is believed that the fundus autofluorescence signal is not due to the accumulation of lipofuscin, a fluorophore that has not been found to be increased in diabetes (Elner et al. 2008). Moreover, increased autofluorescence of mitochondrial flavoproteins, an indicator of mitochondrial oxidative stress, probably correlates with retinal cell dysfunction (Elner et al. 2008) and the apoptosis of retinal cells is a key pathophysiologic mechanism in diabetic retinopathy.

4.2 Functional aspects

4.2.1 Visual acuity (VA)

Visual acuity is not a good test for monitoring the development of the sight-threatening DR. VA in diabetic patients can be within the normal range even in patients with severe proliferative diabetic retinopathy (Rudnicka & Birch

2000) because VA decreases only when maculopathy or vitreous haemorrhage occurs. VA is a test which assesses foveal function only (Bengtsson et al. 2008).

4.2.2 Contrast sensitivity (CS)

Contrast sensitivity decreases at all spatial frequencies in diabetic maculopathy (Rudnicka & Birch 2000). Ismail and Whitaker (Ismail & Whitaker 1998) found that contrast sensitivity declined in their diabetic subjects compared to age-matched controls. However, as with VA, CS is a relatively weak test for identifying the onset or development of DR because it produces an unacceptably high false positive rate. Although a CS reduction has been reported in some studies of diabetic patients (Ismail & Whitaker 1998), it is hard to confirm whether the decrease of CS in diabetic patients is caused by retinopathy or other aspects of aging (Rudnicka & Birch 2000).

4.2.3 Colour vision

Ismail and Whitaker (Ismail & Whitaker 1998) assessed colour vision for the diabetics using the Farnsworth-Munsell 100-Hue test. All diabetic subjects were found to have higher error scores than the control subjects. Error scores increase steadily with the severity of the DR. The acquired colour defect is predominantly along the blue-yellow colour axis. However, screening for tritan deficits usually has low sensitivity and specificity due to individual variations in pre-retinal absorption of wavelength by macular pigment and lens (Rudnicka & Birch 2000).

4.2.4 Automated perimetry

Bengtsson and co-workers (Bengtsson et al. 2005) demonstrated that visual field

(VF) measures correlated better than VA with the severity of DR (Bengtsson et al. 2005). Transient relative scotomas occur over the areas of poorly perfused retina (Rudnicka & Birch 2000) but some VF scotomas cannot be related to any visible lesions in the fundus (Ghirlanda et al. 1997). The conventional white-on-white perimetry (WWP) and short-wavelength automated perimetry (SWAP) show similar validity for the functional changes in DR. Test-retest variability is unaffected by blood glucose fluctuation either for WWP or for SWAP (Bengtsson et al. 2008). Both WWP and SWAP show the same decrease in sensitivity (mean defect) of about 0.40 dB per ETDRS step (Bengtsson et al. 2005). WWP may be better than SWAP in separating groups with different levels of retinopathy, while SWAP for the central field appears superior to WWP in identifying more localized field losses caused by ischemic damage (rather than macular oedema) (Remky et al. 2003; Bengtsson et al. 2005). However the sensitivity and specificity of SWAP are rather low because of the poor differentiation between eyes with and without oedema (Agardh et al. 2006).

It has been suggested that the functional loss in VF sensitivity is relatively unrelated to localized blood-retinal barrier defects (Bek & Lund-Andersen 1990). In a study using microperimetry, retinal regions with macular hard exudates and cystoid oedema were associated with local reduction of sensitivity; regions with focal and diffuse non-cystoid macular oedema (for example, intra-retinal haemorrhage, non-perfusion and serous retinal detachment) were shown to have sensitivity comparable to normal retina. Since hard exudates and cystoid oedema block or scatter the light before it reaches the photoreceptors, these optical effects have been proposed to be major causes of sensitivity loss (Soliman et al. 2010).

4.2.5 Dark adaptation

Elevated rod threshold have been found in diabetic patients. Poor night vision is a symptom of pre-proliferative and proliferative DR. Poor night vision may be due to poor pupil dilation under mesopic and scotopic condition. Extensive scotomas in the peripheral visual field may also contribute (Rudnicka & Birch 2000). Henson and North reported that a large number of diabetics had an elevated final threshold above the age-norm in dark adaptation but there was considerable scatter in their data (Henson & North 1979). They proposed that ischemia in the retina could be the reason for this fairly large amount of data variability. The abnormalities in dark adaptation might imply the inability of the rods to increase their dark current, or a postsynaptic failure to detect minimal rod signals (Arden et al. 1998).

4.3 Electrophysiological objective ocular assessments

4.3.1 Electro-oculogram (EOG)

The EOG is an electrical signal detected by electrodes placed at inner and outer canthus (for the monocular case), and is produced as the ocular dipole rotates in the orbit. It may be measured binocularly by placing electrodes at right and left outer canthus. The EOG is a measure of the functional status of the retinal pigment epithelium (RPE) and the photoreceptors, and is assessed by calculating the ratio of the eye movement signal amplitudes (for a standard eye movement) in light phase and dark phase (Arden ratio) (Van Bijsterveld 2000; Arden & Constable 2006).

Shirao and Kawasaki (Shirao & Kawasaki 1998) suggested that the mean waveforms of the conventional EOG dark trough and light peak in diabetic

patients at various stages of DR were not essentially different. Schneck et al. (Schneck et al. 2008) reported that the Arden ratio was insensitive to alterations in DM, while the reduction of the fast oscillation amplitudes in EOG might reflect the alterations of the RPE and/or photoreceptors. There are conflicting results in this aspect of diabetes, with some reports that the Arden ratio deteriorates with the duration of diabetes and the severity of the retinopathy while others deny this finding (Van Bijsterveld 2000).

4.3.2 Full-field electroretinogram (ERG)

The ERG is a measure of the summated electrical response of the retina to a light stimulus. The rod and cone retinal systems can be isolated by manipulating different stimulus and adaptation conditions. There are several components obtained from ERG. The negative a-wave reflects the proximal photoreceptor response together with some postsynaptic activities (Sieving et al. 1994; Tzekov & Arden 1999; Van Bijsterveld 2000); the positive b-wave reflects the bipolar cell responses (Sieving et al. 1994; Tzekov & Arden 1999; Van Bijsterveld 2000); oscillatory potentials (OPs) are supposed to reflect the inner plexiform layer response and are probably generated by neural interactions (Tzekov & Arden 1999); the photopic negative response (PhNR) originates more distally and overlaps in time with the inner retinal contributions (Rangaswamy et al. 2007).

The b-wave, OPs and PhNR have been reported to have reduced amplitudes and delayed responses in the early stages of DR. The b-wave implicit time has been reported to be delayed in non-proliferative and proliferative DR (Kim et al. 1997). Its amplitude reduction is mostly observed to be reduced in eyes with proliferative DR (Kim et al. 1997). The b-wave implicit time has been shown to

be more sensitive in showing the difference between the diabetic group (without DR) and the control group than is b-wave amplitude (Holopigian et al. 1992).

Reduction of OP amplitudes has been found in diabetic patients (Holopigian et al. 1992; Kim et al. 1997; Shirao & Kawasaki 1998; Tzekov & Arden 1999; Vadala et al. 2002; Kizawa et al. 2006; Chen et al. 2008) and OP amplitudes has been shown to reduce with increased DR severity (Kizawa et al. 2006) and selectively in certain OP wavelets (Ghirlanda et al. 1997). OP wavelets have also been found to be delayed (Ghirlanda et al. 1997; Kim et al. 1997; Shirao & Kawasaki 1998; Tzekov & Arden 1999; Kizawa et al. 2006). The OP amplitudes change prior to the period when retinal disruption is extensive enough to alter the b-wave amplitude (Speros & Price 1981). The OP generator is presumed to be in the intra-retinal feedback neuronal circuitry, mostly probably in the amacrine cells (Shirao & Kawasaki 1998). However, the findings in different studies vary considerably. Some studies have reported that the deterioration of OPs is present even without ophthalmoscopically visible DR (Kim et al. 1997; Shirao & Kawasaki 1998; Tzekov & Arden 1999) while other studies have reported that deterioration of OPs was only found in those with mild NPDR (Kizawa et al. 2006; Chen et al. 2008). Reduced neurosensory retinal function as indicated by reduced OPs before the presence of vascular defects may indicate the risk of developing typical defects of DR (Vadala et al. 2002). Moreover, there is no standard method of analyzing OP data, with some studies summing OP amplitudes (Shirao & Kawasaki 1998; Kizawa et al. 2006; Chen et al. 2008) while others have analyzed individual OP wavelets (Kim et al. 1997; Shirao & Kawasaki 1998). The instrumentation and software for analyzing OPs power and amplitude are less widespread than are those for other ERG components (Kim et

al. 1997). The fluctuation of OP responses from normal to subnormal amplitudes might occur in relation to unsteady metabolic retinal changes even with minimal vascular injury (Vadala et al. 2002). This might lead to the variation of study findings and the sensitivity of OPs.

The PhNR has been proposed to indicate inner retinal activities (Rangaswamy et al. 2007). Chen and co-workers demonstrated that diabetic patients have a delayed PhNR with reduced amplitude (Chen et al. 2008). In their study, the PhNR also had a better sensitivity than OPs in screening diabetic patients without retinopathy (Chen et al. 2008).

However, Kizawa and co-workers stated a contradictory finding. They reported that the PhNR amplitudes were only significantly reduced at the mild NPDR stage (Kizawa et al. 2006) and that its sensitivity was less than that of OPs. However these investigators used different chromatic stimuli in ERG measurement, and this may account for the difference in their findings.

4.3.3 Pattern electroretinogram (PERG)

The PERG is a measure of ganglion cell activity and is thus abnormal in diseases of the optic nerve and ganglion cells (Van Bijsterveld 2000). PERG amplitude is reduced with increasing severity of diabetic retinopathy (Van Bijsterveld 2000). However, different PERG paradigms (for example stimulus size, luminance, frequency etc) in each clinic may produce different or even contradictory experimental results (Kim et al. 1997; Tzekov & Arden 1999; Parisi & Uccioli 2001). There is currently no agreement on the standard stimulus used to generate a PERG (Ghirlanda et al. 1997; Kim et al. 1997; Tzekov & Arden 1999).

Chapter 5: Multifocal electroretinogram (mfERG)

5.1 Background information of mfERG

The mfERG is a photopic, topographic measure of retinal function (Sutter & Tran 1992). The stimulus consists of a pattern of hexagons that are usually scaled to produce approximately equal ERG responses from each stimulus element on the normal retina. The series of stimuli are controlled by a pseudorandom binary m-sequence (Sutter & Tran 1992; Sutter 2000) and displayed as alternating white and black hexagons. These small retinal areas are independently stimulated and the local ERG contributions to the recorded mass potential are extracted using a cross-correlation technique (Hood et al. 1997).

According to the ISCEV guidelines, the basic clinical setting of the mfERG is 103 scaled hexagons extending to a diameter of 50°. The filtering bandpass is 3-300 Hz or 10-300 Hz. The mfERG waveforms are largely shaped by bipolar cell activity, together with small contributions from the photoreceptor cells and inner retinal (amacrine and ganglion) cells (Hood 2003; Ng et al. 2008). The mean flash response is called the first-order component. There are three main components: N1, P1 and N2 (Figure 5.1). They are influenced in different ways by the onset and offset of the bipolar cells responses and, to a much lesser extent, by responses of the photoreceptors. The inner retina exerts a subtle influence on the waveform (Ng et al. 2008).
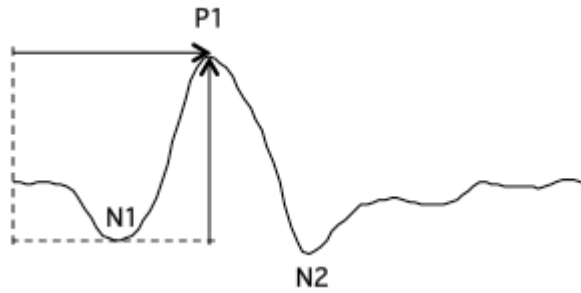
Figure 5.1. Basic resultant waveform of the standard mfERG paradigm

(Adopted from Hood et al. 2012)

5.2 mfERG assessment of DM patients

5.2.1 Standard mfERG paradigm

Palmowski and co-workers (Palmowski et al. 1997) investigated the first-order response component in DM with and without retinopathy. They observed overall reduced amplitudes and delayed implicit times in the diabetic patients with NPDR. For those without retinopathy, they found no such trend; however, Klemp and co-workers (Klemp et al. 2004) found that both the implicit times and amplitudes could be affected by the hyperglycemic condition. The implicit time of P1 and N2 were shortened significantly and the amplitude increased slightly in the hyperglycemic condition. This might indicate some impairment of outer retinal function in diabetes with NPDR (Palmowski et al. 1997) and hyperglycemia might suggest accelerated retinal metabolism in the early stages of DM (Klemp et al. 2004).

5.2.2 Modified mfERG paradigms

The response of the conventional mfERG paradigm (the first-order component) is mainly derived from the outer retina, with much lesser contribution from the inner retina. To investigate the role of the inner retina in the mfERG, several

modified mfERG paradigms have been suggested. As neurodegeneration exists in diabetic retinopathy, the following modified mfERG paradigms have been applied in investigation of DR.

5.2.2.1 Second order mfERG study

Second-order responses reflect the short-term adaptation from a preceding flash. The second-order response is smaller than the first-order response. It is related to the activity of the inner retina and ganglion cells (Lam 2005; Ng et al. 2008).

Palmowski and co-workers (Palmowski et al. 1997) found that diabetics had reduced amplitude and delayed implicit time of the second-order response, whether retinopathy had developed or not. Short-term hyperglycemia could also affect the implicit time of the second-order response (Klemp et al. 2004). This indicated that diabetes might have impaired adaptive mechanisms, and the inner retina might be impaired earlier than the outer retina (Palmowski et al. 1997).

5.2.2.2 Slow flash mfERG (sfmfERG) study

In the commonly used version of the sfmfERG, there are 4 video frames in each interval of the sfmfERG stimulus. The first frame is the multifocal stimulus, which is followed by 3 dark frames to increase the time interval between multifocal flash frames (by 13.33 x 3 = 39.99ms). The basic waveform of the slow flash mfERG is shown in figure 5.2a. his enables the retinal responses to develop and decay more completely and allows a clearer assessment of the first-order component including the oscillatory potentials (OPs) (Lai et al. 2007). OPs are believed to originate from the inner plexiform layer and be generated by neural interaction (Lam 2005).
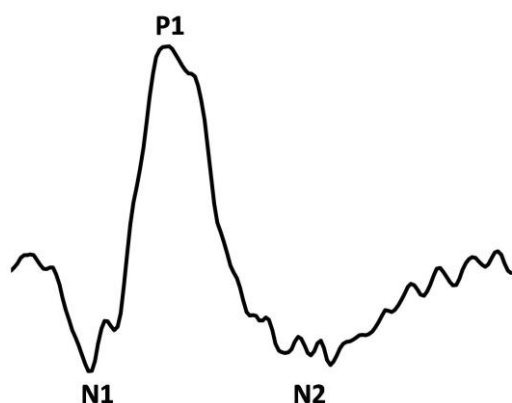
Figure 5.2a. Basic resultant waveform of the slow flash mfERG paradigm

Bearse and co-workers (Bearse et al. 2004) investigated the local multifocal oscillatory potentials (mfOPs) in diabetic eyes. They found that the mfOPs were mostly abnormal at retinal sites containing NPDR. The summed second-order OPs (assessed by combining the first- and second-order sfmfERG and then digitally filtered to form the summed second-order OPs) were more associated with retinal sites of NPDR. They suggested that fast adaptive mechanisms in the retina might be impaired in locations affected by DR.

5.2.2.3 Periodic global flash mfERG (MOFO mfERG) study

In the global flash mfERG paradiagm, there are 4 video frames in each stimulus interval. The first frame is the multifocal stimulus (designated M) followed by a dark frame (O), a global flash (F) and then another dark frame (O) (hence MOFO describes the 4 frame sequence). This paradigm is used to measure fast adaptive retinal mechanism(s) (Chu et al. 2006; Lai et al. 2007). There are two main components in the results: the direct component (DC) which is a response to the focal flash; the induced component (IC) which is the interaction of focal and global flash. The IC is proposed to arise from the inner retina, or from the

ganglion cells.
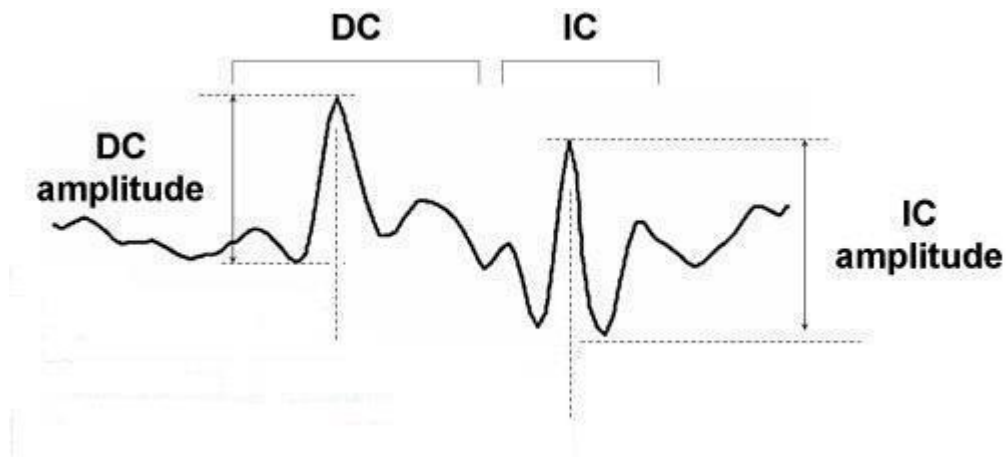
Figure 5.2b. Basic resultant waveform of the global flash mfERG paradigm

Shimada and co-workers (Shimada et al. 2001) applied the global flash paradigm to assess early retinal changes in diabetes. The resultant waveform of the global flash paradigm is as shown in Figure 5.2b. The DC amplitude was much smaller in their diabetic group than in their normal group. For the IC, due to the larger inter-subject variability, no significant difference was found between these two groups. This is unexpected, as IC is supposed to be generated from the inner retinal components (Hood et al. 2002; Chu et al. 2008; Luo et al. 2011), and deterioration in these neural components should exist in diabetes, even prior to the visible retinal lesions (Barber et al. 1998; Barber 2003; Barber et al. 2011).

In 2006, Chu and co-workers (Chu et al. 2006) applied the global flash mfERG to glaucoma patients with altered stimulus luminance difference in multifocal flashes. They attempted to measure the inner retinal signals at different luminance adaptation levels. They found that the peripheral DC luminance-modulated response function was altered by the adaptive mechanism

that was induced by the global flash. This luminance-modulated global flash paradigm might help in reflecting an abnormal adaptive mechanism in ocular diseases.

5.2.2.4 "Long-duration" stimulus mfERG

In the output waveform of the standard mfERG paradigm, there is a large overlap of the on- and off-pathway responses. This may mask the different performance along different pathways in the investigation of normal and abnormal retina. To separate the on- and off-pathways, Kondo and Miyake (Kondo & Miyake 2000) introduced a mfERG paradigm to simulate the "long-duration" flash in the Ganzfeld full-field electroretinogram (Sieving 1993). By increasing the number of multifocal flashes and dark frames, the overlap between the on-response (the retinal signal measured when the light stimulus turns on) and off-response (the retinal signal measured when the light stimulus turns off) in the mfERG can be minimized. The basic resultant waveform is shown in figure 5.2c. This protocol has been applied in some retinal diseases to study the responses of the on- and off-pathways (Kondo et al. 1998; Marmor et al. 1999; Luu et al. 2005).
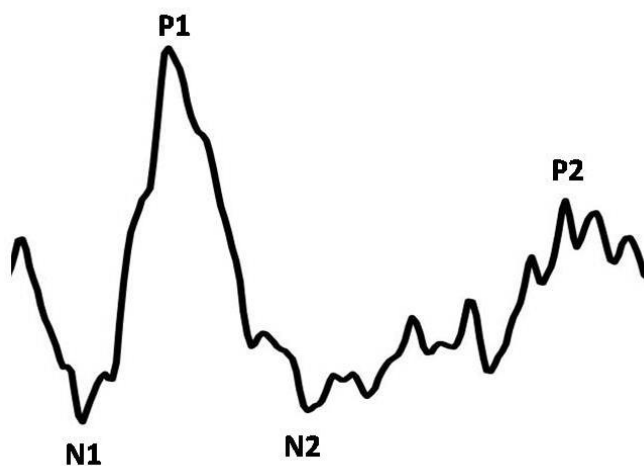
Figure 5.2c. Basic resultant waveform of the "long-duration" mfERG paradigm

5.2.3 Summary of the aims of this study

DR is one of the most common causes of blindness in the world. Two basic hypotheses have been suggested as its cause; however, the exact mechanism of DR development is still unclear. When cellular apoptosis begins and what types of cells involved in the neurodegeneration process are still unknown (Barber et al. 1998). Early detection of neural changes in diabetes helps in understanding what may delay the irreversible stage of DR. Also, neuroprotection might be the direction to consider in the future medical treatment of DR (Westall 2005). The mfERG, in standard form or in a modified paradigm provide a powerful and objective tool which clinicians can assess the early neural changes in DR. This may help in deciding the proper time to start the neuroprotective therapies, and to assess the safety and effectiveness issues involved with various therapies.

In this study, its aims are to:

1) find out the optimal luminance combination for the MOFO mfERG paradigm

2) investigate the localized DR lesions by means of the MOFO mfERG paradigm

3) find out if the MOFO mfERG is sensitive enough to screen out the early DR functional deterioration

4) compare the sensitivity among the three ocular assessments – MOFO mfERG measurement, automated perimetry and the RNFL assessment

5) correlate the objective MOFO mfERG measurement with two common morphological and functional clinical assessments - automated perimetry and optical coherence tomography RNFL assessment in diabetic eyes

6) apply the "Long-duration" mfERG paradigm to investigate the on- and off-pathway responses of the diabetic retina in order to study their lateral antagonistic properties

Part II
Experiments

Chapter 6: Middle and inner retinal responses measured by MOFO mfERG

6.1 Experiment A1 – Effects of luminance combinations on the characteristics of MOFO mfERG

6.1.1 Abstract

Purpose: This study aims to ascertain the characteristics of the response triggered by the global flash multifocal electroretinogram (MOFO mfERG) under various combinations of global and focal flash luminance, and to determine the optimal conditions for this measurement.

Methods: Ten normal subjects with mean age 23.2 years (± 1.14 years) were recruited for the MOFO mfERG measurement. The visual stimulation consisted of four video frames (stimulus frame with 103 scaled hexagonal focal flashes, followed by a dark frame, a global flash and then another dark frame). The focal and global flash intensities were varied independently for four levels (50, 100, 200 and 400 cd/m^2). The subjects then underwent measurements with sixteen combinations of focal and global flash luminance. The direct component (DC) and induced component (IC) of the MOFO mfERG were grouped into central and peripheral regions for analysis.

Results: The central and peripheral DC amplitude increased with the focal flash luminance under constant global flash luminance. Moreover, the proportion of the global flash and focal flash intensity was shown to be important to achieve an optimal IC response. When the ratio of global flash luminance to focal flash luminance (g/f ratio) was kept at about 2:1, the central and peripheral IC

amplitude reached the peak value, and further increasing the global flash luminance did not enhance the IC response magnitude. The implicit time of both central and peripheral DC generally decreased with the increase of g/f ratio. However, the implicit time of central and peripheral IC increased with increasing g/f ratio.

Conclusion: The g/f ratio is important in the MOFO mfERG paradigm since the DC and IC responses change with this ratio. In order to obtain both optimal DC and IC responses, a g/f ratio of 1:1 with focal flash luminance between $100cd/m^2$ and $200cd/m^2$ is recommended. As the global flash mfERG paradigm is used to study the interaction triggered by both flashes, the g/f ratio is a vital parameter for measurement in future studies.

6.1.2 Introduction

The multifocal electroretinogram (mfERG) provides information regarding topographic retinal responses. It helps in examining local functional changes or losses in various retinal diseases such as glaucoma, diabetic retinopathy, age-related macular degeneration and retinitis pigmentosa (Chan & Brown 1998; Chan & Brown 1999; Chan & Brown 2000; Kretschmann et al. 2000; Palmowski-Wolfe et al. 2006; Asano et al. 2007; Palmowski-Wolfe et al. 2007; Nagy et al. 2008; Tyrberg et al. 2008; Gerth 2009; Wolsley et al. 2009). The conventional mfERG signals have been reported to originate mainly from bipolar cells (Hood et al. 2002; Ng et al. 2008). With a modified mfERG protocol suggested by Sutter and his co-workers, the retinal responses from the inner retinal layer, especially ganglion cell activity, can also be studied (Sutter et al. 1999).

This modified multifocal stimulation was used to study the retinal adaptive mechanism by inserting interleaved global flashes between the successive frames of the multifocal stimulus (Sutter et al. 1999). A large non-linear inner retinal response could be triggered. This "global flash" protocol has been further applied to study ocular diseases that involve the inner retina. Shimada et al. (Shimada et al. 2001) used the global flash paradigm for the early detection of functional changes in DR. Chu et al. (Chu et al. 2006; Chu et al. 2007) further modified the global flash protocol to facilitate the early detection of glaucoma.

In the global flash mfERG response, there are two main components: the direct component (DC) and the induced component (IC). The DC is the mean response to the focal flash and the IC is an adaptive response due to the interaction of the

focal and the global flash (Shimada et al. 2005). The DC has been proposed to be composed of outer retinal responses and inner retinal oscillation-like wavelets; the origin of the IC has been proposed to be predominantly from the inner retinal layers (Sutter & Bearse 1999; Chu et al. 2008). This modified protocol demonstrates its capability in diagnosing inner retinal dysfunction. Since the luminance intensities of the focal and global flashes can influence the retinal physiology that alters the characteristics (i.e. amplitude, implicit time) of the DC and IC, apart from applying it as a clinical tool, it is important to understand the effects of luminance on this protocol.

Shimada and colleagues have studied the effect of different combinations of focal and global flash luminance in the MOFO paradigm (Shimada et al. 2005) but used only three subjects with a wide age range (23-63 years) for all experimental conditions. This did not provide an adequate description of MOFO mfERG response characteristics. Moreover, a thorough understanding of the relationship between the global and focal flash luminance and the DC and IC characteristics should help to increase the value of the MOFO global flash mfERG for different purposes. Hence, the optimal setting of the focal and global flash luminance would help in maximizing the measurement of outer and inner retinal responses. This is necessary to achieve the most effective paradigm, especially in the clinical assessment of retinal diseases. In this study, we investigated the characteristics of the DC and IC at different retinal regions under various luminance combinations (both global and focal flashes) in the global flash (MOFO) mfERG paradigm. We attempted to suggest the optimal luminance setting for this particular mfERG paradigm.

6.1.3 Methods

6.1.3.1 Subjects and inclusion criteria

Ten normal subjects (age range 21-24 years, mean age 23.2 ± 1.14 years) were recruited for this study. The subjects had visual acuity of 6/6 without any ocular or systemic disorders. Their refractive errors were within +3.00 to -6.00 D with less than -1.25 D of astigmatism. One eye was randomly selected for measurement. Pupil dilatation was carried out on the tested eye of the subjects with room illumination (about 100 lux) throughout the whole experiment. All procedures of the study followed the tenets of the Declaration of Hesinki. The study was approved by the Ethics Committee of The Hong Kong Polytechnic University. Informed consent was obtained from each subject after the experimental procedures were described.

6.1.3.2 Experimental set-up and procedures

6.1.3.2.1 Stimulus conditions

The VERIS Science 5.1 system (Electro-Diagnostic-Imaging; San Mateo, CA, USA) was used for the mfERG measurement. The visual stimulus consisted of 103 scaled hexagons subtending a visual angle of about 45°. The stimulus was displayed on a high luminance CRT monitor (FIMI, Medical Electronic Equipment, Italy). The hexagonal stimulation followed a pseudo-random binary m-sequence (2^{13}-1) with a video frame rate of 75 Hz. There were four video frames in the stimulation sequence: a frame with pseudo-random focal flash followed by a full screen dark frame, a full screen global flash and another full screen dark frame. The total duration of these four video frames was 53.2 ms, with 13.3 ms between frames. The luminances of the focal flash and the global flash were varied independently, with four different luminance levels used (50,

100, 200 and 400 cd/m^2); the dark frame was set to a luminance of 2 cd/m^2. This gave sixteen combinations of global (g) and focal (f) flash luminance for this study. The background luminance was set at 100 cd/m^2. A central cross on the stimulus pattern was used for fixation.

6.1.3.2.2 Recording conditions

Before testing, the pupil of the tested eye was fully dilated with 1% tropicamide (Alcon, Fort Worth, TX). The untested eye was occluded by an eye patch. A Dawson-Trick-Litzkow (DTL) electrode was used as the active electrode. Gold-cup electrodes were placed at the ipsilateral temporal side and forehead respectively as reference and ground electrodes. The refractive error of the tested eye was corrected by the spherical equivalent power for a viewing distance of 33 cm. The signals were amplified by 100,000 with a band-pass filter from 3 to 300 Hz (Grass Instrument Co., Quincy, MA, U.S.A.). The recording time for each luminance combination was about eight minutes. There were a total of sixteen recordings for each subject. The sequence of the sixteen recordings was randomized. The sixteen recordings took place over two days over to minimize subjects' fatigue. Each recording was divided into thirty-two segments of approximately 14 seconds and a break was allowed between each segment. The recording quality, including the fixation quality, was monitored using the real time display from VERIS. Any segment contaminated by poor fixation, eye movements, or blinks was rejected and re-recorded immediately.

6.1.3.3 Statistical analysis and g/f ratio calculation

The mfERG responses were grouped into two regions: central (Ring 1-2, about 7° of the central visual field) and peripheral (Ring 4-6, about 17.2° to 44.5° visual field). Ring 3 was a transitional region between the central and peripheral regions (Chu et al. 2006), and it was excluded from the analysis. The first-order kernel of the mfERG response was extracted and analysed. The DC and IC peak-to-peak amplitudes of the mfERG were measured and compared among different combinations of the global and focal flash luminance as shown in Figure 6.1a and 6.1b. The implicit times of the DC and IC were also measured for analysis. All the comparisons were performed by repeated measures ANOVA with Bonferroni post-hoc test. The ratio of global flash luminance to focal flash luminance (g/f ratio) was also applied to correlate with changes in the DC and IC responses.
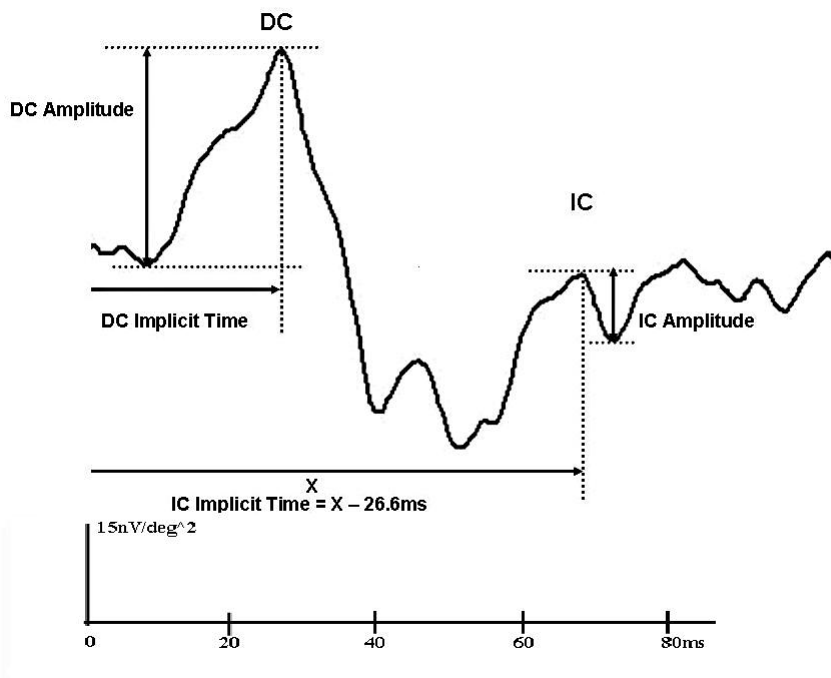
Figure 6.1a. Central MOFO mfERG waveform
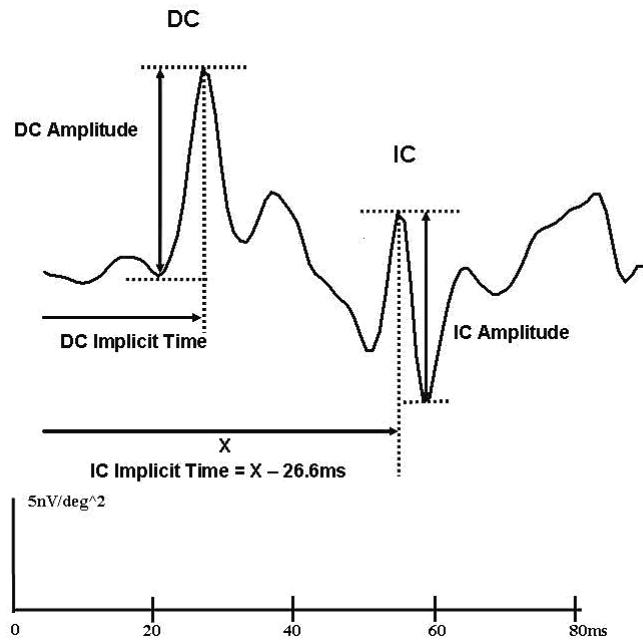
Figure 6.1b. Peripheral MOFO mfERG waveform

6.1.4 Results

6.1.4.1 Direct components (DC)

6.1.4.1.1 DC Amplitude

In the central retinal region, the DC amplitude increased with focal flash luminance under a fixed global flash luminance. Figure 6.2a shows the change in amplitude of DC with different g/f ratios (i.e. ratio of global flash to focal flash luminance) for four focal flash luminance levels. When the focal flash luminance was within the range from 100 to 400 cd/m^2, the DC amplitude achieved the maximum value when the g/f ratio was minimal (with the global flash set at the lowest value, i.e. 50 cd/m^2). Further increasing the g/f ratio decreased the DC amplitude and the central DC amplitude was significantly affected by the luminance of focal flash (f) (p<0.001), global flash (g) (p<0.001) and was also affected by their interaction (p<0.05).

In the peripheral retinal region, the DC amplitude increased with the focal flash luminance but decreased with the global flash luminance. When the focal flash luminance was within the range of 100 to 400 cd/m^2, the DC response reached the maximum value while the g/f ratio was the smallest (Figure 6.2b). It was significantly affected by the luminance of focal flash ($p<0.001$), global flash ($p<0.005$) and their interaction ($p<0.025$).

When the global flash intensity was less than the focal flash intensity (i.e. g/f ratio < 1), the DC responses for the focal flash intensity from 100 to 400 cd/m^2 showed a similar trend. Post-hoc testing revealed that with the combination of g/f at 50/400, the DC amplitude achieved the maximum value in both the central and peripheral regions; when the combination of g/f was at 400/50, amplitude was at its minimum value. These findings show that a focal flash luminance greater than or equal to 100 cd/m^2, together with a global flash of not more than 400 cd/m^2 gives rise to a better DC signal. Under constant focal flash luminance, if the global flash is less than or equal to the focal flash luminance (i.e. g/f ratio $\leq$ 1), a reasonable DC signal is obtained.
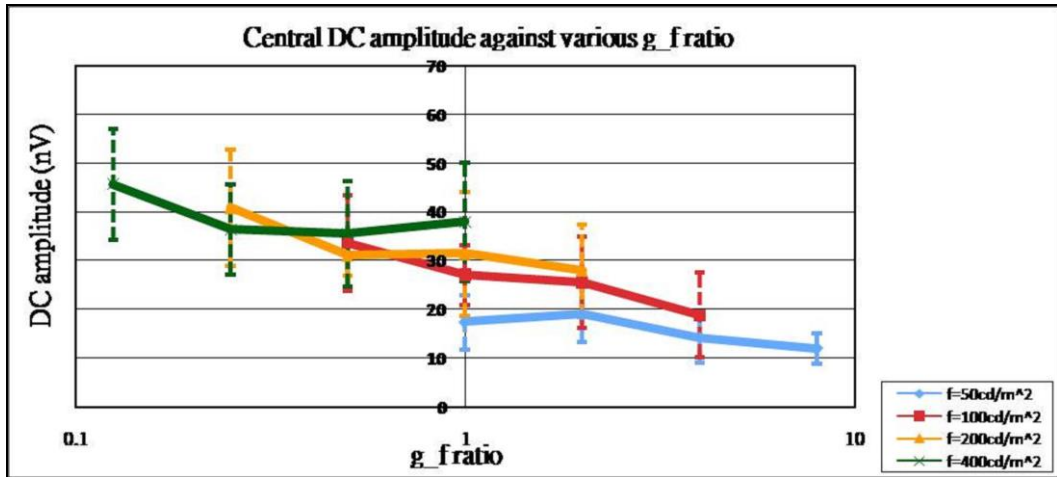
Figure 6.2a. The central DC amplitude at various g/f ratios. Each coloured line represents the DC amplitude under different focal flash intensities. The error bar shows ± 1 standard deviation.
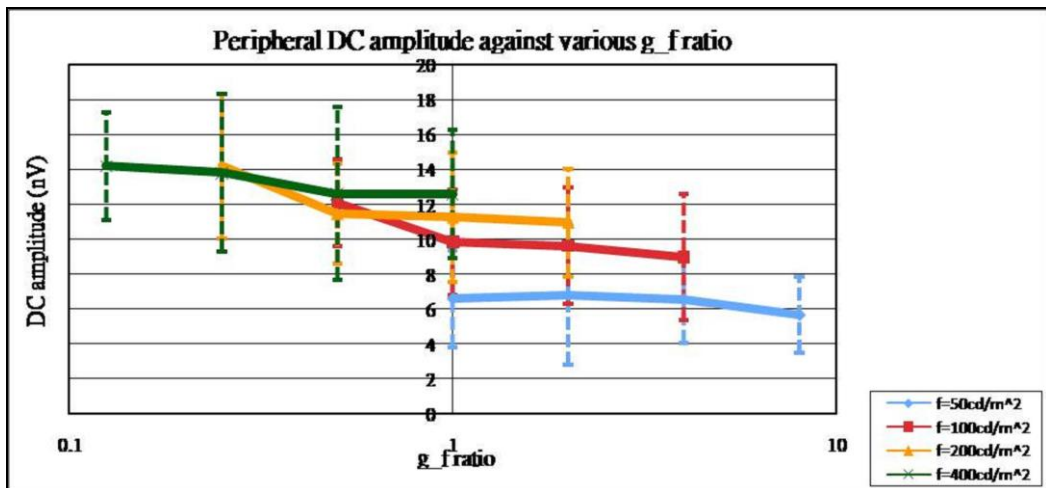
Figure 6.2b. The peripheral DC amplitude at various g/f ratios. Each coloured line represents the DC amplitude under different focal flash intensities. The error bar shows ± 1 standard deviation.

6.1.4.1.2 DC Implicit time

The change in the central DC implicit time as a function of the g/f ratio is shown in Figure 6.3a. When the global flash was dimmer than the focal flash (g/f ratio < 1), the higher the focal flash intensity, the longer was the delay in the DC implicit time, at the same g/f ratio. Initially, the implicit time increased with the g/f ratio. After increasing to a certain level, it would then decrease. It was significantly affected by changes in the focal flash luminance ($p<0.001$). The scattered points of the DC implicit time in the central region converged with the increase in g/f ratio (Figure 6.3a).

The peripheral DC implicit time decreased with an increasing g/f ratio. In other words, a brighter global flash would trigger the DC to occur earlier (Figure 6.3b). It was affected by the intensity of the focal flash ($p<0.001$), global flash ($p<0.001$) and their interaction ($p<0.001$). The peripheral DC implicit time seemed to reach the maximum as the g/f ratio was less than 1. Thereafter, the implicit time decreased.
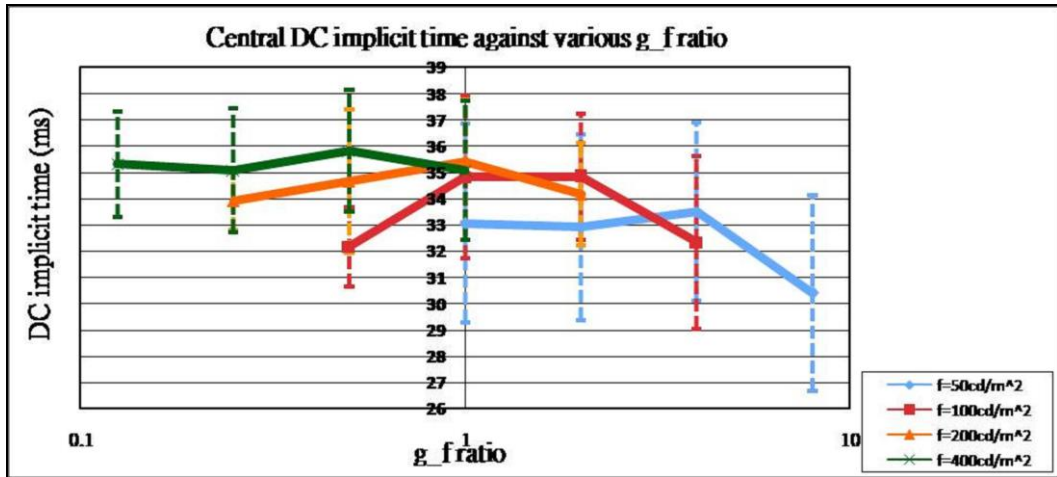
Figure 6.3a. The central DC implicit time at various g/f ratios. Each coloured line represents the DC amplitude under different focal flash intensities. The error bar shows ± 1 standard deviation.
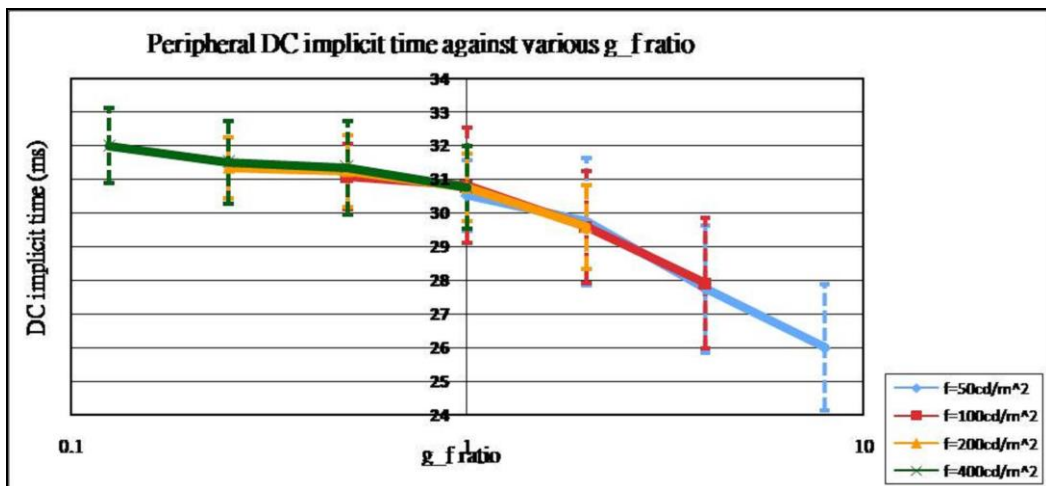
Figure 6.3b. The peripheral DC implicit time at various g/f ratios. Each coloured line represents the DC amplitude under different focal flash intensities. The error bar shows ± 1 standard deviation.

6.1.4.2 Induced components (IC)

6.1.4.2.1 IC Amplitude

In the central retinal region, when the focal flash luminance ranged from 50 to 200 cd/m^2, the IC amplitude increased with the global flash luminance until the g/f ratio reached 2 (i.e. the global flash luminance was twice the focal flash luminance). Thereafter, the IC amplitude began to decrease even with further increase in the global flash intensity (Figure 6.4a). The central IC signal was significantly affected by the luminance of the focal flash ($p<0.005$) and its interaction with the global flash luminance ($p<0.025$) as described below.

The IC amplitude in the peripheral region showed the same characteristic as in the central region. When the focal flash luminance was within the range of 50 to 200 cd/m^2, the IC response increased with the global flash luminance until the g/f ratio was about 2 (Figure 6.4b). Beyond this point, the IC amplitude decreased. The peripheral IC response was significantly affected by the focal flash ($p<0.025$), global flash ($p<0.001$) and their interaction ($p<0.005$).

Post-hoc testing showed that the g/f combinations of 100/50 and 200/100 led to the maximum IC amplitude in the central and peripheral regions respectively, while the combinations of 50/200 and 50/100 led to the minimum IC amplitude in the central and peripheral regions respectively. A focal flash luminance less than or equal to 400 cd/m^2 and a global flash greater than or equal to 100 cd/m^2 gave rise to a better IC response. For a focal flash between 50 and 200 cd/m^2, the global flash luminance should be greater than or equal to the focal flash in order to achieve a reasonable IC signal (i.e. g/f ratio$\geq$1), except for the combination with focal flash of 200 cd/m^2 and global flash of 100 cd/m^2. The IC signal

generated by this combination did not show a significant difference compared with other combinations.
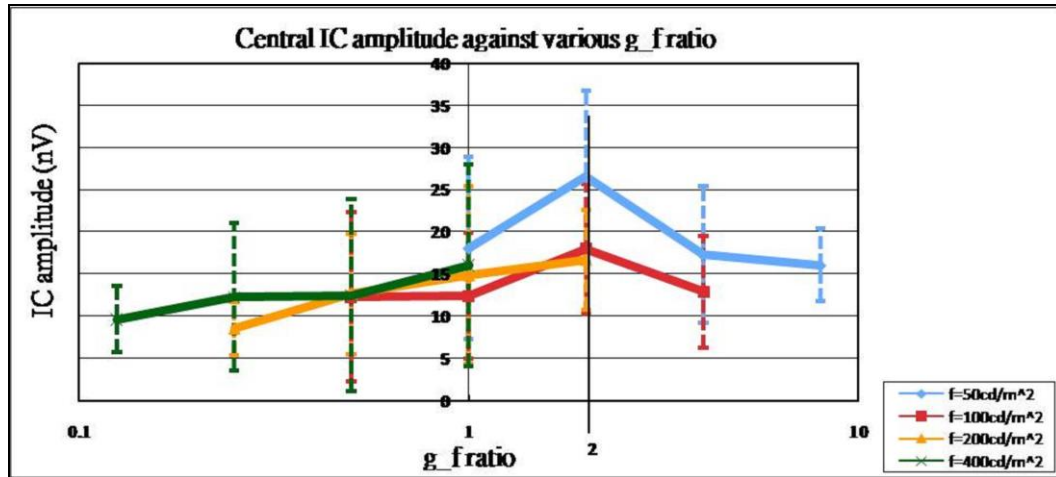
Figure 6.4a. The central IC amplitude at various g/f ratios. Each coloured line represents the DC amplitude under different focal flash intensities. The error bar shows $\pm$ 1 standard deviation.
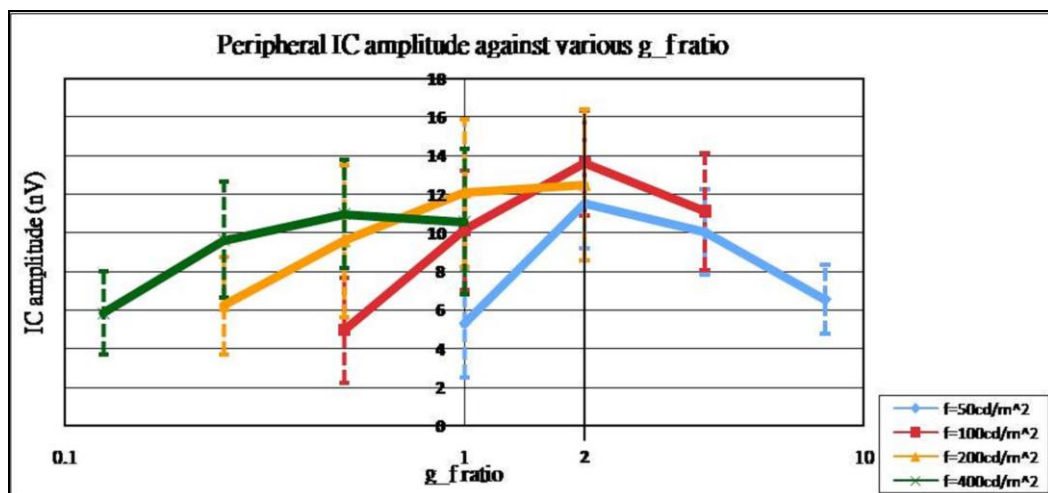
Figure 6.4b. The peripheral IC amplitude at various g/f ratios. Each coloured line represents the DC amplitude under different focal flash intensities. The error bar shows $\pm$ 1 standard deviation.

6.1.4.2.2 IC Implicit time

The IC implicit time in the central retina was significantly affected by the global flash luminance ($p < 0.01$) and it was generally delayed with increased g/f ratio (Figure 6.5a). The changes were variable at different focal flash luminance levels. IC implicit time increased within each set of focal luminance measures, peaking at the third and fourth g/f measure.

However in the peripheral retinal region, the IC implicit time was delayed with an increase in the g/f ratio, that is, the IC implicit time was lengthened with brighter global flash than with the focal flash. IC implicit time increased for g/f rations up to 1 in the periphery. The delay of response then seemed not to increase when the g/f ratio exceeded 1 (Figure 6.5b). It was significantly affected by both the intensities of the focal ($p < 0.001$) and global flashes ($p < 0.01$).
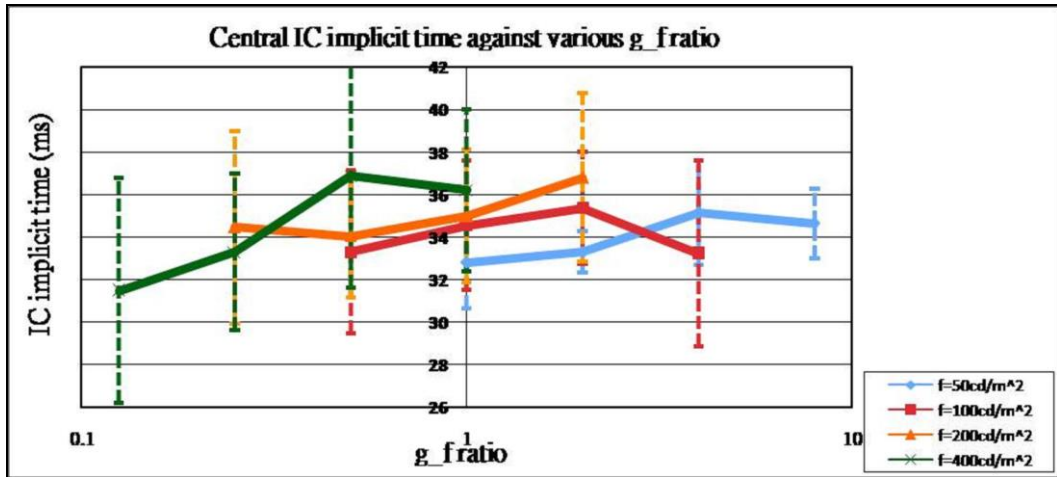
Figure 6.5a. The central IC implicit time at various g/f ratios. Each coloured line represents the DC amplitude under different focal flash intensities. The error bar shows ± 1 standard deviation.
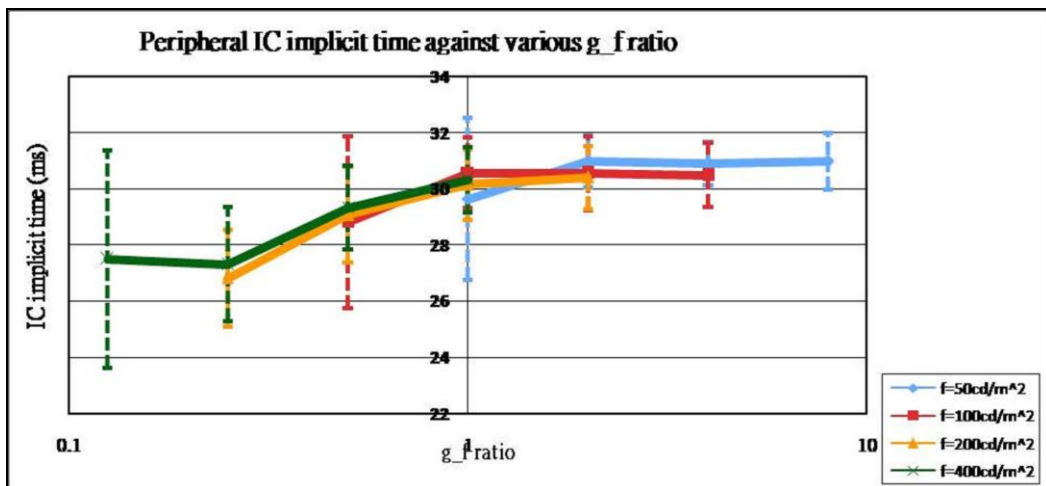
Figure 6.5b. The peripheral IC implicit time at various g/f ratios. Each coloured line represents the DC amplitude under different focal flash intensities. The error bar shows ± 1 standard deviation.

6.1.5 Discussion

6.1.5.1 Changes of MOFO mfERG responses with g/f ratio

In the periodic global flash mfERG measurement, the resultant waveform contains two sharp peaks: the direct component (DC) and the induced component (IC). These findings clearly show that the amplitudes and implicit times of both responses are influenced by the intensity of global and focal flashes as well as by the combination of these two flashes (i.e. g/f ratio). The DC contains the response predominantly from the ON- and OFF-bipolar cells with oscillatory wavelets from the inner retina forming a small component; this is generated from the inner retina, mainly from ganglion cells and amacrine cells (Chu et al. 2008).

The mfERG waveforms and amplitudes change with retinal eccentricity (Sutter & Tran 1992; Sutter & Bearse 1999; Sutter et al. 1999; Chu et al. 2006); therefore, in this study, we divided retinal responses into central (about central 7°) and peripheral regions (about 17.2° to 44.5°) examine the variations of DC and IC responses under conditions with different luminance. A new parameter, the g/f ratio for this MOFO measurement, is introduced to assist in understanding how the interaction of the global and focal flashes influences both DC and IC in terms of amplitude and implicit time.

In a previous study (Shimada et al. 2005), the DC amplitude was found to increase approximately linearly with increasing log units of focal flash intensity. These findings were consistent with those of Shimada and both the central and peripheral DC amplitudes increased with the focal flash intensity. The DC amplitude seemed to achieve its largest value when the g/f ratio was kept at the minimum. Different proportions of global flash intensity and focal flash intensity

produced a larger DC response instead of increasing the focal flash intensity alone. A greater flash intensity could improve the signal-to-noise ratio, but the greater luminance would cause irritation to the subjects during measurements. By applying the g/f ratio, an optimal DC response can be obtained even under a focal flash with dimmer and more comfortable intensity.

The IC is the response change to the global flash from the preceding focal flash and it has been reported to be related to the inner retina (Chu et al. 2008). After the IC amplitude peaked at a g/f ratio of 2:1, the retinal response did not increase further with the increased global flash intensity. This demonstrated the non-linear characteristics of the inner retinal adaptive mechanisms. Shimada et al (Shimada et al. 2005) found a point of inflexion for the individual data when both intensities of focal flash and global flash were equal to 200 cd/m^2. This point was absent in the present study. There are two possible explanations. Firstly, ring 3, regarded as a transition zone, was discarded in the retinal area grouping for analysis in the current study. Secondly, the adaptive mechanisms of the central and peripheral IC may not be similar. Figure 6.1a and 6.1b illustrate the waveforms from the central and peripheral regions. Due to the shift of implicit time, the waveform at the central and peripheral regions showed different patterns. This may be why the waveforms from the present findings differed from the grouped responses shown in their study. The separated analysis of the central and peripheral responses may make the point of inflexion less obvious. This may also explain why the IC property at g/f ratio equal to 2:1 was not obvious in Shimada's study.

Under constant focal flash intensity, a shortened DC implicit time was reported

with increasing global flash intensity (Shimada et al. 2005). Their findings were only similar to the present results when g/f ratio was less than or equal to 1. The performance of the central DC implicit time was opposite to that reported when g/f ratio was greater than 1. The peripheral DC implicit time was initially stable as g/f ratio increased and it decreased when the ratio was greater than 1. This showed that the implicit time of the DC in different retinal regions behaved differently according to the ratio. The IC implicit time in the central region was initially delayed with an increase in the g/f ratio until it reached a saturated level with the ratio more than 1. Its variation was more obvious in the peripheral region. It was also very similar to the findings reported in Shimada's study (Shimada et al. 2005) which showed a shorter IC implicit time when the focal flash intensity was greater than the global flash intensity. When comparing their reported implicit times in both central and peripheral regions, different behaviors under different g/f ratios suggested that the adaptive mechanism had different characteristics across the retina. In terms of the implicit times between DC and IC, the trends of the variations in both DC and IC implicit times were totally different. The DC became less delayed but the IC became more delayed as the g/f ratio increased in value. This clearly demonstrated different physiological characteristics of the DC and IC in response to the combinations of the global and focal flash intensities.

6.1.5.2 Optimal conditions of MOFO mfERG

Considering the stray light problem suggested by the ISCEV guideline (2007) (Hood et al. 2008) and the patients' discomfort, the focal flash luminance, according to the current findings, should be between 100 and 200 cd/m^2. Together with a global flash dimmer than the focal flash, a considerable DC

amplitude with good signal-to-noise ratio can be obtained (i.e. 100 cd/m^2 < f $\leq$ 200 cd/m^2, f $\geq$ g). My recommended focal flash luminance is higher than the range suggested by Shimada et al. (i.e. 50 cd/m^2 < f < 100 cd/m^2) (Shimada et al. 2005).

For a reasonable IC amplitude, it is recommended, that the focal flash should be less than or equal to 200 cd/m^2 and the global flash higher than or equal to 100 cd/m^2. The g/f ratio should be kept at greater than or equal to 1 (i.e. f $\leq$ 200 cd/m^2; g $\geq$ 100 cd/m^2; f $\leq$ g). The focal flash luminance suggested in this study is higher than that of Shimada et al. (Shimada et al. 2005) .

Thus, in order to obtain both optimal DC and IC responses, a g/f ratio of 1:1 and with focal flash luminance greater than 100 cd/m^2 and smaller than 200 cd/m^2 would be recommended.

6.2 Experiment A2- Early local functional changes in human diabetic retina: a global flash mfERG study

Modified from the manuscript published in: Graefes Arch Clin Exp Ophthalmol 2012; 250: 1745-54

6.2.1 Abstract

Purpose: To investigate early functional changes of local retinal defects in type II diabetic patients using the global flash multifocal electroretinogram (MOFO mfERG).

Methods: Thirty-eight diabetic patients and fourteen age-matched controls were recruited. Nine of the diabetics were free from diabetic retinopathy (DR) while the remainder had mild to moderate non-proliferative diabetic retinopathy (NPDR). The MOFO mfERG was performed at high (98%) and low (46%) contrast levels. MfERG responses were grouped into 35 regions for comparison with DR classification at those locations. Z-scores of the regional mfERG responses were compared across different types of DR defects.

Results: The MOFO mfERG waveform indicated a local reduction in DC and IC amplitudes in diabetic patients with and without DR. With increasing severity of retinopathy, there was a further deterioration in amplitude of both components. Under the MOFO mfERG paradigm, DC and IC amplitudes were useful screening parameter as compared to their implicit times.

Conclusion: The MOFO mfERG can help in detecting early functional anomalies before the appearance of visible signs of DR, and may assist in monitoring further functional deterioration in diabetic patients.

6.2.2 Introduction

Diabetic Retinopathy (DR) is the most frequent cause of new cases of blindness in the working population (Porta & Bandello 2002; Fong et al. 2003; Carmichael et al. 2005). In the first two decades after diagnosis of the disease, over half of the patients with Type II DM have retinopathy (Fong et al. 2003; Carmichael et al. 2005). Diabetic patients are usually assessed using ophthalmoscopy and fundus photography (Aldington et al. 1995; Fong et al. 2003). The main focus is to detect visible sign of vascular retinopathy in order to monitor progress of DR and to avoid its sight-threatening complications (Harding et al. 1995; Carmichael et al. 2005), however the basis of functional changes in the retina, especially in the early stages, has not been determined.

The Ganzfeld full-field electroretinogram has been used to study the changes of retinal function in diabetic patients (Yamamoto et al. 1996; Holopigian et al. 1997; Kizawa et al. 2006; Luu et al. 2010). The defects of DR are not distributed uniformly across the retina and show a range of stages of development (Kern & Engerman 1995). The fullfield electroretinogram, which is a summated retinal response measurement, is not likely to reflect local or eccentric functional changes in diabetes. The multifocal electroretinogram (mfERG) provides objective topographical measurements of retinal responses across the visual field (Sutter & Tran 1992). Palmowski et al. (Palmowski et al. 1997) and Shimada et al. (Shimada et al. 2001) examined retinal function in diabetes using the mfERG; however, the mfERG responses were either grouped into rings, quadrants or summed across the retina. Such groupings lose the fine topographic details in studying various types of vascular defect (Fortune et al. 1999; Bearse et al. 2004). Bearse et al. applied the slow flash mfERG in a study of local oscillatory

potentials in the diabetic retina and suggested that retinal adaptation was more likely to be abnormal at sites with early retinopathy (Bearse et al. 2004). Bronson-Castain et al. and Fortune et al. applied the conventional mfERG to the diabetic retina and observed an implicit time delay increasing with the severity of retinopathy. However, local response amplitudes failed to show a consistent relationship with retinal abnormalities in diabetic eyes (Fortune et al. 1999; Bronson-Castain et al. 2009).

Sutter and Bearse used the MOFO mfERG to study retinal adaptive effects. In the global flash mfERG, waveform (Figure 6.6), the direct component (DC) arises predominantly from bipolar and N-methyl-D-aspartic-acid (NMDA)-sensitive cells; the induced component (IC) is predominantly from NMDA-sensitive cells and ganglion cells from the inner retina (Chu et al. 2008). This global flash mfERG allows separate examination of the response from the outer and inner retina. In addition, Hood and co-workers found that nonlinear retinal responses saturate at high contrast levels and they suggested that low contrast stimuli would enhance the inner retinal response (Hood et al. 1999).

The aim of this study was to investigate the early local functional changes in diabetic retina at both high (98%) and low (46%) contrast levels. The use of the periodic global flash multifocal electroretinogram (MOFO mfERG) in diabetic patients assisted in correlating the local functional changes with retinopathy, and in investigating the depth of retinal dysfunction in diabetic patients.

6.2.3 Methods

6.2.3.1 Subject recruitment and inclusion criteria

Thirty-eight type II diabetic patients were examined: nine (aged 49.7 ± 6.4 years) did not have DR while twenty-nine (aged 49.8 ± 6.4 years) had mild to moderate NPDR. Fourteen control subjects (aged 49.4 ± 7.0 years) were also examined. All subjects had visual acuity better than 6/9. Their refractive errors were between +3.00 and -6.00 D, and astigmatism was less than -1.25 D. None had any clinically significant ocular or systemic disorders other than DM or DR. The plasma glucose level of the subjects was measured during the visit using a blood glucose meter (Accu-Chek Compact Plus, F. Hoffmann-La Roche Ltd, Basel, Switzerland), at least two hours after any food intake. Ten healthy controls and thirty-six diabetic patients consented to plasma glucose measurements. The duration of DM was based on patient's own report, and was represented by an ordinal parameter (DM diagnosed less than 5 years, DM diagnosed for 5 to 10 years, DM diagnosed for more than 10 years).

All procedures of the study followed the tenets of the Declaration of Hesinki. This study was approved by the Ethics Committee of The Hong Kong Polytechnic University. Informed consent was obtained from each subject following full explanation of the experimental procedures.

6.2.3.2 Experimental set-up and procedures

6.2.3.2.1 Stimulus conditions

The VERIS Science 5.1 system (Electro-Diagnostic-Imaging, San Mateo, CA, USA) was used for mfERG measurement. The stimulus was shown on a high luminance CRT monitor (FIMI Medical Electrical Equipment, Saronno, Italy).

The stimulus pattern contained 103 scaled hexagons with an angular subtense of 44° vertically and 47° horizontally. The sequence of hexagonal pattern stimulation followed a pseudo-random binary m-sequence (2^{13}-1) with a video frame rate of 75 Hz. In each MOFO stimulation, there were four video frames: a frame with pseudo-random m-sequence focal flash, followed by a full-screen dark frame, a full-screen global flash, and another full-screen dark frame. The duration of one MOFO stimulation sequence was 53.3 ms. The background luminance of the mfERG display was 100 cd/m^2. At the high contrast level (98%), both the luminance of the bright phase of the multifocal stimulus and the global flashes were set at 200 cd/m^2 as suggested in Experiment A1 (Ch. 6.1) (Lung & Chan 2010), in order to obtain optimal DC and IC responses. The dark phase was set at a luminance of 2 cd/m^2. At the low contrast level (46%), the bright phase of the multifocal stimulus was set at 166 cd/m^2, while the dark phase was set at 61 cd/m^2. A central cross on the stimulus pattern was used as a fixation target. One eye was randomly selected for mfERG measurement. The recording was carried out with room illuminance of about 100lux.

6.2.3.2.2 Recording conditions

Detailed eye examination (including subjective refraction, biomicroscopy and indirect ophthalmoscopy) with fundus photodocumentation was carried out for each subject. Slit-lamp biomicroscopic assessment was performed and the crystalline lens was graded according to the Lens Opacities Classification System III (Chylack et al. 1993). Best-corrected VA was measured in order to exclude subjects with clinically significant cataract condition which led to non-age-related visual impairment. Stratus optical coherence tomography (Carl Zeiss Meditec, Inc., Dublin, CA, USA) was used to measure macular thickness in

a fast scanning mode in order to rule out any subjects with macular oedema. In the MOFO mfERG measurement, the pupil of the tested eye was dilated with 1% tropicamide (Alcon, Fort Worth, TX, USA) to at least 7 mm diameter. The untested eye was occluded. A Dawson-Trick-Litzkow (DTL) electrode was placed on the lower bulbar conjunctiva as the active electrode. Gold-cup electrodes were used as reference and ground electrodes, on the temporal side of the tested eye and forehead respectively. The ERG signal was amplified (x100,000) and band-pass filtered (3-300 Hz) (Grass Instrument Co., Quincy, MA, USA). The MOFO mfERG protocol was randomly carried out at high (98%) and low (46%) contrast levels. The mfERG recording time for each contrast level was about 8 minutes and was divided into 32 segments. Each segment lasted approximately 14 seconds, and a short break was provided between segments. The refractive error of the tested eye was corrected for the viewing distance of 33 cm. The recording quality as well as the fixation quality was monitored using the real time display of the VERIS program. Segments contaminated by poor fixation, eye movement or blinks were rejected and re-recorded immediately.

6.2.3.3 Data Analysis

6.2.3.3.1 Analysis of the MOFO mfERG responses

The 103 MOFO mfERG trace arrays were grouped into 35 regions as suggested by Bearse and colleagues. This grouping combines similar waveforms while maintaining their nasal, temporal and eccentricity locations (Figure 6.7) (Bearse et al. 2003; Bearse et al. 2004). For each region, signal amplitudes of the DC and IC were measured. The DC implicit time was measured from the onset of the multifocal stimulus to the peak of DC; the IC implicit time was measured from the onset of the global flash to the peak of IC (Figure 6.6). Left eye MOFO

mfERG signals were transposed so that all eyes were apparently right eyes for the purposes of data analysis.
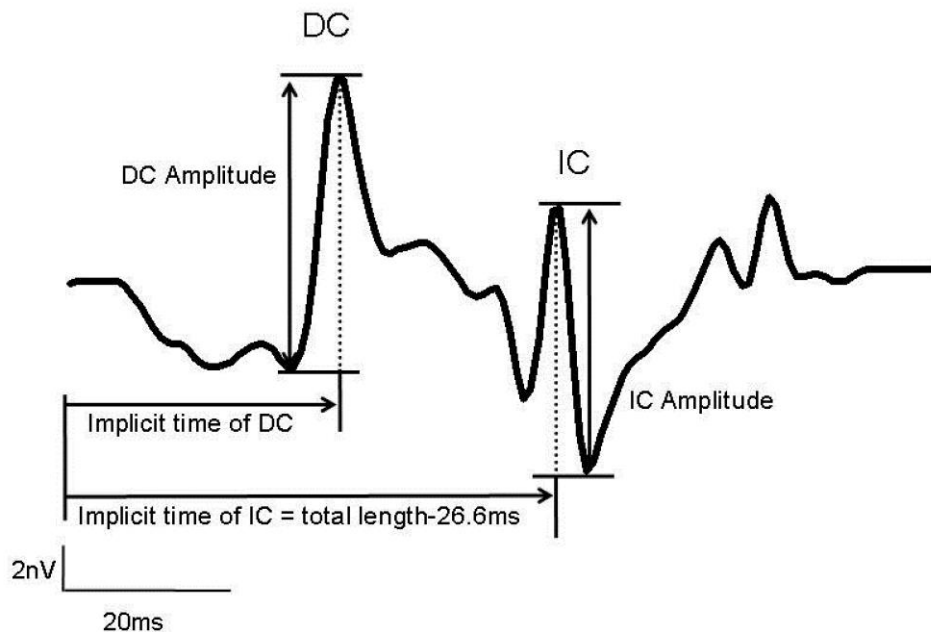
Figure 6.6. Waveform of the MOFO responses contains two main components: the direct component (DC) and the induced component (IC). Note that the implicit time of the DC is measured from the onset of the multifocal stimulus to the response peak of the DC, while the implicit time of the IC is measured from the onset of the global flash 26.6ms to the response peak of the IC.

The MOFO mfERG responses from the 35 regions were grouped according to the fundus photographs grading (see below) for further analysis. To account for the topographic asymmetry of the mfERG and provide the same baseline for comparison, a z-score scale was established for the MOFO mfERG responses (Wu & Sutter 1995; Sutter & Bearse 1999). The MOFO mfERG responses in the control group were used to calculate the means and standard deviations for each specific location across the 35-division of the mfERG topography. The means

and standard deviations obtained above were then used to calculate the z-score of the MOFO mfERG responses for each subject at that specific region (by subtracting the mean from the individual mfERG response and then dividing it by the standard deviation obtained from the control group.

Equation:

Z-score of the MOFO mfERG response =

(Individual response - Mean response of the control group)

Standard deviation

6.2.3.3.2 Relating the plasma glucose level, DM duration and averaged mfERG responses in the control and diabetic subjects

The plasma glucose level was compared between the control and diabetic subjects by independent t-test. The MOFO mfERG responses from the 35-division array were averaged so that each subject gave a mean z-score of the mfERG responses. The correlation between the individual plasma glucose level and DM duration with the averaged mfERG responses of the diabetic subjects was then obtained.

6.2.3.3.3 Mapping between fundus photographs and MOFO mfERG topography

A Topcon IMAGEnet Fundus camera was used to take colour fundus photographs with one central 45° field and eight peripheral surrounding fields. The fundus photographs from various fields were grouped into a single photograph in mosaic format. The 103 hexagonal pattern of the mfERG topography was aligned with the mosaic of fundus photos for each subject. The

blind spot depression and the central peak were aligned with the optic disc and fovea respectively. The 103 hexagons were then grouped into the 35-division pattern as shown in Figure 6.2 (Calculations including the range of corrections used in these experiments and the range of axial lengths expected suggest that the variation in magnification of the retinal image of the stimulus pattern would be small, in the range of 3%).

Figure 6.7. The multifocal stimuli pattern was mapped with the automated mosaic fundus photo (each circle indicates the fundus photo taken at a particular gaze position. There are in total nine gaze positions, one central gaze position and eight peripheral gaze positions, to form a mosaic fundus photo). Both were divided into 35 regions as in previous studies (about two to three hexagons were grouped as one region in the mfERG topography as indicated by the dark polygons). This figure illustrates the regional mfERG waveform of a diabetic

patient with DR lesions at different locations. Those regional mfERG samples with DR (in red lines) are compared with the averaged regional samples from the control group (in blue lines).

6.2.3.3.4 Grouping of data

The regional retinal defects were then graded by a masked retinal specialist according to the following scales based on the severity of retinopathy:

Group 0	Regional samples from control subjects
Group 1	Regional samples from DM patients without retinopathy ("No NPDR" group) (equivalent up to the ETDRS level 10) (Early Treatment Diabetic Retinopathy Study Research Group 1991; Early Treatment Diabetic Retinopathy Study Research Group 1991)
Group 2	Regional samples containing hard exudates ("HE" group) (equivalent up to the ETDRS level 14) (Early Treatment Diabetic Retinopathy Study Research Group 1991; Early Treatment Diabetic Retinopathy Study Research Group 1991) For the regional samples with definite haemorrhage (equivalent up to the ETDRS level 35 and 43) (Early Treatment Diabetic Retinopathy Study Research Group 1991; Early Treatment Diabetic Retinopathy Study Research Group 1991), they were further divided into two types (outer and inner retinal haemorrhage) based on the retinal depth of the haemorrhage
Group 3	Regional samples containing outer retinal haemorrhage – Dot/ Blot haemorrhage, together with or without hard exudates ("Outer retinal haemorrhage +/- HE" group)
Group 4	Regional samples containing inner retinal defect – Flame haemorrhage, together with or without cotton-wool-spots ("Inner +/- Outer retinal haemorrhage +/- CWS +/- HE" group)

(Note that retinal regions with small drusen and the retinal regions lacking

retinopathy signs from the NPDR groups were excluded).

6.2.3.3.5 Statistical analysis

Based on the above grading in the 35 retinal regions, the corresponding regional MOFO mfERG responses were then associated with these grades of different retinal defect for multiple comparisons. It was assumed that the mfERG from those 35 divisions were independent of each other (Fortune et al. 1999). The statistical analysis was performed using SPSS 16.0 (SPSS, Chicago IL). Repeated measures Analysis of Variance with Bonferroni's adjustment was applied to study the group differences (Group 0 to 4). Bonferroni's adjustment was based on the contrast levels (a within-subject factor with 2 levels) and retinal defect groups (a between-subject factor with 5 levels). In case of the existence of interaction between factors, simple effect of the group factor was then reported.

6.2.3.3.6 Evaluation of the diagnostic values of the MOFO mfERG parameters

For each MOFO mfERG parameter (amplitude and implicit time of the DC and IC) at each contrast level, a receiver-operating-characteristic curve was constructed and the area-under-the-curve was calculated (GraphPad Prism 5, CA) to estimate the predictive ability of each parameter in the detection of DR.

6.2.4   Results

6.2.4.1 Correlation of the plasma glucose level and DM duration with the averaged MOFO mfERG parameters

The plasma glucose levels of the diabetic subjects were significantly higher than those of the control subjects (independent t-test, $p < 0.0001$). Among the

thirty-eight diabetic subjects, no significant correlation was found between the averaged MOFO mfERG responses and the DM duration (Spearman's r ranged from -0.09 to 0.1, p-value ranged from 0.57 to 0.94). For the plasma glucose level measured from the thirty-six diabetic subjects, significant correlation was only found with the mean z-score of IC implicit time at low contrast level. The higher the plasma glucose level was, the greater was the delay of the mean IC implicit time at low contrast level (Pearson's r=0.412; p=0.012) (Table 6.1).

Averaged MOFO parameters	Contrast levels	Plasma glucose level (mmol/L) n = 36 persons		DM duration (ordinal parameters) n = 38 persons	
		Pearson's r	p-value	Spearman's r	p-value
DCA_z	46%	-0.136	0.427	0.012	0.943
	98%	-0.054	0.752	-0.081	0.631
ICA_z	46%	0.027	0.876	-0.022	0.897
	98%	0.082	0.636	-0.084	0.617
DCIT_z	46%	0.162	0.345	-0.048	0.776
	98%	0.134	0.435	-0.028	0.868
ICIT_z	46%	0.412	0.012 *	0.058	0.730
	98%	0.293	0.083	0.095	0.569

Table 6.1. Correlation of the plasma glucose level and DM duration with the averaged MOFO mfERG parameters in diabetic subjects (*: p<0.05)

6.2.4.2 Local MOFO mfERG responses in different types of retinopathy defects

A total of 1019 MOFO regional samples was collected. The number of regional samples from each group were: Group 0 – 486 regional samples (47.7%), Group 1 – 302 regional samples (29.6%), Group 2 – 28 regional samples (2.8%), Group 3 – 168 regional samples (16.5%), Group 4 – 35 regional samples (3.4%).

DC and IC amplitude measures, and DC and IC implicit time measures, showed statistically significant effects of contrast levels (Repeated measures ANOVA, p<0.001), groups (p<0.001) and their interaction (p<0.001). The differences

between the subgroups of subjects were further studied by applying One-way ANOVA and Bonferroni's *post-hoc* test.

6.2.4.2.1 Amplitude of DC (DCA_z) between groups

There were significantly smaller DC amplitudes at high and low contrast levels for all diabetic groups than for the control subjects ($p<0.02$) (Figure 6.8). At the low contrast level, the DC amplitude showed a greater decrease in the presence of retinopathy signs. The DCA_z from the regions in Group 4 deteriorated even more compared to the regional samples from Group 1 ($p=0.011$) (Figure 6.8). It should be noted that the diabetic subjects showed considerable variation in response.
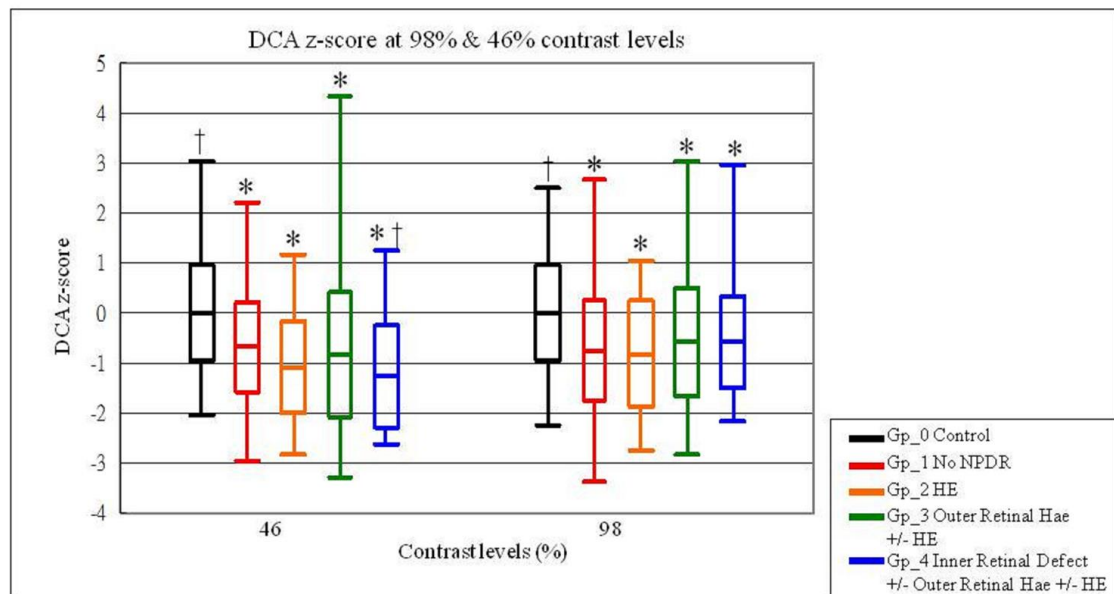
Figure 6.8. Comparison of the DC amplitude z-scores (DCA_z) for groups 0 to 4 at high (98%) and low (46%) contrast levels. *: $p<0.05$ when compared with group 0; †: $p<0.05$ when compared with group 1. Boxplot: central line - the mean; the edges of the box - ± 1 standard deviation; the edges of the vertical bars - range.

6.2.4.2.2 Amplitude of IC (ICA_z) between groups

At the high contrast level (Figure 6.9), all the diabetic groups (Group 1-4) showed a reduction in ICA_z compared to Group 0 (p<0.001). With the presence of visible retinopathy, there was a further reduction in IC amplitude. Among the diabetic groups, the ICA_z of Group 2 was significantly reduced compared to Group 1 (p=0.0034) and Group 3 (p=0.018).

At the low contrast level (Figure 6.9), the trend of the ICA_z was similar to that at the high contrast level. Again, with the existence of visible retinopathy, there was a further reduction in IC amplitude. However, statistical significance was only seen between these two pairs of comparison: Group 0 and Group 2, Group 0 and Group 3 (p<0.02). The ICA_z of Group 3 was also significantly smaller than Group 1 (p<0.00023). The lack of statistically significant findings between the "No NPDR" and control groups here may be attributed to the considerable variation in response.
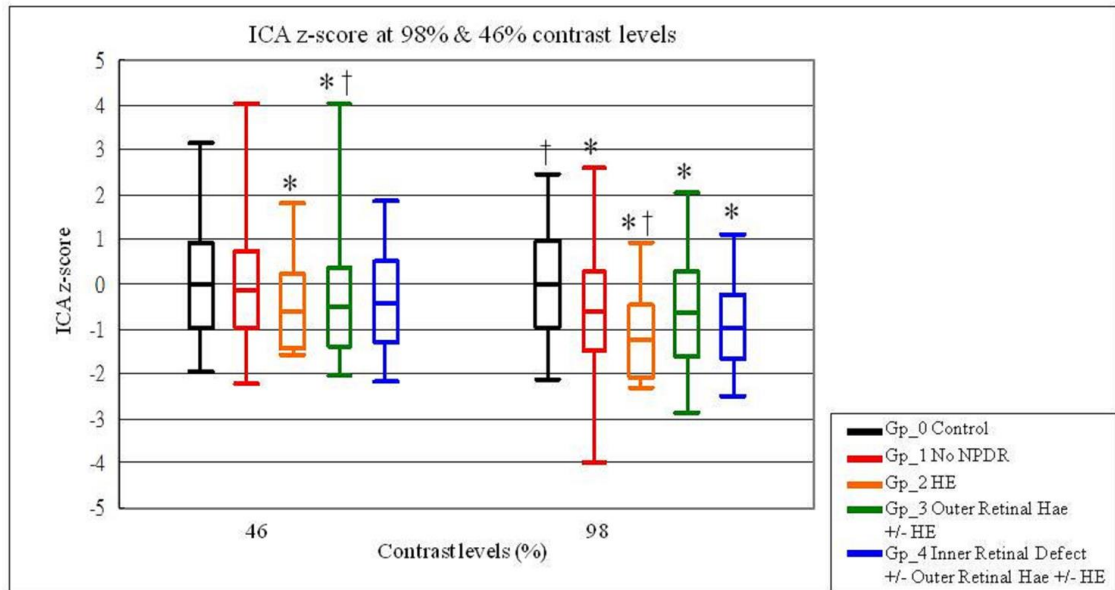
Figure 6.9. Comparison of IC amplitude z-scores (ICA_z) for groups 0 to 4 at high (98%) and low (46%) contrast levels. *: p<0.05 when compared with group 0; †: p<0.05 when compared with group 1. Boxplot: central line - the mean; the edges of the box - ±1 standard deviation; the edges of the vertical bars - range.

6.2.4.2.3 Implicit time of DC (DCIT_z) between groups

For high contrast level stimulation (Figure 6.10), all the locations with retinopathy (Group 2 – 4) showed a significant delay in response compared to Group 0 (p<0.002) and Group 1 (p<0.01). The existence of visible retinopathy led to a greater delay in the DC implicit time than the regions without retinopathy. However, no statistically significant difference was seen for the regional samples at low contrast level. This was largely due to the increased variability of the responses in the DR groups, with a few patients showing very much faster responses, especially to the low contrast stimuli (Figure 6.10).
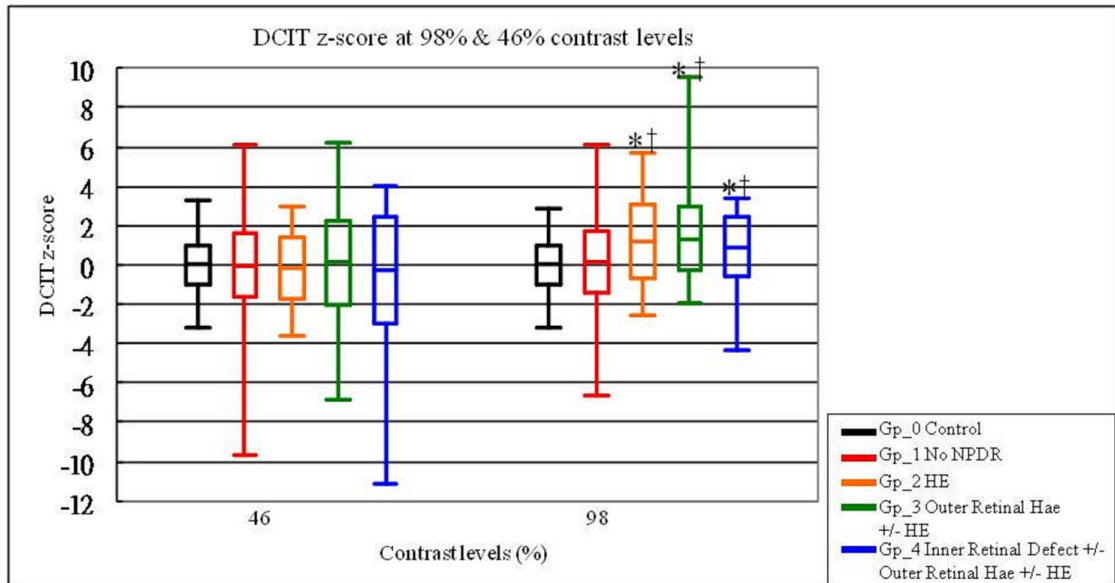
Figure 6.10. Comparison of DC implicit time z-scores (DCIT_z) for groups 0 to 4 at high (98%) and low (46%) contrast levels. *: $p<0.05$ when compared with group 0; †: $p<0.05$ when compared with group 1. Boxplot: central line - the mean; the edges of the box - ±1 standard deviation; the edges of the vertical bars - range.

6.2.4.2.4 Implicit time of IC (ICIT_z) between groups

At the high contrast level (Figure 6.11), the mfERG responses from the diabetic groups were, on average, slower than those from Group 0. With visible retinopathy (Group 2-4), the delay was larger than those without DR (Group 1). Group 2 and Group 3 showed a significant delay compared to Group 0 in the IC implicit time ($p<0.02$). The IC implicit time of Group 3 also had a significant delay in response compared to Group 1 ($p=0.0022$).

At the low contrast level (Figure 6.11), only Group 1 showed a significant delay in IC implicit time compared to Group 0 ($p=0.0013$).

75
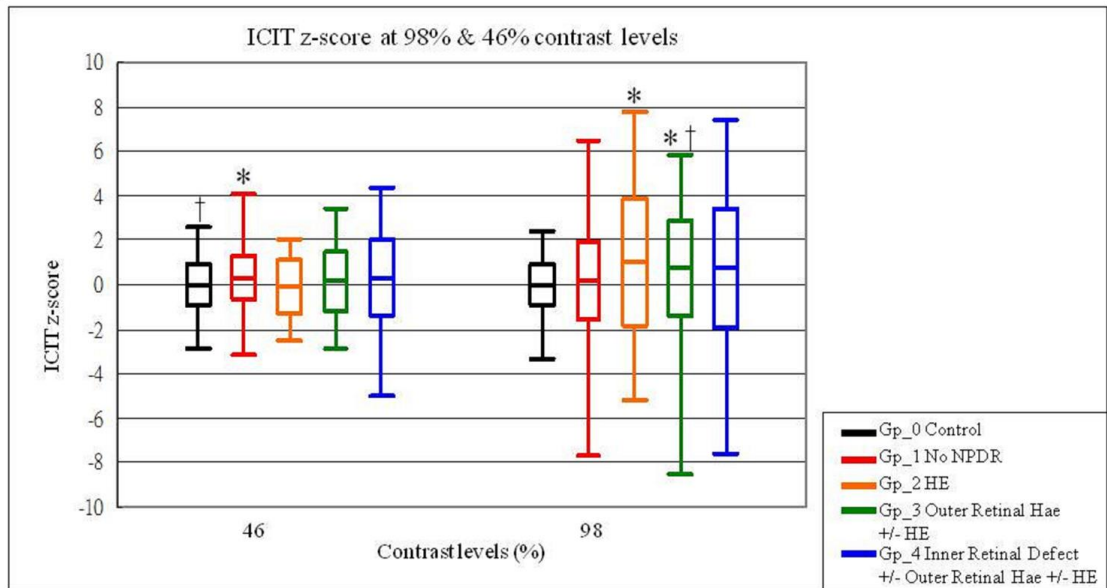
Figure 6.11. Comparison of IC implicit time z-scores (ICIT_z) for groups 0 to 4 at high (98%) and low (46%) contrast levels. *: p<0.05 when compared with group 0; †: p<0.05 when compared with group 1. Boxplot: central line - the mean; the edges of the box - ±1 standard deviation; the edges of the vertical bars - range.

6.2.4.2.5 Diagnostic value of the MOFO mfERG parameters

In order to determine the diagnostic value of the MOFO mfERG parameters, receiver operating characteristics (ROC) curves were plotted and the area-under-the-curve (AUC) was calculated; these values are summarized in Table 6.2. When differentiating the retinopathy groups (Group 2-4) from Group 0, DCIT_z at 98% contrast level resulted in the highest AUC (76.6%). However, the AUC value of DCIT_z declined to 62.6% if it was used to differentiate the diabetic groups (Group 1-4) from Group 0 (Table 6.2).

DCA_z at low and high contrast levels and the ICA_z at high contrast level showed the highest potential for screening out functional defects due to diabetes

(including those without visible vascular defects) having AUC values ranging from 69.1 to 70.9% (Table 6.2).

MOFO parameters	Contrast levels	AUC for screening out the regional sample with visible DR signs (Group 2 - 4)	AUC for screening out the regional sample from DM group (Group 1 - 4)
DCA_z	46%	74.47%	70.89%
	98%	67.14%	69.28%
ICA_z	46%	65.90%	58.20%
	98%	71.73%	69.10%
DCIT_z	46%	56.45%	53.63%
	98%	76.59%	62.58%
ICIT_z	46%	53.30%	56.67%
	98%	68.39%	61.31%

Table 6.2. Summary of the area-under-the-curve (AUC) for each MOFO parameter used in screening the regional samples with visible DR signs and screening the regional samples from DM groups (those with and without DR signs)

(Light-grey shaded cell: MOFO parameter with the highest screening power of the retinal samples with DR signs)

(Dark-grey shaded cells: MOFO parameters with the relatively high screening power of the retinal samples from the DM patients with and without DR signs)

6.2.5 Discussion

This study illustrated the variations of MOFO mfERG responses under high (98%) and low (46%) contrast levels in the diabetic retina. By inserting a periodic global flash between two successive multifocal stimuli, retinal adaptation activity should be enhanced (Sutter et al. 1999). In MOFO mfERG assessment, there are two main components: the direct component (DC) and the induced component (IC). The DC response is the average response to the focal stimulation, while the IC response shows the effect of the preceding focal stimulation on the response to the global flash (Shimada et al. 2001).

In this study, using the high contrast MOFO paradigm, the delay and reduction of the mfERG responses suggests that both middle and inner retinal layers (i.e. DC and IC responses respectively) were impaired even in diabetic patients without signs of retinopathy. Greater delay of response (on average) and reduction of response amplitude in the mfERG were seen when retinopathy signs were present. This implies that certain local functional deterioration started before the visible signs of vascular retinopathy could be detected in the clinical screening assessment.

Previous studies have reported reduced responses in DR in the pattern ERG (Parisi & Uccioli 2001), the second order kernel responses of mfERG (Palmowski et al. 1997), the oscillatory potentials (OPs) and photopic negative responses (PhNR) of the standard full-field ERG (Simonsen 1980; Brinchmann-Hansen et al. 1992; Vadala et al. 2002; Chen et al. 2008) and mfERG (Kurtenbach et al. 2000; Onozu & Yamamoto 2003; Bearse et al. 2004; Shinoda et al. 2007). All these previous studies proposed that inner retinal

function(s) were affected in the diabetic retina. In experiments on pigs in which pharmacological dissection techniques have been used, the IC has been found to arise from third order neurons and ganglion cells (Chu et al. 2008). The reduction of IC response here further supports the localized nature of functional changes in the inner retina of the diabetic patients. However, Shimada et al. (Shimada et al. 2001) did not report similar findings, perhaps because of differences in the subject selection. In their study, data from both type I and II diabetic patients were merged for analysis, while only type II diabetic patients were recruited in the current study.

The DC in MOFO mfERG has been found to be predominantly from the bipolar cells with partial contribution from third order neurons (Chu et al. 2008). Its amplitude reduction among diabetic patients before observable vascular lesions in this study suggests that the middle retinal layers may deteriorate early in DR. Shimada et al. (Shimada et al. 2001) reported similar findings for the high contrast mfERG. Considering that the minimum oxygen supply occurs in the region of the inner nuclear layer (INL) (Alder et al. 1983), the present results support the hypothesis that the middle retina is at risk of hypoxic damage in diabetic patients.

6.2.5.1 MOFO mfERG amplitude

The reductions in the DC and IC responses provide crucial evidence that the middle and inner retina are actually impaired at an early stage in diabetic patients. Recent studies have reported that hypoxia can affect the photoreceptors and the INL (Alder et al. 1983; Linsenmeier 1986; Linsenmeier et al. 1998; Wangsa-Wirawan & Linsenmeier 2003; Arden et al. 2010) while excito-toxicity

also plays a role in affecting the neurotransmission among amacrine and glial cells in the diabetic retina (Barber et al. 1998; Kaneko et al. 2000; Barber 2003). It seems that multiple retinal layers are affected in diabetes at the early stage (Greenstein et al. 1989). In the present study, low contrast MOFO mfERG stimulation was applied to avoid saturation of the non-linear retinal response. Hood and co-workers (Hood et al. 1999) reported that mfERG stimulation at a contrast level of 50% evokes a waveform with more involvement of the inner human retina (Bearse & Sutter 1999; Sutter et al. 1999). The low contrast mfERG stimulus has been used to investigate inner retinal activity in glaucoma (Chu et al. 2006; Chan et al. 2011). In this study, diabetic patients demonstrated reduced DC and IC amplitudes in both high and low contrast conditions. However, reducing contrast of the stimulus does not appear to improve discrimination between the control and diabetic patients and additional delay of implicit time for low contrast stimuli was not obvious; this might be due to a large inter-subject variability or, more likely, the problems in the inner retina induced by DR are different from those induced by glaucoma. Since amplitude and implicit time responses at different contrast levels appear to be different in diabetes and glaucoma (Chu et al. 2006; Chan et al. 2011), the basis of these two diseases is believed to be different (e.g. cell loss or cellular dysfunction). This finding further supports the hypothesis by Greenstein and co-workers (Greenstein et al. 1989) that the mechanism of the retinal dysfunction at the early stage of DM is unlike that of glaucoma.

6.2.5.2 MOFO mfERG implicit time

Previous mfERG studies reported that the implicit time was a more "sensitive" parameter in detecting functional anomalies than response amplitude in DM

patients (Fortune et al. 1999; Kurtenbach et al. 2000; Bearse et al. 2004; Schneck et al. 2004; Harrison et al. 2011). In the current study, the implicit time of DC was only maximally sensitive on screening retinal locations with retinopathy signs with delayed response in average. However, some very fast responses were obtained from the diabetic patients especially for the low contrast condition. This could not be fully explained by the range of plasma glucose levels among subjects as there was no significant correlation with the DCIT. Moreover, Klemp and co-workers (Klemp et al. 2004) found the short-term hyperglycemia leads to a shorter implicit time in the first and second order mfERG responses, presumably because of increased retinal metabolism. This seems to contradict to the positive correlation here between of the plasma glucose level and the ICIT_z at low contrast level. The discrepancy may be due to the effect of chronic instead of short-term hyperglycemia in these diabetic subjects. Studies on the effect of the stability of the plasma glucose level (e.g. glycated hemoglobin) in type II diabetic patients should also be considered.

6.2.5.3 Difference between current and previous studies

Based on the current findings, to screen out functional abnormalities at a very early stage in the diabetic patients without retinopathy, the amplitudes of IC from high contrast stimuli, and DC at both high and low contrast levels were preferred. Compared with the longitudinal study by Harrison and co-authors (Harrison et al. 2011) which showed the implicit time as a more sensitive parameter than amplitude, a number of possibilities may account for any differences: 1) The MOFO paradigm dissociates the original mfERG retinal responses into two different components. The MOFO mfERG with the insertion of a global flash is used to enhance the retinal adaptation mechanism. By splitting the retinal

81

components, subtle changes in the waveform amplitude may thus become more obvious; 2) Modifying the electrophysiological protocols may favor the activities of different types of retinal cells (Kaneko et al. 2000; Masland 2001; Lung & Chan 2010). The mfERG protocol used in Harrison et al.'s study (Harrison et al. 2011) was the standard mfERG. Without the dissociation of the inner retinal responses by the global flash, the standard mfERG responses would not separate the middle and inner retinal responses, and thus subtle changes of the resultant waveform may be masked. And additionally the bandpass filter applied in Harrison et al's study was 10-100 Hz which screened out some high-frequency oscillatory potentials contributed from the retinal ganglion cells and third order neurons (Zhou et al. 2007); in this study, filtering from 3-300 Hz was applied to cover the range of both high- and low-frequency retinal responses to study the middle and inner retinal layer performance. The involvement of the high-frequency component may thus lead to the difference; 3) In the present study, only type II diabetic patients were recruited while both type I and II diabetic patients were recruited by Harrison et al. Differences in the subject pools may contribute to this discrepancy because the underlying mechanism, medical treatment and prevalence of DR progression of type I and type II DM show different patterns (Barber et al. 1998; Fong et al. 2003; LeRoith et al. 2004).

The MOFO mfERG paradigm provides more detailed information in terms of the retinal adaptive changes or the retinal recovery rate than does the conventional paradigm. However, as this study was limited by its cross-sectional nature, a longitudinal follow-up study should be performed to determine the prediction ability of the MOFO mfERG for DR onset. It is surprising that the duration of DM does not correlate with the individual mean MOFO responses, but this may

be due to the variability of the latent period before DM can be diagnosed.

The multifocal electroretinogram, together with the MOFO paradigm, provides a means of detecting early functional anomalies in the diabetic retina before visible vascular defects appear. Comparing with the other standard electrophysiological assessments (full-field ERG, pattern ERG and Visual Evoked Potential), the MOFO mfERG not only provides assessment of retinal adaptation but also provides topographic details. It aids in differentiating the early functional deterioration(s) of the middle and inner retina in the diabetic retina. This result suggests potential retinal sites (middle and inner retina) for future pharmaceutical therapies. The MOFO mfERG is helpful in monitoring disease progression before sight-threatening retinopathy supervenes. Moreover it may be useful in evaluating the effectiveness of the potential therapies, so as to restore retinal function or delay the deterioration of the retina (Simo & Hernandez 2009).

Chapter 7: The correlations of the MOFO mfERG with traditional functional and morphological clinical assessments

7.1 Experiment B- MOFO mfERG: Early detection of local functional changes and its correlations with optical coherence tomography (OCT) and visual field (VF) tests in diabetic patients

7.1.1 Abstract

Purpose: To investigate the correlations of the global flash multifocal electroretinogram (MOFO mfERG) with common clinical visual assessments − Humphrey perimetry and Stratus circumpapillary retinal nerve fiber layer (RNFL) thickness measurement in type II diabetic patients.

Methods: Forty-two diabetic patients participated in the study: ten were free from diabetic retinopathy (DR) while the remainder suffered from mild to moderate non-proliferative diabetic retinopathy (NPDR). Fourteen age-matched controls were recruited for comparison. MOFO mfERG measurements were made under high and low contrast conditions. Humphrey central 30-2 perimetry and Stratus OCT circumpapillary RNFL thickness measurements were also performed. Correlations between local values of implicit time and amplitude of the mfERG components (direct component (DC) and induced component (IC)), and perimetric sensitivity and RNFL thickness were evaluated by mapping the localized responses for the three subject groups.

Results: MOFO mfERG was superior to perimetry and RNFL assessments in showing differences between the diabetic groups (with and without DR) and the

controls. All the MOFO mfERG amplitudes (except IC amplitude at high contrast) correlated better with perimetry findings (Pearson's r ranged from 0.23 to 0.36, $p<0.01$) than did the mfERG implicit time at both high and low contrasts across all subject groups. No consistent correlation was found between the mfERG and RNFL assessments for any group or contrast conditions.

Conclusion: The responses of the local MOFO mfERG correlated with local perimetric sensitivity but not with RNFL thickness. Early functional changes in the diabetic retina seem to occur before morphological changes in the RNFL.

7.1.2 Introduction

Diabetes mellitus (DM) is a group of systemic disorders resulting in hyperglycemia. Vascular anomalies are common complications of DM. The earliest visible sign of vascular anomalies in the eyes are microaneurysms, which lead to the diagnosis of diabetic retinopathy (DR) (Van Bijsterveld 2000).

In a rat model, Barber and co-workers demonstrated that neural apoptosis occurs shortly after DM is induced (Barber et al. 1998; Barber 2003; Kern & Barber 2008; Barber et al. 2011). Neural apoptosis was proposed to cause functional and anatomical changes of the inner retina even before the existence of visible vascular lesions. With the development of new diagnostic instruments, changes in the retinal nerve fiber layer (RNFL) thickness have been evaluated in diabetic patients. Optical coherence tomography (OCT) is an optical diagnostic instrument which provides an objective and non-invasive measurement of cross-sectional retinal thickness. Thinning of the neuronal layer has been reported in the human diabetic retina (Lopes de Faria et al. 2002; Ozdek et al. 2002; Parravano et al. 2008; Takahashi & Chihara 2008; Oshitari et al. 2009). Visual function, assessed by automated perimetry, which provides a subjective measurement of luminance increment sensitivity at different visual field locations, has also been shown to be disturbed before visible DR lesions occur (Bresnick et al. 1985; Ismail & Whitaker 1998; Kurtenbach et al. 2002; Bengtsson et al. 2005; Parravano et al. 2008). These two common clinical assessments have been reported to be useful in detecting early changes in diabetic retina (Lopes de Faria et al. 2002; Ozdek et al. 2002; Bengtsson et al. 2005; Bengtsson et al. 2008; Parravano et al. 2008; Takahashi & Chihara 2008; Oshitari et al. 2009).

In Experiment A2 (Ch. 6.2) above, the MOFO mfERG was shown to be helpful in separating the "middle" and "inner" retinal responses. It has been found that both the middle and inner retinal functions deteriorate before vascular lesions are visible in DM patients.

In the present study, the aim was to compare electrophysiological assessment with automated perimetry and with OCT RNFL thickness measurements in the diabetic retina; this would enrich our knowledge of their relationships at the early stages of DM and further our understanding of the relationships between tests at various levels of DR severity.

7.1.3 Methods

7.1.3.1 Subjects inclusion and recruitment

Forty-two patients with type II DM were recruited for the study: ten (aged 51.0 ± 6.9 years) were free from DR while thirty-two (aged 49.5 ± 5.8 years) had non-proliferative diabetic retinopathy (NPDR). Fourteen healthy controls (aged 49.4 ± 7.0 years) were recruited for comparison. All subjects had visual acuity better than 6/9. Their refractive errors were between +3.00 D and -6.00 D and astigmatism was less than -1.25 D. Subjects with systemic or ocular diseases other than DM or DR were excluded. Detailed eye examination (including subjective refraction, biomicroscopy and indirect ophthalmoscopy) with fundus photodocumentation was carried out for each subject. Slit-lamp biomicroscopic assessment was performed and the crystalline lens was graded according to the Lens Opacities Classification System III (Chylack et al. 1993). Best-corrected VA was measured in order to exclude subjects with clinically significant cataract condition which led to non-age-related visual impairment. One eye was

randomly selected for this study.

Instantaneous plasma glucose data were obtained from ten controls and forty diabetic patients using a plasma-glucose meter before the mfERG measurement (Accu-Chek Compact Plus, F. Hoffmann-La Roche Ltd, Basel, Switzerland); testing was conducted more than 2 hours after any food intake.

All procedures of the study followed the tenets of the Declaration of Hesinki. This study was approved by the Ethics Committee of The Hong Kong Polytechnic University. Informed consent was obtained from each subject following full explanation of the experimental procedures.

7.1.3.2 Experimental set-up and procedures
7.1.3.2.1 mfERG stimulation and recording

A VERIS Science 5.1 system (Electro-Diagnostic-Imaging, Redwood City, CA, USA) was used for the MOFO mfERG measurement. The instrumental set-up was similar to that described in our previous studies (Experiments A1 and A2 in Ch. 6) (Lung & Chan 2010; Lung et al. 2012). Briefly, the mfERG stimulation was a 103 scaled hexagonal pattern (stretch factor: 10.46) which subtended 47° horizontally and 44° vertically. It was displayed on a high luminance CRT monitor (FIMI Medical Electrical Equipment, MD0709BRM, Saronno, Italy) with a frame rate of 75 Hz. A cycle of the MOFO mfERG stimulation included four video frames: a multifocal flash frame, a dark frame, a global flash frame and a further dark frame. The multifocal frame was modulated between bright and dark phases according to a binary pseudo-random m-sequence (2^{13}-1). Each subject had the mfERG measurement made at both high contrast (98% contrast;

bright phase: 200 cd/m^2; dark phase: 2 cd/m^2) and low contrast (46% contrast; bright phase: 166 cd/m^2; dark phase: 61 cd/m^2) in a random order with the background luminance set at 100 cd/m^2. The measurement for each contrast level was divided into 32 segments and lasted for about 8 minutes. Short breaks were provided between segments. Any segment with blinks or eye movements was discarded and re-recorded immediately.

One eye of each subject, with the pupil dilated using 1% tropicamide (Alcon, Fort Worth, TX, USA), was randomly selected for mfERG measurement. A Dawson-Trick-Litzkow (DTL) electrode was used as the active electrode. A gold-cup reference electrode was placed 10 mm lateral to the outer canthus of the tested eye, and a similar ground electrode was placed on the central forehead. The signal was amplified 100,000 times with bandpass from 3 to 300 Hz (Grass Instrument Co., Quincy, MA, USA). The amplitudes and implicit times of the DC and IC for both contrast conditions (Figure 7.1) were measured as previously described in Experiments A1 and A2 in Ch. 6.

7.1.3.2.2 Optical coherence tomography (OCT)

The circumpapillary retinal nerve fiber layer (RNFL) thickness was measured using the Stratus OCT (Carl Zeiss Meditec, Inc., Dublin, CA, USA) set to the fast scanning mode. The scanning area was circular with a 3.4 mm diameter. The circle centre was aligned with the centre of the optic nerve head. The RNFL thickness within the circular region was further divided into 12 sectors and the sectoral RNFL thickness values were then used for analysis (see below).

7.1.3.2.3 Visual field (VF)

The Humphrey Field Analyzer (Carl Zeiss Meditec, Inc., Dublin, CA, USA) was used to measure monocular visual field in this study. The white-on-white static protocol "Central 30-2 (SITA-fast)" was chosen to assess the central 60 degree field; full-aperture lenses were placed in front of the patient's tested eye to correct refractive errors for the viewing distance of the VF analyzer. The locations of the VF test spots were plotted on a grid; the grid was then overlaid with the mfERG topography which was divided into 35 regions for further analysis as in Experiment A2 in Ch. 6.2 (Lung et al. 2012) and previous studies (Bearse et al. 2003; Bearse et al. 2004; Han et al. 2004). The overlay is shown as in Figure 7.2. Details of the grid scaling and alignment are discussed below.

7.1.3.2.4 Fundus photodocumentation

A Topcon IMAGEnet fundus camera was used to take fundus photographs of the tested eye centrally and at eight peripheral locations for each subject. The photographs were then combined to form a mosaic for each subject.

7.1.3.3 Data analysis

7.1.3.3.1 MOFO mfERG parameters

The 103 mfERG trace arrays were divided into 35 regions as suggested by Bearse and co-workers (Bearse et al. 2003; Bearse et al. 2004). The mfERG from left eyes was reflected so that all data resembled those from right eyes. The amplitudes and implicit times of the local MOFO mfERG responses (i.e. DC and IC) were collected for analysis (Figure 7.1). For each region, data of mfERG parameters from the control group were used to calculate the means and standard deviations (SD) which were then used to calculate z-scores of the mfERG

parameters. Using z-scores for further analysis as in Experiment A2 in Ch. 6.2 helps in eliminating topographic asymmetry of the mfERG and provides the same basis for comparison (Wu & Sutter 1995; Sutter & Bearse 1999; Bearse et al. 2003; Bearse et al. 2004; Lung et al. 2012). Each subject had 35 regional z-scores (calculated based on the regional means and SD of the control group) across the subject's mfERG topography. An averaged z-score could thus be obtained across the 35 regions for individual subjects.
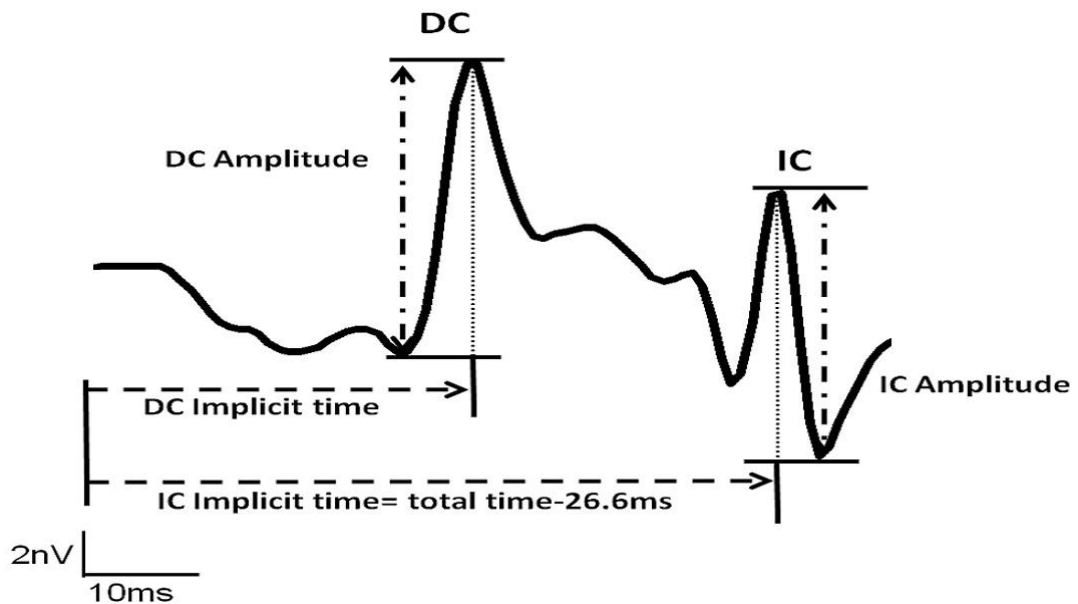
Figure 7.1. MOFO mfERG resultant waveform. The measurement of amplitudes and implicit times of DC and IC are also shown.

7.1.3.3.2 Visual field (VF) sensitivity

In the Humphrey visual field analyzer, two parameters could be obtained directly from the results: mean deviation (MD) and local total deviation (TD). MD is the numerical value of averaged VF sensitivity difference from the age-norm provided by the manufacturer of Humphrey analyzer. TD is the numerical value which indicates the difference from the age-norm at each tested location on the

field. In this experiment, the VF from left eyes was reflected and all data resembled those from right eyes. The MD and local TD were used for analysis in order to provide the same basis for comparison among different subject groups (Heijl & Patella 2002; Dersu & Wiggins 2006). The MD was also correlated with the plasma glucose level to evaluate the relationship between and among the three subject groups. The TD of each VF test spot which fell in the mfERG topography was associated with the mfERG responses in order to evaluate its correlation with the electrophysiological assessment.

7.1.3.3.3 RNFL thickness

The mean RNFL thickness and the RNFL thickness values obtained in each of the 12 sectors measured by the OCT within the circular scanning region were used for analysis. The averaged RNFL thickness of each subject was correlated with the plasma glucose level and compared among the three subject groups. To eliminate topographic asymmetry, the sectoral RNFL thicknesses of the control group were used to calculate the sectoral z-scores for individual subject as suggested by Bronson-Castain and co-workers (Bronson-Castain et al. 2009). The RNFL data from left eyes was reflected and resembled those from right eyes. For each sector of RNFL thickness, the values from the control group were initially averaged and this value was used to calculate the sectoral z-score of each subject using the equation:

Sectoral z-score of RNFL thickness =

$$\frac{\text{(Individual sectoral thickness} - \text{Averaged sectoral thickness from controls)}}{\text{Averaged sectoral thickness from controls}}$$

This provides the same basis for comparison among the three groups of regional data after mapping between mfERG topography and RNFL profile.

7.1.3.3.4 Duration of DM, plasma glucose level and averaged findings of the three ocular assessments (mfERG, RNFL thickness and VF sensitivity)

Duration of DM among the diabetic patients was ranked into three categories: less than 5 years, duration from 5 to 10 years, duration more than 10 years. The median of the duration ranking is reported for the diabetic groups in the results below.

Plasma glucose level and the results of the three ocular assessments were compared among the control subjects, the DM patients without DR and the DM patients with NPDR using one-way ANOVA; significance levels were adjusted using Bonferroni's correction. Pearson's correlation (r) was evaluated between the plasma glucose level and the averaged mfERG responses, mean RNFL thickness and VF MD among the three subject groups.

7.1.3.4 Correlations of the local retinal responses among three ocular assessments by mapping

Fundus photographs, mfERG data and VF data were all provided at different scales. They were converted to a common scale by measuring the distance from fovea/ fixation point to disc centre/blindspot depression. This was used as a baseline to adjust the scale of the two-dimensional data.

7.1.3.4.1 Overlay of fundus photographs with MOFO mfERG topography

As mentioned above, a mosaic photograph was formed for each individual. By overlapping the fovea and optic disc of the photographs with the central peak and blindspot depression of the mfERG topography respectively, the mosaic photographs were aligned with the 103-hexagonal mfERG topography. Fundus

photographs were then divided into 35 regions following the mfERG topography in Figure 7.2 (Bearse et al. 2003; Bearse et al. 2004). A retinal specialist who was masked to each patient's diagnosis then rated each region for presence or absence of a DR lesion.

This was done for the three groups of subjects, thus allowing creation of three groups of regional data:

Group I – Regional data from the control group only

Group II – Regional data from the DM patients (without any DR signs) only

Group III – Regional data from the DM patients with NPDR only, but only those with DR lesions were included. Those regions without DR lesions were discarded to avoid confusion with group II

7.1.3.4.2 Overlay of VF and MOFO mfERG topography

The 103 hexagonal stimulus pattern of mfERG was aligned with the VF test grid. The locations of the blindspot and the fixation point (i.e. foveal peak) in mfERG topography were overlaid with the blindspot and fixation point of the VF test grid, respectively. By overlaying the VF test grid with the 35-division mfERG topography as shown in Figure 7.2, the mfERG parameters measured at each division could be grouped with the TD of the VF test spot that fell within the division. If more than one VF test spot fell within the same mfERG division, the TD of those VF test spots were averaged before matching with the mfERG parameters. As the Humphrey central 30-2 program (central 60°) provides a larger field of view than that of mfERG (about central 47°), those VF test spots which fell outside the mfERG topography were excluded from the study. Once groupings of mfERG parameters and VF TD values were accomplished,

correlation values were calculated.
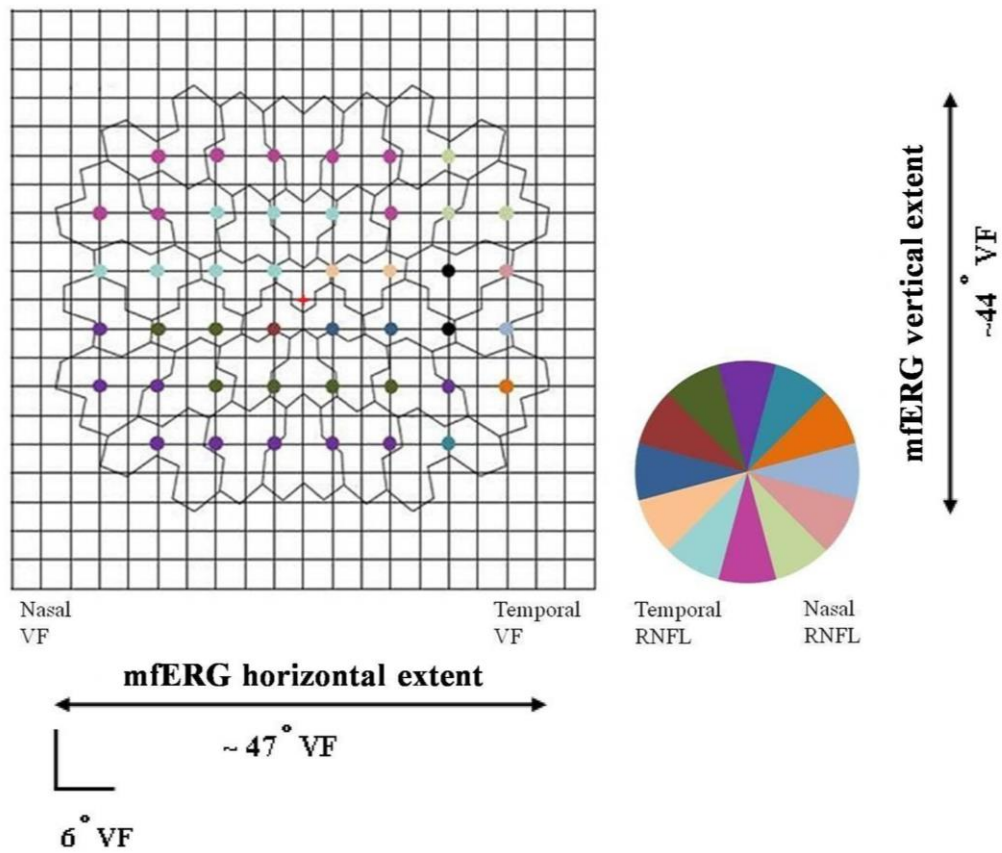
Figure 7.2. Mapping between the data of the mfERG, VF test and OCT RNFL profile. Left side: mapping of the overlays between the mfERG topography (35 polygonal patches) and the VF test spots (coloured spots). Right side: The sectoral RNFL profile measured by the OCT. Colour indication: Through mapping the VF test spots with the corresponding sectoral RNFL thickness (Garway-Heath et al. 2000; Garway-Heath et al. 2002), the regional mfERG data could be matched with the corresponding RNFL thickness (the central red cross represents the fixation point of the mfERG and VF assessments).

7.1.3.4.3 Overlay of OCT RNFL and MOFO mfERG topography

The OCT RNFL profile at the optic disc was mapped with the VF test grid (Figure 7.2) according to the overlay generated by Garway-Heath and co-workers (Garway-Heath et al. 2000; Garway-Heath et al. 2002). The fundus locations mapped by Garway-Heath et al. are on a $3°$ grid, simplifying alignment of the two data sets. Together with the mapping applied in the above section between the mfERG topography and the VF test grid, it was possible to link the MOFO mfERG topography to its corresponding sectoral RNFL profile obtained from the OCT measurement (Figure 7.2). If more than one mfERG division fell along a sector of the RNFL profile, the z-scores of the mfERG parameters at that sector were averaged before mapping with the RNFL thickness. The correlation between the regional MOFO mfERG responses and the sectoral RNFL thickness could then be calculated.

The correlations (Pearson's r) between the local z-scores of the MOFO mfERG responses and the results of two clinical assessments (VF and OCT) were calculated for groups I (regional data from the control group), II (regional data from the DM patients without any DR signs) and III (regional data from the DM patients with NPDR).

The regional responses of the three ocular assessments (mfERG, RNFL thickness and VF sensitivity) were also compared among groups I, II and III. Due to the repeated contribution from individual subject, generalized estimating equation (GEE) with Bonferroni's post-hoc adjustment was used for statistical analysis with the assumption of an unstructured working matrix.

7.1.4 Results

7.1.4.1 Correlation between local mfERG responses with the local sensitivity deviation (TD) of VF

After overlaying the MOFO mfERG topography with VF test spots, there were 76 VF test spots which fell into the mfERG topography. This gave a total of 854 VF regional data points: 392 in group I, 280 in group II and 182 in group III (Table 7.1). The correlations of the local mfERG responses with the local VF TD are shown in Table 7.2 for different groups of data (Groups I, II and III). The mfERG amplitude provides a more consistent relationship with the VF findings across various groups than implicit time does.

	Group I	Group II	Group III
Visual field (VF)	(n= 392)	(n= 280)	(n= 182)
Total deviation (TD)	-1.51 ± 1.55	-1.84 ± 2.06	-3.30 ± 2.39 (* p=0.005)
OCT	(n= 168)	(n= 120)	(n= 110)
Sectoral RNFL thickness (z-score)	0.00 ± 0.97	0.02 ± 1.25	0.029 ± 1.21
MOFO mfERG	(n= 490)	(n= 350)	(n= 234)
98% contrast level (z-scores)			
DCIT _z	0.00 ± 0.96	0.02 ± 1.50	1.23 ± 1.66 (* p<0.001) († p=0.013)
DCA_z	0.00 ± 0.96	-0.67 ± 1.01	-0.62 ± 1.09
ICIT_z	0.00 ± 0.96	0.06 ± 1.68	0.75 ± 2.31 (* p=0.013)
ICA_z	0.00 ± 0.96 († p=0.045)	-0.64 ± 0.85 (* p=0.045)	-0.80 ± 0.92 (* p=0.007)
46% contrast level (z-scores)			
DCIT_z	0.00 ± 0.96	-0.15 ± 1.85	-0.02 ± 2.22
DCA_z	0.00 ± 0.96 († p=0.014)	-0.66 ± 0.90 (* p=0.014)	-0.93 ± 1.20 (* p=0.003)
ICIT_z	0.00 ± 0.96	0.20 ± 1.08	0.12 ± 1.39
ICA_z	0.00 ± 0.96	-0.12 ± 0.85	-0.47 ± 0.89

Table 7.1. Regional data from each measurement (VF TD, OCT sectoral RNFL thickness and MOFO mfERG parameters) according to its mapping with the MOFO mfERG topography

(*: Significantly different from the control group (Group I) with p< 0.05)

(†: Significantly different from the DM patients without DR (Group II) with p<0.05)

Contrast conditions	MOFO mfERG parameters	Control Samples (Group I)		No DR Samples (Group II)		DR Samples (Group III)	
		Pearson r	p-value	Pearson r	p-value	Pearson r	p-value
98%	DCIT_z	0.26	<0.001*	-0.10	0.109	-0.05	0.532
	DCA_z	0.36	<0.001*	0.28	<0.001*	0.32	<0.001*
	ICIT_z	0.22	<0.001*	-0.20	0.001*	0.03	0.719
	ICA_z	0.24	<0.001*	0.01	0.909	0.42	<0.001*
46%	DCIT_z	0.18	<0.001*	0.09	0.142	0.02	0.794
	DCA_z	0.25	<0.001*	0.24	<0.001*	0.23	<0.001*
	ICIT_z	0.16	0.002*	-0.22	<0.001*	0.06	0.427
	ICA_z	0.30	<0.001*	0.23	<0.001*	0.27	<0.001*

Table 7.2. Summary of Pearson's correlation (r) between local responses of VF (TD) and MOFO mfERG parameters (*: Statistically significance level achieved with $p < 0.05$).

7.1.4.1.1 MOFO mfERG amplitude z-scores

At both high and low contrast levels, the DC and IC amplitudes showed a positive correlation with VF local sensitivity deviation in all three groups of data (except the IC amplitude of group II at high contrast level). Retinal regions with higher luminance sensitivity also showed greater mfERG amplitudes. The Pearson's correlation value ranged from 0.24 to 0.42 ($p < 0.05$) (Table 7.2) (Figure 7.3 and 7.4). However, the variations of the correlation did not show any trend in terms of the DR lesions or contrast levels.
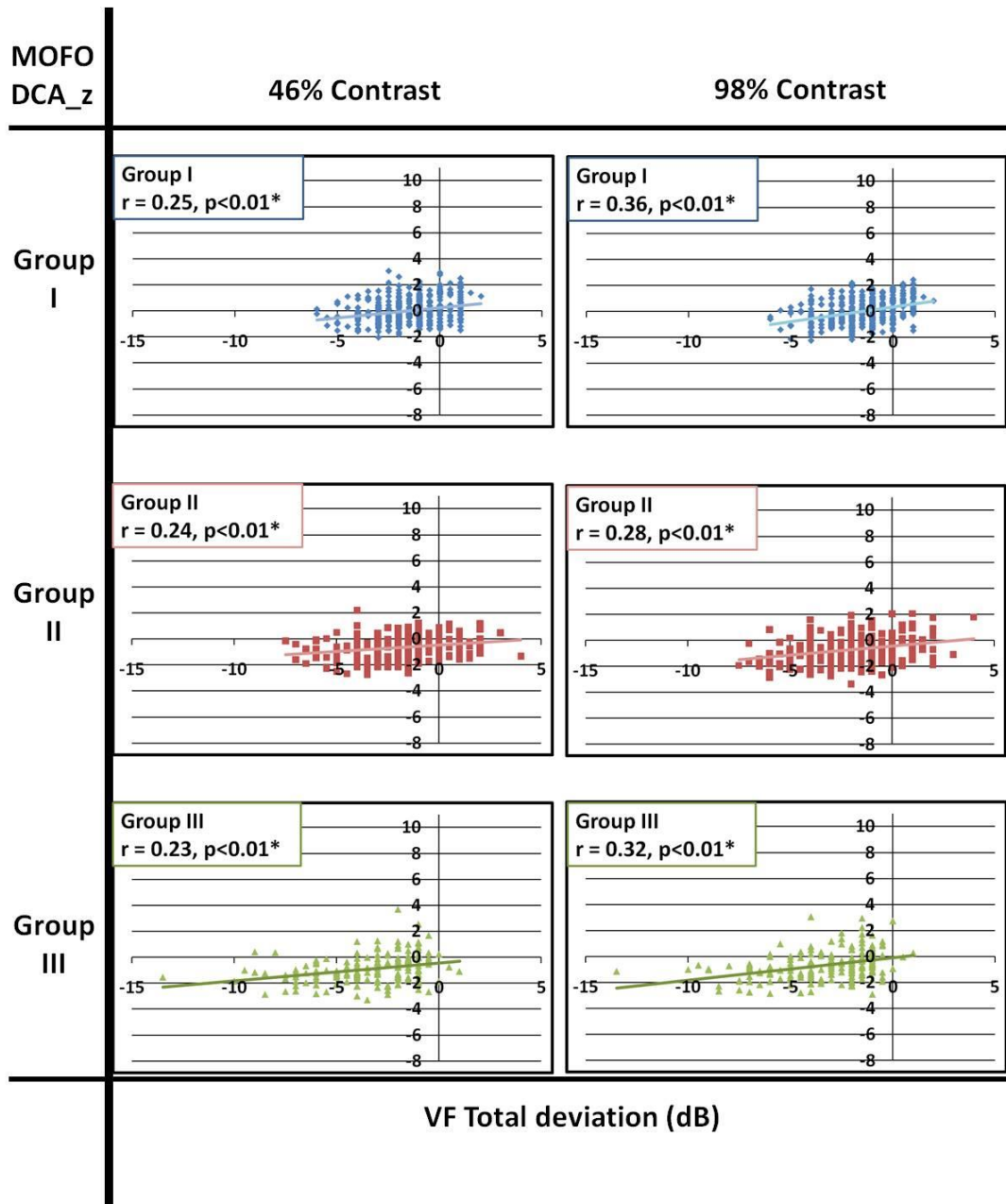
Figure 7.3. Correlation between the local responses of the VF (TD) and DCA_z of the MOFO mfERG at 98% and 46% contrast condition from groups I, II and III.
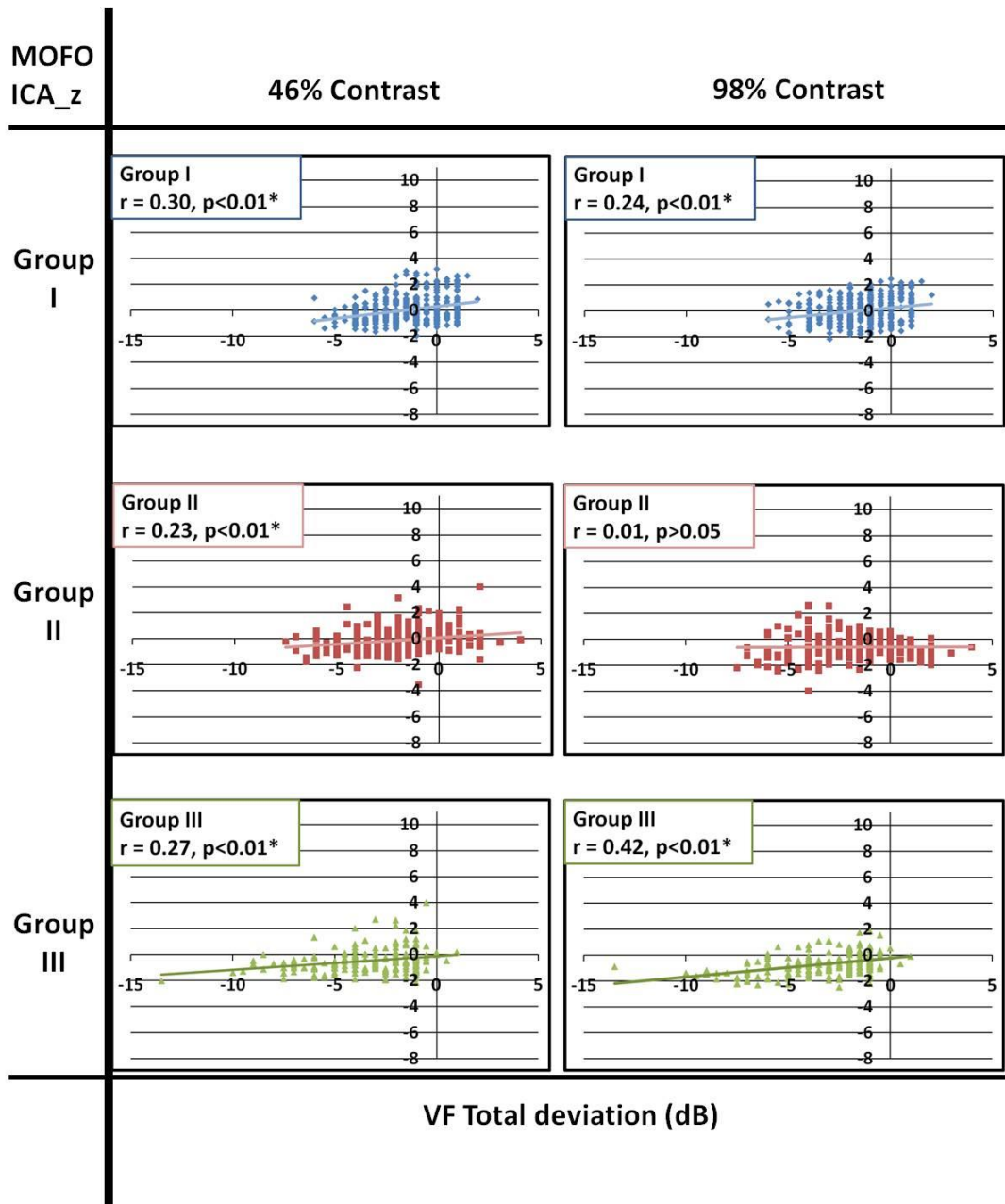
Figure 7.4. Correlation between the local responses of the VF (TD) and ICA_z of the MOFO mfERG at 98% and 46% contrast conditions from groups I, II and III.

7.1.4.1.2 MOFO mfERG implicit time z-scores

No significant correlations with visual field results were found in the diabetic groups (groups II and III) in terms of the DC implicit time at either contrast level. For the IC implicit time, significant correlations were found in group II but not in group III at high and low contrast levels. However, the relationship between the IC implicit time and luminance sensitivity was inconsistent across the diabetic groups.

7.1.4.2 Correlations between the local MOFO mfERG responses with the sectoral RNFL thickness z-scores

There were 398 sectoral RNFL thickness z-scores after mapping with the mfERG topography: 168 in group I, 120 in group II and 110 in group III (Table 7.1). However, no significant differences were found among these three groups of data ($p > 0.05$). The correlations between the mfERG responses with the sectoral RNFL thickness are listed in Table 7.3. No significant trends were found in correlations between MOFO mfERG parameters and sectoral RNFL thickness; few statistical significant correlations were found between in terms of IC amplitude z-score. However, these correlations were not consistent with the changes of contrast levels or among the various subject groups.

Contrast conditions	MOFO mfERG parameters	Control Samples (Group I)		No DR Samples (Group II)		DR Samples (Group III)	
		Pearson r	p-value	Pearson r	p-value	Pearson r	p-value
98%	DCIT_z	-0.08	0.309	-0.09	0.330	0.18	0.067
	DCA_z	0.02	0.799	0.13	0.159	0.03	0.770
	ICIT_z	-0.05	0.520	-0.06	0.492	0.04	0.718
	ICA_z	-0.06	0.437	0.00	0.995	0.27	0.005*
46%	DCIT_z	-0.08	0.331	0.07	0.432	0.14	0.139
	DCA_z	-0.14	0.081	-0.00	0.968	-0.08	0.392
	ICIT_z	0.09	0.233	-0.05	0.596	-0.00	0.966
	ICA_z	-0.20	0.008*	-0.06	0.491	-0.15	0.128

Table 7.3. Summary of Pearson's correlation (r) between local responses of
RNFL sectoral z-score and MOFO mfERG parameters
(*: Statistically significance level achieved with $p < 0.05$).

7.1.4.3 Regional data of groups I, II and III from each measurement (MOFO mfERG, VF and RNFL) after mapping based on mfERG topography

For the MOFO mfERG, there were a total of 1074 regional data values: 490 in
group I, 350 in group II and 234 in group III (Table 7.1). Only the amplitudes of
the DC at low-contrast level and IC at the high contrast level were able to
differentiate the diabetic data (groups II and III) from the control data (group I)
($p < 0.05$). The amplitudes from the diabetic groups were significantly smaller
than those of the control group. There was a significant delay in high contrast DC

and IC for group III (p<0.05), compared to group I data (p<0.05). There was a further delay of DC response in group III in high contrast condition than group II (p<0.05). DC and IC implicit time findings did not differentiate between diabetic data (groups II and III) and the control data.

Compared with the corresponding VF regional data points after overlaying the MOFO mfERG topography with VF test spots as shown in Table 7.1, it was found that only the regions with DR lesions demonstrated a marked reduction in VF sensitivity (p<0.01) compared to the regional data from the controls (group I). However, for the sectoral RNFL thickness z-scores collected after mapping with the MOFO mfERG topography (Table 7.1), no significant differences were found among these three groups of data (p>0.05).

7.1.4.4 Relationship of the plasma glucose levels with the averaged mfERG responses, VF sensitivity deviation and RNFL thickness

The control subjects had significantly lower plasma glucose levels than did the diabetic patients, either with or without DR (p<0.02 and p<0.01 respectively) (Table 7.4). The MOFO mfERG IC amplitude z-score for the low contrast condition in the control group increased with the plasma glucose level (r=0.731, p<0.02). There were no significant correlations between DC or IC amplitude z-scores at either contrast level and glucose level for either group of diabetic patients. No significant correlations were found between plasma glucose levels and RNFL thickness or VF assessments in all groups of subjects (controls, DM patients with or without DR).

Visual assessment parameters		Controls		DM patients without DR		DM patients with NPDR	
		(n= 10persons)		(n= 10persons)		(n= 30persons)	
		Pearson's r	p-value	Pearson's r	p-value	Pearson's r	p-value
VF mean deviation (dB)		-0.011	0.976	-0.044	0.904	-0.034	0.857
Mean RNFL thickness (um)		-0.367	0.297	-0.245	0.494	0.017	0.928
MOFO mfERG							
98% contrast level (z-scores)							
	DCIT_z	-0.049	0.892	0.520	0.124	-0.110	0.565
	DCA_z	-0.386	0.270	-0.091	0.803	-0.225	0.233
	ICIT_z	0.224	0.534	0.510	0.132	0.133	0.485
	ICA_z	0.371	0.291	-0.028	0.938	0.020	0.917
46% contrast level (z-scores)							
	DCIT_z	-0.215	0.552	0.585	0.076	-0.071	0.710
	DCA_z	0.454	0.187	-0.287	0.421	-0.183	0.333
	ICIT_z	0.543	0.104	0.580	0.079	0.206	0.276
	ICA_z	0.731	0.016*	0.010	0.979	-0.146	0.440

Table 7.4. Summary of Pearson's correlation (r) between plasma glucose level
(mmol/L) with each mean visual assessment parameters (VF mean deviation
[dB], RNFL mean thickness [um] and the averaged MOFO mfERG parameters
[z-scores]) (*: Significance level with $p < 0.05$).

7.1.5 Discussion

The current findings demonstrated that the MOFO mfERG responses generally correlated better with the results of perimetric testing than those of the RNFL thickness measurement in diabetes. Among these three assessments, only the MOFO mfERG differentiates the "No DR" regional data (group II) from the control group (group I). The MOFO mfERG amplitude provides a more consistent relationship with the perimetric test across retinal regions than does implicit time. RNFL thickness has no relationship with the functional testing performed in this study.

These results showed that the local VF sensitivity deviation (i.e. TD), rather than the RNFL thickness, was moderately correlated with most of the MOFO mfERG parameters in the control data. It is not surprising that an electrophysiological assessment correlates better with a clinical functional test than with a morphological test in these subjects. Visual field assessment has been applied in studies of DM patients, but whether VF measures can differentiate diabetic patients without DR from healthy controls is still controversial. It is generally accepted that the VF mean deviation should decrease with increasing DR severity (Remky et al. 2003; Bengtsson et al. 2005; Nitta et al. 2006; Bengtsson et al. 2008; Parravano et al. 2008).

7.1.5.1 Correlation between MOFO mfERG and VF assessments

Correlations between mfERG amplitudes and VF parameters were more consistent than correlations between implicit time and VF parameters in the diabetic samples (groups II and III). Only group II showed a significant negative association between the VF sensitivity and the IC implicit time. There was an

opposite change in the correlation direction from group I to group II (as shown in Table 7.2) for the high and low contrast conditions. Although the mechanisms for the mfERG amplitude and implicit time changes in DM patients are not understood, neither reduced contrast levels nor the increased DR severity led to a great change in the values of Pearson's r value between MOFO mfERG parameters and VF sensitivity deviations. This result should be repeated to determine whether the relationship between VF and IC implicit time can be substantiated or whether it is anomalous. In both previous studies (Shimada et al. 2001; Lung et al. 2012) and current experiment, the amplitudes of the MOFO mfERG paradigm demonstrated a greater ability in showing the group difference between the healthy and diabetic groups (with or without DR). Moreover, it also showed a better and more consistent correlation with the perimetric functional test than the implicit time. These findings are different from those reported in other mfERG paradigm studies (Fortune et al. 1999; Han et al. 2004; Han et al. 2004; Bearse et al. 2006; Ng et al. 2008; Harrison et al. 2011) that delay of implicit time existed earlier before the amplitude changes in DM patients. This discrepancy between the amplitude and implicit time findings would be probably due to the different mfERG paradigms involved in the studies which may in turn trigger a different cellular performance.

Similar to a previous study (Han et al. 2004), Pearson's correlation r between the mfERG and VF was maintained at about 0.2 to 0.4. The relatively weak to moderate correlations between these two functional tests may be due to different underlying mechanisms. MOFO mfERG provides an objective measurement of the retinal adaptation activity predominantly from retinal components beyond the secondary neural level, while VF provides a subjective measurement of the

retinal threshold detection from the whole visual system. Although the MOFO mfERG was shown to be better than VF in differentiating DM patients without DR from the control group, it cannot be concluded that mfERG is superior to VF. One of the major differences between VF and mfERG is that VF provides a static stimulus for assessing luminance sensitivity while mfERG measures activities to luminance changes and temporal interactions. The information from these two tests is supplementary and gives rise to a clearer picture of the underlying changes in DM.

7.1.5.2 Correlation between MOFO mfERG and RNFL assessments

However, the functional deterioration in the diabetic retina found in this study cannot be purely explained by the luminance detection/sensitivity or the morphological changes of the RNFL. The changes observed in MOFO mfERG and its weak to moderate correlations with RNFL thickness and luminance sensitivity indicated the alteration of adaptive function in the middle and/or inner retinal layers (with the RNFL excluded).

While there are some conservative opinions on the ability of OCT to detect RNFL thinning for the DM patients without visible DR lesions (Ozdek et al. 2002; Takahashi & Chihara 2008), many studies have proposed that there is RNFL thinning, at least in a specific quadrant of the optic disc, in the early stages of NPDR (Lopes de Faria et al. 2002; Ozdek et al. 2002; Sugimoto et al. 2005; Takahashi & Chihara 2008; Oshitari et al. 2009). In the present study, functional deterioration was found, but no structural anomalies were detected in early DM. Only the IC amplitude findings provided a weak correlation with RNFL morphological changes. Zhang et al. (Zhang et al. 2000) suggested that

retrograde axonal transport was impaired in the early stage of DM. The ganglion cells would be adversely affected before morphological impairment of the optic nerve fibers. This may indicate why the retinal functional deterioration found by the MOFO mfERG paradigm in DM patients does not match with RNFL changes, and the optic neuropathy found in DM patients is very different from the glaucomatous optic neuropathy (Ozdek et al. 2002; Oshitari et al. 2009). This weak electrophysiological-morphological association further supports the hypothesis raised by Greenstein et al. (Greenstein et al. 1989) that the problematic site of DM is at/near the middle retinal layers which is different from glaucoma or retinitis pigmentosa (RP). Further investigation of the electrophysiological-morphological association in the more severe DR group will help to understand the nature of the disease progression.

7.1.5.3 Limitations of this experiment

Hyperglycemia is an underlying problem in DM. Unexpectedly, the high correlation of the plasma glucose level to the IC amplitude in the low contrast condition was shown only in the healthy controls but not in the diabetic patients. This might be due to the large variations of plasma glucose level as well as different effects caused by glycemic control and chronic hyperglycemia (Klemp et al. 2004; Jeppesen et al. 2007; Parravano et al. 2008). Further studies on how glycemic control and chronic hyperglycemia affect middle/inner retinal responses (as reflected in mfERG responses) in both normal and diabetic patients would be useful. Another limitation of this study is the mapping between the RNFL bundles with the OCT which was based on a Caucasian population. Whether there is any ethnic difference in the mapping of the RNFL to each OCT sector needs to be investigated.

Chapter 8: The on- and off-responses in diabetic patients assessed using the long-duration stimulus mfERG with white (Broad-spectrum) and blue (Narrow-spectrum) stimuli

8.1 Experiment C – Characteristics of the on- and off-responses in diabetic retina with white and blue stimuli – a mfERG study

8.1.1 Abstract

Purpose: To investigate the characteristics of the on- and off-responses in the human diabetic retina using a "long-duration" multifocal electroretinogram (mfERG) paradigm. Changes in retinal antagonistic interaction were also evaluated in the early stage of diabetes mellitus (DM).

Methods: Twenty type II diabetic patients with no or mild non-proliferative diabetic retinopathy (NPDR) and twenty-one age-matched healthy controls were recruited for "long-duration" mfERG measurements. A 61-hexagon mfERG stimulus was displayed under acromatic (white/black) and chromatic (blue/black) conditions with matched luminance. The amplitudes and implicit times of the on-response components (N1, P1 and N2) and off-response (P2) components of the mfERG were analysed using conventional ring analysis.

Results: The blue stimulation generally triggered greater mfERG amplitudes in on-response (P1, N2) and off-response (P2) ($p<0.05$) than those from white stimulation in both control and diabetic groups. The diabetic group showed significantly greater N2 amplitude than the controls under white stimulation in Rings 2 and 4 ($p<0.05$). When the stimulus was changed from white to blue, the diabetic group showed a smaller percentage of enhancement in N2 amplitude than the controls in the periphery (Ring 5) ($p<0.02$).

Conclusion: When the stimulus changes from white (broad-band spectral stimulation) to blue (narrow-band spectral stimulation), a decrease in involvement of lateral antagonism would be expected. The larger amplitude of the on-response component (N2) in the diabetic patients suggested an imbalance of lateral antagonism, and the lesser percentage change of N2 amplitude in the diabetic group may indicate an impairment of interaction at the middle retinal level in the early stages of DM.

8.1.2 Introduction

Diabetic retinopathy (DR) is an ocular vascular complication associated with diabetes mellitus (DM) which has shown a rapid increase of incidence in Asia (Wild et al. 2004). DR is one of the leading causes of blindness among the working population (Porta & Bandello 2002). It has been proposed that due to the damage of the endothelium and pericytes, together with the acceleration of apoptosis, vascular leakage results and leads to the clinically visible signs of DR (Cunha-Vaz 2007). Both reduction of sensitivity in automated perimetry (Bengtsson et al. 2005; Bengtsson et al. 2008) and thinning of the retinal nerve fiber layer (RNFL) (Lopes de Faria et al. 2002; Sugimoto et al. 2005; Takahashi & Chihara 2008; Oshitari et al. 2009; Cho et al. 2010) have been reported in diabetic patients. In previous Experiments A2 and B in this thesis (Ch. 6.2 and 7) (Lung et al. 2012; Lung et al. 2012), the mfERG has been shown to be superior to two common clinical assessments (automated white-on-white perimetry and RNFL thickness measurement by optical coherence tomography) in demonstrating early physiological changes before the existence of visible vascular lesions.

The multifocal electroretinogram (mfERG) provides an objective assessment of retinal function and provides topographic details of retinal function (Sutter & Tran 1992). The mfERG reflects neural activities mainly in the middle and inner retinal layers (Hood et al. 1999). Functional deterioration detected by the mfERG indicates disturbance of retinal adaptation at or beyond the level of secondary neurons. Several studies have applied the mfERG with different protocols to provide objective evaluation of functional changes in diabetic patients, and to assess topographic details of these changes (Palmowski et al. 1997; Fortune et al.

1999; Shimada et al. 2001; Onozu & Yamamoto 2003; Bearse et al. 2004; Bearse et al. 2004; Han et al. 2004; Han et al. 2004; Tyrberg et al. 2005; Bearse et al. 2006; Ng et al. 2008; Tyrberg et al. 2008; Bronson-Castain et al. 2009; Harrison et al. 2011; Lung et al. 2012). The retinal dysfunction detected in diabetic patients cannot be fully explained by either reduced luminance sensitivity or by morphological changes of the RNFL (Lung et al. 2012). It is believed that the possible site for the functional changes is within the middle to inner layers of the retina.

However, there is a large overlap of the on- and off-pathway responses in the responses of the conventional mfERG paradigm, and these responses are important in the investigation of normal and abnormal retinal physiology. In order to dissociate the on- and off-pathways, Kondo and Miyake (Kondo & Miyake 2000) modified the mfERG paradigm to mimic the "long-duration" flash which is applied in the Ganzfeld full-field electroretinogram (Sieving 1993). By increasing the number of multifocal flashes and dark frames, the overlap between the on-response and off-response in the mfERG can be minimized. In using this protocol, the mfERG can be used to separately assess the on- and off-pathways (Kondo & Miyake 2000). Such a protocol has been applied in some retinal disorders to study the activities of the on- and off-pathways (Kondo et al. 1998; Marmor et al. 1999; Luu et al. 2005).

Previous studies have demonstrated that narrow-band spectral stimulation can trigger a larger retinal signal than broad-band stimulation in electroretinogram measurements. This is probably due to antagonistic interactions initiated by networks of long-, middle- and short-wavelength cones and their secondary

neurons (Rangaswamy et al. 2007). Colour discrimination ability has been shown to deteriorate early in diabetic retinopathy (Bresnick et al. 1985; Kurtenbach et al. 2002; Ong et al. 2004). A generalized loss of chromatic discrimination has been suggested by Feitosa-Santana et al. (Feitosa-Santana et al. 2006), while various authors have proposed a reduction of short-wavelength sensitivity in diabetic patients (Bresnick et al. 1985; Greenstein et al. 1989; Yamamoto et al. 1996). Selective loss of short-wavelength cone sensitivity in diabetic patients has also been illustrated by electrophysiological assessment (Yamamoto et al. 1996; Yamamoto et al. 1997).

In this experiment, the modified long-duration mfERG paradigm described above was used to study the on- and off-responses of the middle and inner retinal layers at different retinal regions in diabetic patients. Furthermore, the mfERG stimulus pattern was used under achromatic (white/black) and chromatic (blue/black) conditions to manipulate the antagonistic interactions, in order to evaluate the changes of the interaction at or beyond the middle retinal level in the early stages of DM.

8.1.3 Methods

8.1.3.1 Subject recruitment and inclusion criteria

Twenty type II diabetic patients (aged 46.6±7.4 years) with no or mild non-proliferative diabetic retinopathy (NPDR) and twenty-one age-matched healthy controls (aged 46.6±7.4 years) were recruited for this study. All of the participants had best corrected visual acuity equal to or better than 6/9 and their refractive errors were between +3.00D and -6.00D with astigmatism less than -1.25D. Detailed eye examination (including subjective refraction,

biomicroscopy and indirect ophthalmoscopy) with fundus photodocumentation was carried out for each subject. Slit-lamp biomicroscopic assessment was performed and the crystalline lens was graded according to the Lens Opacities Classification System III (Chylack et al. 1993). Best-corrected VA was measured in order to exclude subjects with clinically significant cataract condition which led to non-age-related visual impairment. Fundus photodocumentation was performed in the central retina and in the eight cardinal gaze directions using a fundus camera (Topcon IMAGEnet, Japan). Participants with ocular diseases other than DR or systemic diseases other than DM were excluded

All of the study procedures fulfilled the tenets of the Declaration of Hesinki. This study was approved by the Ethics Committee of The Hong Kong Polytechnic University. Written consent was obtained from each individual subject after full explanation of the experimental procedures.

8.1.3.2 Experimental set-up and procedures

8.1.3.2.1 mfERG recording

The VERIS Science 5.1 system (Electro- Diagnostic- Imaging, Redwood City, CA, USA) was used for the mfERG measurement with the "long-duration" protocol. A scaled 61-hexagon pattern (Figure 7.1) (stretch factor: 10.46) which subtended 49° horizontally and 47° vertically was displayed on a high luminance CRT monitor with P45 phosphor (FIMI Medical Electrical Equipment, Saronno, Italy). Each base period of the mfERG stimulation contained 16 video frames: 8 successive multifocal flash frames and 8 successive dark frames, as suggested by Kondo and Miyake (Kondo et al. 1998; Kondo & Miyake 2000). Each base period lasted about 213.3 ms (bright phase duration: 106.6 ms, dark phase

duration: 106.6 ms). The stimulus was displayed at a frame rate of 75 Hz and the pseudo-random m-sequence chosen had 2^{11}-1 steps. The mfERG signal was amplified by 100,000x and was bandpass filtered from 3 to 300 Hz (Grass Instrument Co., Quincy, MA, USA).

Measurements were made under two conditions: In the white condition, the bright phase was displayed at 22 cd/m^2 and the dark phase was displayed at 0.3 cd/m^2. The background luminance was maintained at the mean luminance level at 10 cd/m^2. The room illuminance was dimmed and maintained at about 10 lux.
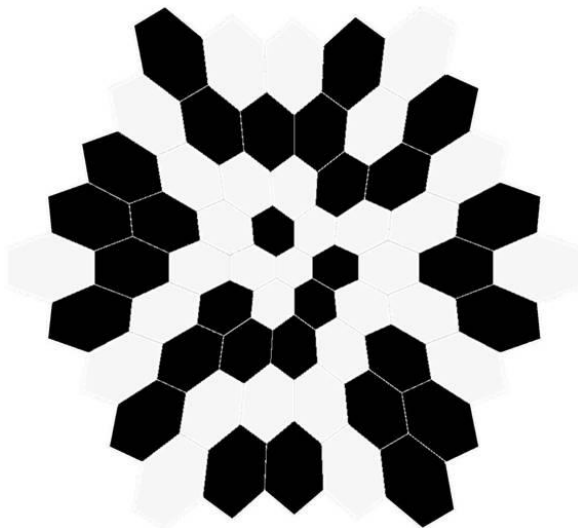
Figure 8.1a. The 61-hexagonal mfERG stimulus pattern for the white condition.
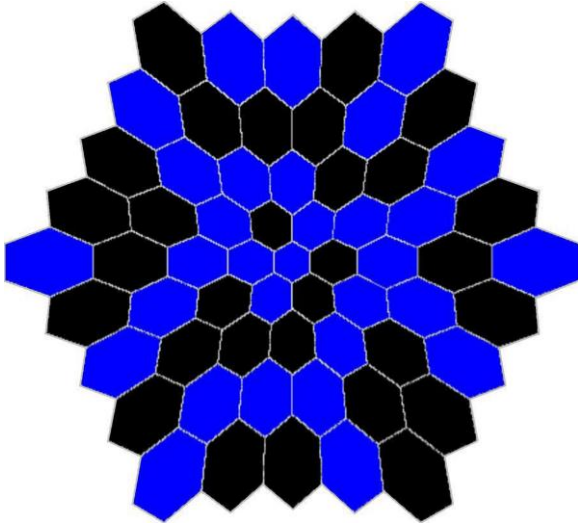
Figure 8.1b. The 61-hexagonal mfERG stimulus pattern for the blue condition.

A Wratten 47A filter was inserted between the display and the eye to achieve the blue stimulation condition. The Wratten 47A filter has peak transmission at 450 nm, with cutoff at half-height at about 500 nm. The spectrum of visible wavelengths emitted from P45 phosphor is broader than the cutoff of the Wratten 47A filter, and the combination of P45 and Wratten 47A produces a deep blue stimulus which stimulates mainly the short-wavelength (SW) and partly middle-wavelength (MW) cone systems (Poloschek & Sutter 2002; Ozawa & Itoh 2003). The luminance of the white and black hexagons on the FIMI monitor under the 47A filter was adjusted so that the same luminance was achieved as for the white stimulation condition. The luminance measurements were made using a Konica Minolta LS-110 photometer (Konica Minolta Optics, Inc., Tokyo, Japan). Both the white and blue mfERG stimulations with the same luminance were displayed randomly to the subjects.

One eye of each subject was randomly selected for mfERG measurement and dilated using 1% Tropicamide (Alcon, Fort Worth, TX, U.S.A.) until the pupil

reached at least 7 mm diameter. A Dawson-Trick-Litzkow (DTL) electrode was used as the active electrode. A gold-cup electrode was placed at the outer canthus as the reference electrode, and another at the central forehead as the ground. Subjects were corrected for the viewing distance of 33 cm using ophthalmic trial lenses. Each subject was instructed to fixate the central cross of the mfERG stimulus pattern throughout the measurement. The measurement for each condition was divided into 32 segments. Any recorded segment contaminated by blinks or other artifacts was rejected and re-measured immediately.

8.1.3.3 Data analysis

8.1.3.3.1 Grouping of mfERG responses

The mfERG responses from the 61-hexagon pattern were grouped into 5 rings for analysis. There are two sections of the resultant waveform: the on-response triggered by the mfERG bright phase (stimulus-on) and the off-response triggered by the mfERG dark phase (stimulus-off) (Figure 8.2). The on-response is the initial part of the waveform, which is similar to the conventional mfERG waveform, including a negative trough (N1) followed by a positive peak (P1) and then another trough (N2). After a plateau following N2, there is a second peak (P2) which is the off-response. The relevant amplitude and time parameters are shown in Figure 8.2.
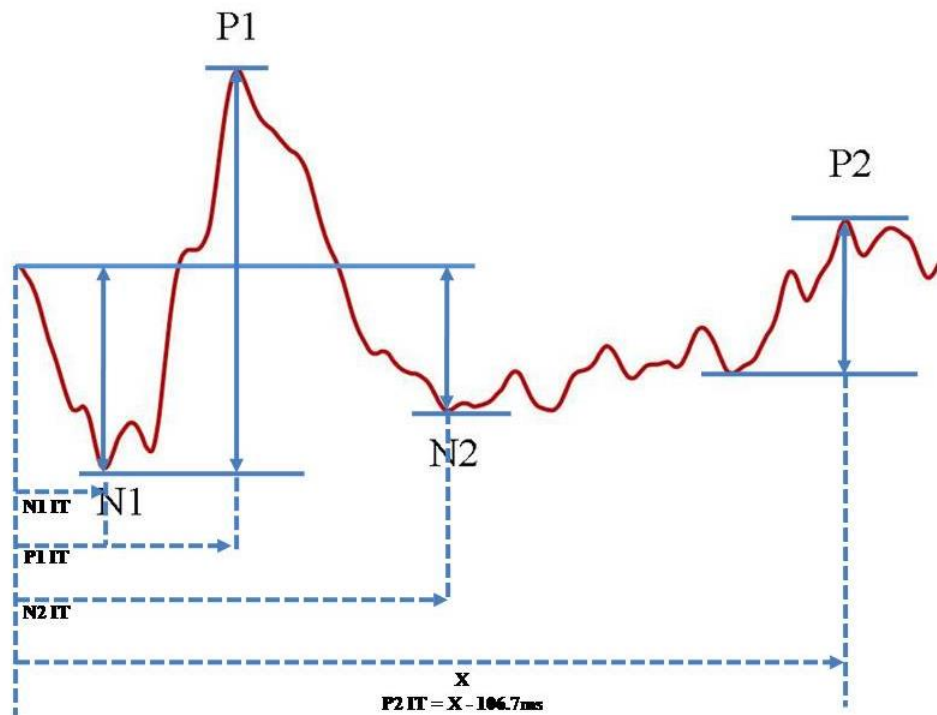
Figure 8.2. The waveform under the "long-duration" mfERG paradigm showing the parameters measured.

8.1.3.3.2 Calculation of percentage changes of mfERG responses under achromatic and chromatic conditions

When the mfERG stimulus changed from white to blue stimulation, the percentage change for the mfERG responses was calculated using:

(mfERG response under blue stimulus – mfERG response under white stimulus) x 100%

(mfERG response under white stimulus)

This value was used to investigate the changes of the antagonistic interaction within the retina.

8.1.3.3.3 Statistical analysis

Three factors were evaluated in this study. The within-subject factors were "Rings" (5 rings) and "Colours" (white and blue) while the between-subject factor was "Groups" (control and diabetic groups). A three-way mixed design analysis of variance (ANOVA) was used for statistical analysis. Post-hoc test with Bonferroni's adjustment was used to account for the multiple comparisons. Statistical significance level was set at $p < 0.05$.

If the within-subject factors or their combinations showed significant effect(s) on the mfERG parameters, two-way repeated measures ANOVA (Factors "Colours" and "Rings") were carried out to examine which mfERG parameters were affected by the within-subject factors in each subject group. A further one-way ANOVA or unpaired t-test was carried out to locate the effect.

If the between-subject factor or its combination showed a significant effect on the mfERG parameters, a mixed design two-way ANOVA (Factors "Rings" and "Groups") was carried out to examine which mfERG parameters were affected in different stimulations. A further unpaired t-test was carried out to locate the significant difference between subject groups.

For the percentage change of the mfERG responses, two-way mixed design ANOVAs (Factors "Rings" and "Groups") were carried out in order to compare the difference between two subject groups. When there was a significant group difference, further unpaired t-tests were carried out to find out their location(s).

8.1.4 Results

8.1.4.1 Effect of retinal eccentricity

Both the amplitudes of mfERG on-responses (N1, P1, N2) and off-response (P2) decreased with increasing retinal eccentricity (Ring number). All the amplitudes (N1, P1, N2 and P2) were affected by the interaction of the factors "Colours", "Rings" and "Groups" with the statistically significance level $p < 0.05$ (Figure 8.3a-d). Further two-way repeated measures ANOVA (Colours x Rings) indicated that a similar significant difference existed in both the control and diabetic groups. Post-hoc testing of ring amplitudes indicated that the greatest mfERG amplitudes for all measures was in Ring 1, the second greatest in Ring 2 and the smallest amplitudes were in Ring 5 ($p < 0.02$) under both white and blue stimulation conditions. The third greatest amplitudes under both stimulation conditions were in Ring 3 ($p < 0.01$) in the control and diabetic groups except for the N2 amplitude under the blue stimulation in the control group.
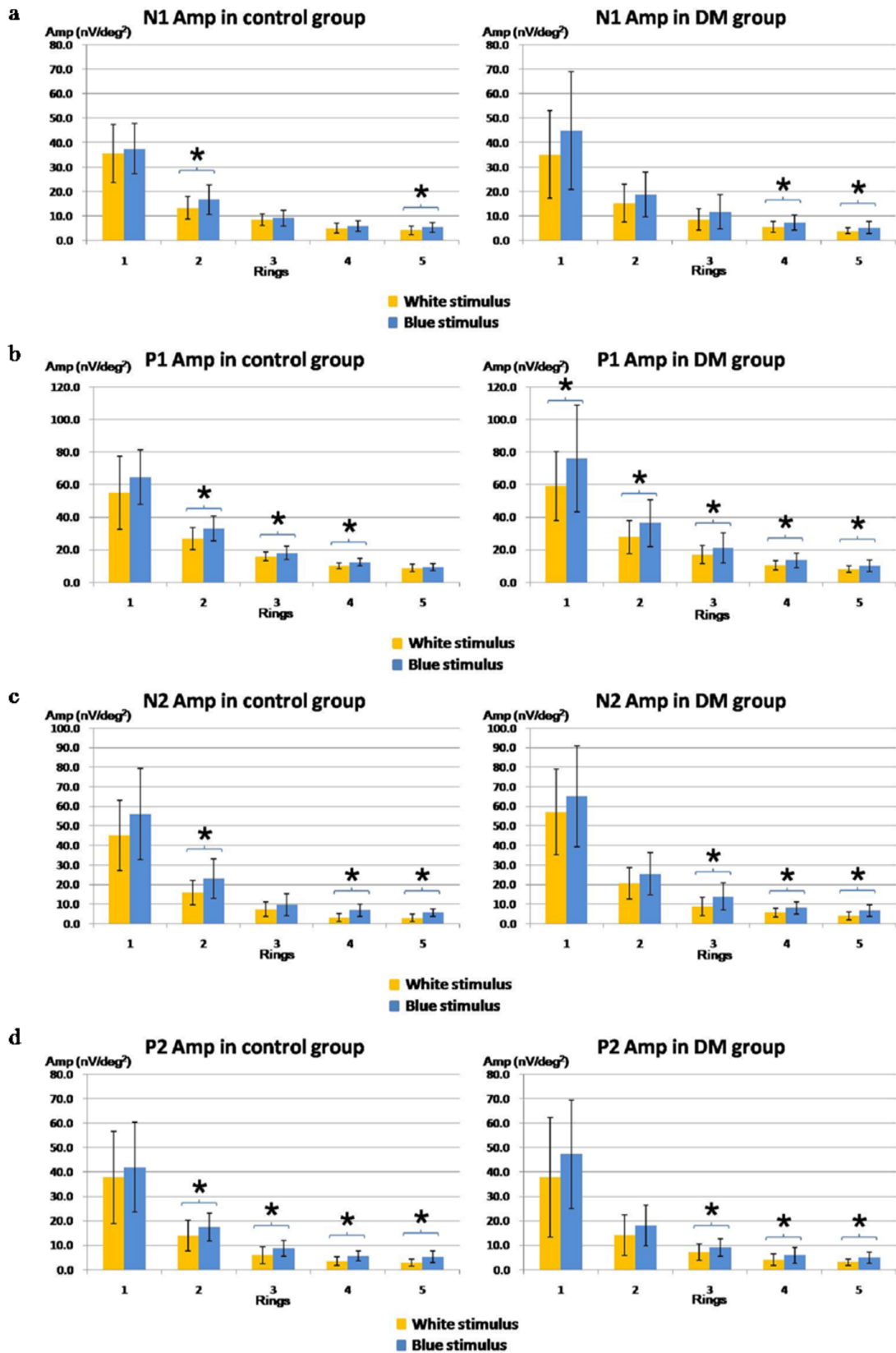
Figure 8.3. a) The N1 amplitude in the DM and control groups under both the white and blue stimulus conditions; b) The P1 amplitude in the DM and control

groups under both the white and blue stimulus conditions; c) The N2 amplitude
in the DM and control groups under both the white and blue stimulus conditions;
d) The P2 amplitude in the DM and control groups under both the white and blue
stimulus conditions

(*: indicates parameters that archived statistically significance level with $p<0.05$)

(Error bar: indicates $\pm$ 1 standard deviation)

In general, no common trend of implicit time was shown for the on- and
off-response components across eccentricity for either the control or diabetic
groups. Three-way mixed design ANOVA showed that the factor "Rings"
affected the mfERG on-response implicit time of N1 ($p<0.005$), P1 ($p<0.001$)
and N2 ($p<0.001$) while no significant difference was found in the implicit time
of the off-response P2 ($p>0.05$). Further two-way repeated measures ANOVA
(Colours x Rings) and one-way repeated measures ANOVA (Rings) with
Bonferroni's post-hoc test indicated that the implicit time of P1 in the central
Ring 1 was significantly longer than those in the peripheral Rings 3 and 4
($p<0.01$) in the control group under both stimulation conditions. In the diabetic
group, the implicit time of P1 in central Rings 1 and 2 was found to be longer
than that in peripheral Rings 3 to 5 ($p<0.05$) under blue stimulation only.

8.1.4.2 Effect of chromatic (white and blue) mfERG stimulation

The factor "Colours" showed significant differential effects on the amplitudes of
on- and off-response (Three-way mixed design ANOVA, $p<0.01$). Therefore,
two-way repeated measures ANOVA (Colours x Rings) were carried out in the
control and diabetic group respectively.

In the control group, two-way repeated measures ANOVA (Colours x Rings) indicated that the blue stimulation triggered greater P1 ($p=0.006$), N2 ($p=0.03$) and P2 ($p=0.034$) amplitudes than the white stimulation. Further paired t-tests on the ring amplitudes were performed. For the P1 amplitude, a significant chromatic effect was found at Rings 2 to 4 ($p<0.05$) (Figure 8.3b, left panel); for the N2 amplitude, the significant chromatic effect was found at Rings 2, 4 and 5 ($p<0.02$) (Figure 8.3c, left panel); for the P2 amplitude, a significant chromatic effect was found at Rings 2 to 5 ($p<0.05$) (Figure 8.3d, left panel).

In the diabetic group, two-way repeated measures ANOVA (Colours x Rings) indicated that the blue stimulation triggered greater amplitudes for all mfERG responses than the white stimulation ($p<0.04$). Further paired t-tests on the ring amplitudes showed where the significant effect existed. For the N1 amplitude, a significant chromatic effect existed in Rings 4 to 5 ($p<0.01$) (Figure 8.3a, right panel); for the P1 amplitude, this effect was found in all five rings ($p<0.02$) (Figure 8.3b, right panel); for the N2 and P2 amplitudes, a chromatic effect was mainly found in Rings 3 to 5 ($p<0.01$) (Figure 8.3c and 8.3d, right panels).

Under different chromatic stimuli, it was observed that the implicit times of the on-responses (P1 and N2) of the blue stimulation were shorter than those of the white stimulation in the diabetic group only. The chromatic factor had a statistically significant effect on the implicit time of P1 at Rings 3 and 4 only in the diabetic group. The P1 implicit time in response to the white stimulation was longer than to blue stimulation ($p<0.01$) (Figure 8.4). No other consistent trend in implicit time was observed for the remaining mfERG components.
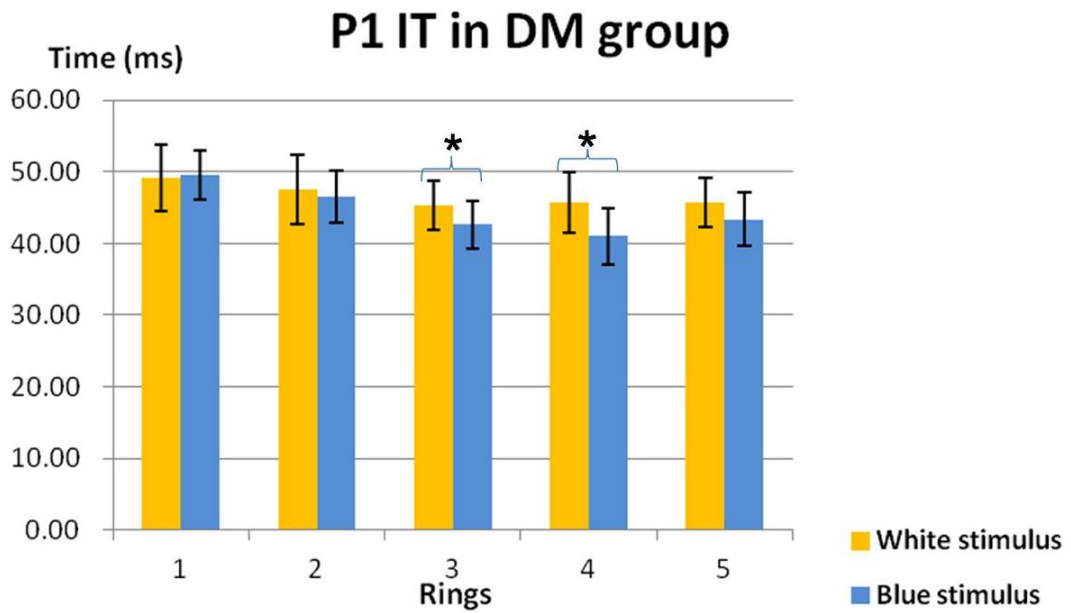
Figure 8.4. The P1 implicit time in the diabetic groups under both the white and blue stimulus conditions

(*: indicates parameters that achieved statistically significance level with p<0.05)

(Error bar: indicates ± 1 standard deviation)

8.1.4.3 Comparison between the control and diabetic groups

The diabetic subjects showed significantly greater N2 amplitudes than did the healthy controls (Three-way mixed design ANOVA, p<0.05). Two-way mixed design ANOVA indicated that a significant "Groups" difference occurred only for white stimulation (p<0.03). Unpaired t-tests showed that this effect achieved a statistical significance level at Ring 2 (p<0.05) and Ring 4 (p<0.001) (Figure 8.5).
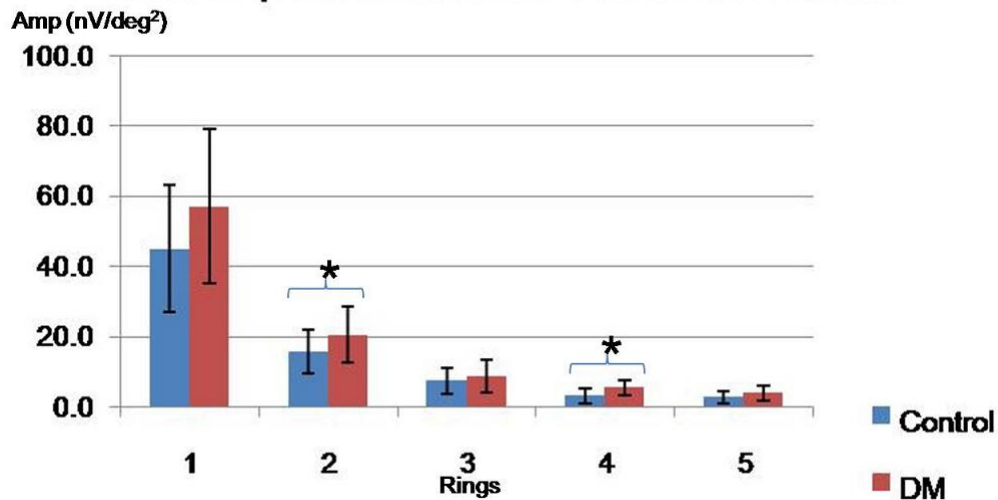
Figure 8.5. The N2 amplitude in the control and diabetic groups under the white stimulus condition.

(*: indicates parameters that achieved statistically significance level with p<0.05)

(Error bar: indicates ± 1 standard deviation)

Considering the amplitude changes of major components (as a percentage) when the stimulus was changed from white to blue, although there was a great variation of the percentage value, the P1 amplitude consistently showed a greater increase across retinal eccentricity in the diabetic than in the control group (Figure 8.6a), while the on-response component N2 showed an opposite trend. Two-way mixed design ANOVA (Rings x Groups) showed that the N2 amplitude of the diabetic group had a significantly smaller increase than the control group (p<0.02) especially for Ring 5 as found by the unpaired t-tests (Figure 8.6b).

a

% of P1 Amplitude Change

Percent (%)

Rings

■ Control group
■ DM group

b

% of N2 Amplitude Change

Percent (%)

*

Rings

■ Control group
■ DM group

c

% of P2 Amplitude Change

Percent (%)

Rings

■ Control group
■ DM group
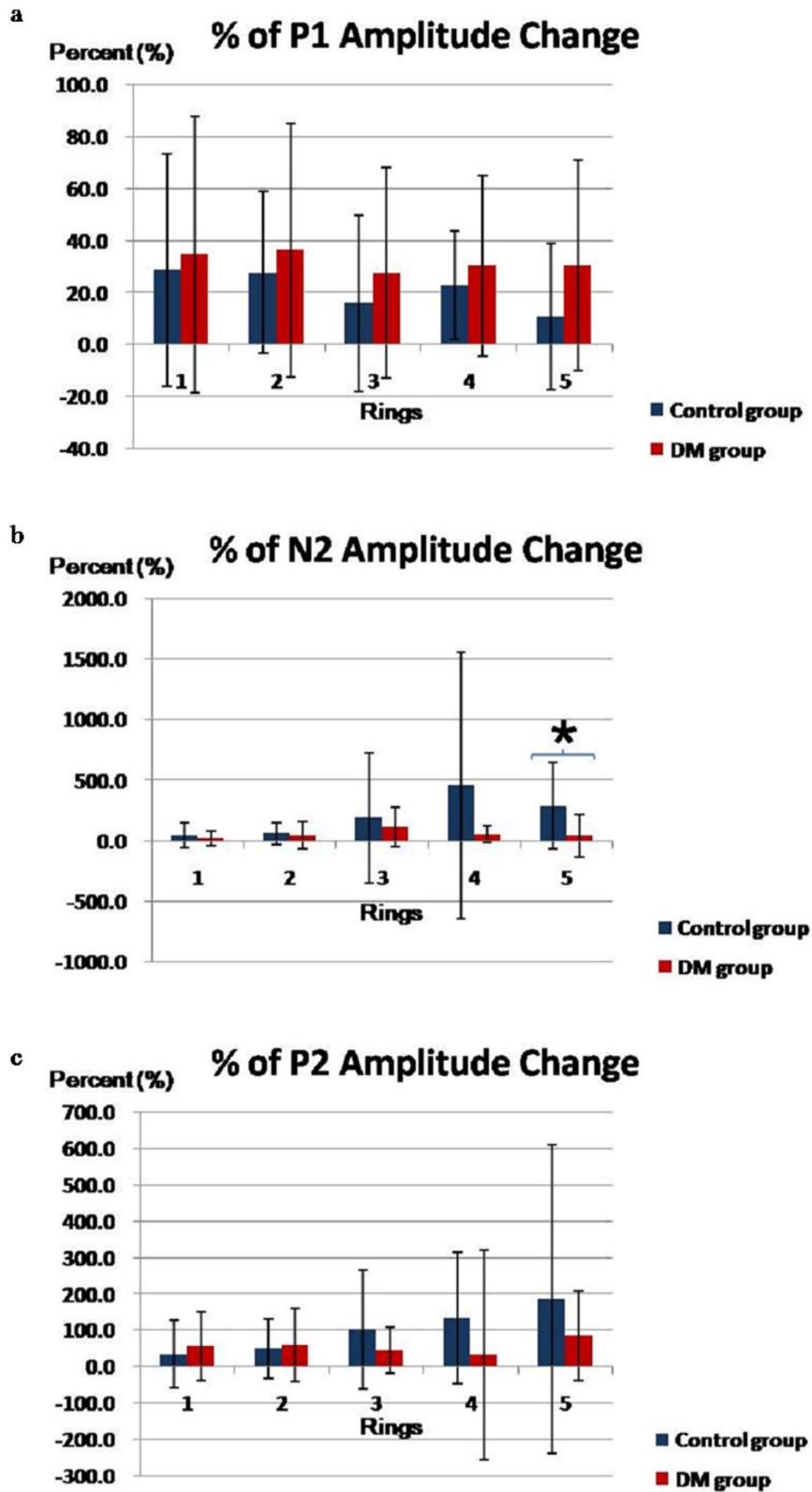
Figure 8.6. a) The amplitude changes (in percentage) of the P1 amplitude due to the change from white to blue stimulus between the control and the diabetic groups; b) The amplitude changes (in percentage) of the N2 amplitude due to the

change from white to blue stimulus between the control and the diabetic groups;

c) The amplitude changes (in percentage) of the P2 amplitude due to the change

from white to blue stimulus between the control and the diabetic groups.

(*: indicates parameters that achieved statistically significance level with p<0.05)

(Error bar: indicates $\pm$ 1 standard deviation)

For the P2 amplitude, when the stimulation changed from white to blue, the diabetic group also had a greater increase than the control at Rings 1 and 2 but a lesser increase for Rings 3 to 5 as shown in Figure 8.6c; however, no statistical significance was shown in the two-way mixed design ANOVA (p>0.05). No consistent trend was observed in the N1 amplitude change. Both the diabetic and control groups showed an increase in the P2 implicit time but no consistent change was observed in the implicit time of the other mfERG components.

8.1.5 Discussion

By using white and blue stimuli in the "long-duration" mfERG paradigm, waveforms contain two positive peaks which are similar to the resultant waveform in the long-duration full-field electroretinogram. This "long-duration" mfERG paradigm is based on the Ganzfeld full-field electroretinogram with a long-duration stimulus. The mfERG stimulus applied here was not a true continuous flash, but a series of flash impulses at high frequency up to 75 Hz. Saeki and Gouras (Saeki & Gouras 1996) demonstrated that a high frequency flash series produces an effect similar to that produced by a light pulse of long-duration which can generate a positive off-response.

8.1.5.1 Spectral difference between the white and blue stimuli

In this study, the blue stimulus generally triggered stronger mfERG signal than the white stimulus in both diabetic and control groups. The mfERG paradigm was conducted at the same luminance level under white and blue conditions. The white stimulus has a broad-band spectrum which stimulates the long (L)-, middle (M)- and short (S)-wavelength sensitive cones; while the blue stimulus has a narrow-band spectrum and it mainly stimulates the S-wavelength sensitive cones. The Wratten 47A filter used (λmax = 450um) minimizes but does not totally eliminate the involvement of the L- and M-cone pathways. This would reduce the lateral antagonism between different cone pathways (Rangaswamy et al. 2007), an effect which is expected to enhance the mfERG responses.

8.1.5.2 The waveform and its representative components under long-duration stimulus mfERG

Because of the similarity of the "long-duration" protocols in the full-field electroretinogram and mfERG (Saeki & Gouras 1996; Kondo & Miyake 2000; Rangaswamy et al. 2007), it is proposed that the N2 trough found beyond the first P1 peak originates from the inner retinal layer, probably a site near the ganglion cell layer (Saeki & Gouras 1996; Kondo & Miyake 2000; Rangaswamy et al. 2007). Although, under the "long-duration" mfERG paradigm, the overlap between the on- and off-pathway responses was minimized, the on- and off-responses were not completely dissociated. The on-response is predominantly from the depolarizing bipolar cells shaped by the hyperpolarizing bipolar cells, while the off-response is predominantly from the hyperpolarizing bipolar cells shaped by the depolarizing bipolar cells (Miyake et al. 1987; Sieving 1993; Kondo & Miyake 2000; Ueno et al. 2006; Rangaswamy et al. 2007).

8.1.5.3 mfERG response in diabetic retina

Under both the white and blue stimulation conditions, the N2 amplitude in the diabetic group was larger than that in the control group. The on-response component under blue stimulus conditions increased in the diabetic group. Four possibilities may lead to an increase of the N2 amplitude in the DM patients: 1) Stronger activity of the inner retina (near the ganglion cell layer); 2) Reduced on-pathway activity; 3) Enhanced off-pathway activity; 4) Weakening of the lateral antagonistic interaction. However, the first three possibilities appear unable to explain the changes in the DM patients. Firstly, previous morphological studies (Barber et al. 1998; Lopes de Faria et al. 2002; Ozdek et al. 2002; Barber 2003; Sugimoto et al. 2005; Kern & Barber 2008; Sato et al. 2008; Takahashi & Chihara 2008; Oshitari et al. 2009; Barber et al. 2011) have indicated that the inner retinal structure is altered, with increased neural apoptosis, reduced rather than increased inner retinal responses have been reported (Palmowski et al. 1997; Fortune et al. 1999; Kurtenbach et al. 2000; Onozu & Yamamoto 2003; Bearse et al. 2004; Bearse et al. 2004; Han et al. 2004; Han et al. 2004; Han et al. 2004; Bearse et al. 2006; Ng et al. 2008; Bronson-Castain et al. 2009; Harrison et al. 2011). Secondly, the P1 and N2 amplitudes in the diabetic group were generally greater than in the control group. This seems to oppose the possibility stated above as point 2). Thus, the increased N2 amplitude cannot be simply explained by changes in the activities of the ganglion cells, the on- or off-pathways alone. Probably the antagonistic interactions within retinal cellular components play a role on the enhancement of the N2 amplitude.

8.1.5.4 Role of lateral antagonism

Considering the hypothesized changes in lateral antagonism, when the stimulus

was changed from white (broad-band) to blue (narrow-band), it was proposed that there was a reduction in antagonistic interaction (Rangaswamy et al. 2007) and this resulted in an increase of the mfERG amplitude. This was reflected by the positive percentage amplitude change found in our results as seen in Figures 8.6a-c.

The higher the percentage value of the mfERG amplitude change calculated in the results (Figure 8.6), the greater would be the hypothesized reduction in lateral antagonistic interaction due to the change of stimulus colours from white to blue. Comparing the percentage change of the mfERG amplitude in both subject groups, the control group initially showed a greater percentage change than the diabetic group in terms of the on-response P1, but a reverse trend was apparent in the later on-response component N2 and the off-response component P2, although these data do show marked variability. It is suggested that both the N2 and P2 components share a common origin, most likely the off-pathway, which, we suggest, exerts less antagonistic interaction to the on-pathway in the early stage of DM. These effects were consistent across the retina, but only reached statistical significance for ring 5 (see Figure 8.6b). Whether the peripheral retina is more prone to this functional loss still needs further investigation.

8.1.5.5 Proposed explanations of the long-duration stimulus mfERG changes in DM patients

Previous electroretinogram studies (Brinchmann-Hansen et al. 1992; Palmowski et al. 1997; Fortune et al. 1999; Kaneko et al. 2000; Kurtenbach et al. 2000; Shimada et al. 2001; Bearse et al. 2003; Onozu & Yamamoto 2003; Bearse et al. 2004; Han et al. 2004; Han et al. 2004; Tyrberg et al. 2005; Bearse et al. 2006;

Kizawa et al. 2006; Chen et al. 2008; Ng et al. 2008; Bronson-Castain et al. 2009; Harrison et al. 2011; Laron et al. 2011; Lung et al. 2012; Lung et al. 2012) reported a decrease in the inner retinal responses rather than an enhanced response. However, in this experiment, greater amplitude was recorded from the diabetic subjects when the blue stimulus was used. The dissociation of the on- and off-retinal pathway activities by the long-duration paradigm can allow subtle changes in responses of the diabetic retina to be more readily observed. It is possible that the changes or weakening of the inhibitory interaction between different retinal pathways will cause this enhancement of mfERG response. In the full-field electroretinogram, a decrease of photopic negative response has been reported for a brief blue flash stimulus. (McFarlane et al. 2012) The dark frames in this mfERG paradigm help to eliminate the temporal adaptive effect of the successive flash stimuli, but there may be a certain spatial lateral effect from the neighboring hexagons which may affect the high-order retinal response. Thus the N2 component may not be directly comparable to the photopic negative response in the conventional full-field electroretinogram. Further studies on the long-duration full-field electroretinogram on diabetic patients and on animal models using pharmacological dissection of the response (Sieving 1993; Hood et al. 1999; Ueno et al. 2006; Rangaswamy et al. 2007) should be conducted in order to increase our understanding of the cellular origin of the N2 component.

Chapter 9: Summary of experimental results, conclusions and suggestions for future research

9.1 Summary of experimental results

DM has become one of the health problems of greatest concern in Hong Kong. According to a recent report from the Hong Kong Society for Endocrinology, nearly 10% of the Hong Kong population was suffering from DM (Diabetes Division, Hong Kong Society for Endocrinology, Metabolism and Reproduction 2000). DM can lead to DR, which is one of the most common causes of blindness. About 28.4% of DM patients in Hong Kong have developed DR with levels ranging from the minimal non-proliferative type to the sight-threatening proliferative type (Tam et al., 2005).

Since the prevalence of early-onset type II diabetes is continuously increasing globally (Rosenbloom et al. 1999; WHO 2012) and it is estimated that nearly all type I DM patients and more than 60% of the type II DM patients will progress to have DR during the first two decades after diagnosis of DM (Fong et al. 2003). This public health issue will create a heavy financial burden on society. With appropriate assessment and treatment, more than 90% of visual loss resulting from DR can be prevented (Li et al. 2004). Better knowledge of the abnormalities in diabetic retinopathy will help to delay as well as to prevent visual loss in DM patients.

By using current clinical tests, only obvious retinal defects or damage can be ruled out (Carmichael et al. 2005). DM affects the capillary circulation and thus leads to ocular disorders. This has a large impact on the inner retinal segment and is believed to affect retinal signal transmission and efficiency. The mfERG offers

a technique that can reflect the abnormalities of retinal functions before the presence of significant observable signs (Shimada et al. 2001). Here, a modified mfERG paradigm (MOFO mfERG) was applied in order to screen out the potential retinal sites with the functional changes in the early stage of DR. Before the paradigm can be used, it is necessary to determine the optimal luminance combination for the MOFO mfERG measurement.

In Experiment A1, sixteen luminance combinations of the global (g) and focal (f) flashes in the MOFO mfERG paradigm were investigated. The experiment demonstrated the variations of the amplitudes and implicit time of the two main parameters, DC and IC under different g/f ratios. The DC amplitude increases approximately with the focal flash intensity and achieves the maximum value when the g/f ratio is kept at the minimal value among the sixteen luminance combinations. The IC amplitude achieves the peak value when the g/f ratio is kept at 2:1. DC and IC implicit times change in opposite directions. With the increasing g/f ratio, DC is less delayed while the IC is more postponed.

Considering together with the ISCEV guideline (2007) (Hood et al. 2008) and patient's discomfort, a focal flash intensity between 100 and 200 cd/m^2 with g/f $\leq$1 (i.e. 100 cd/m^2 < f $\leq$ 200 cd/m^2, f $\geq$ g) is recommended to obtain an optimal DC response. To obtain an optimal IC response, with a g/f ratio 2:1 is recommended.

Therefore, in order to obtain a considerable DC and IC amplitudes together, a g/f ratio equals to 1, and a focal flash intensity above 100 cd/m^2 and equal to or below 200 cd/m^2 is recommended.

In Experiment A2, the MOFO mfERG was applied to investigate the early functional changes in different types of localized diabetic retinal lesions under high and low contrast conditions. With the increase of DR severity, greater delay and amplitude reduction were found, which indicates a further deterioration of retinal function. The amplitudes of IC from the high contrast condition and DC at both high and low contrast conditions are sensitive indicators which can be used to screen out early functional anomalies before DR is seen in the diabetic retina. Both the reduction and delay of the DC and IC parameters suggest that the middle and inner retinal layers are impaired in diabetic patients even before visible DR can be detected by the usual clinical assessments.

In Experiment B, three ocular measurements were carried out in the diabetic retina. The measurements were the MOFO mfERG, visual field and retinal nerve fiber thickness assessment by OCT. A combination of the topographic mapping among the localized data from these three ocular assessments was performed. It was used to compare the sensitivity of these three assessments in diabetic patients and to investigate the localized morphological and functional changes in diabetic lesions. The MOFO mfERG responses generally correlate better with automated perimetry data than do the morphological RNFL thickness measures. The amplitude of mfERG parameters has a more consistent correlation with the perimetric sensitivity than does the implicit time. The MOFO mfERG is superior to the other two assessments in differentiating the diabetic retinal area without DR from other retinal areas. However, only a moderate correlation exists between the MOFO mfERG and localized luminance sensitivity as found in the visual field tests. The changes observed in the MOFO mfERG and its weak to moderate correlations with the RNFL thickness and luminance sensitivity

indicate that the alteration of the adaptive function in the diabetic retina is in the middle and/or inner retinal layers, but appears not to show any effects on the RNFL. The correlation between the MOFO mfERG and luminance sensitivity exists across all diabetic samples, including those without any visible DR signs. This implies that the functional deterioration should exist much earlier than the vascular changes in the human diabetic retina.

From the above experiments, it has demonstrated that the functional deterioration exists at the middle and /or inner retina even before the visible DR lesions. The functional deterioration can only be partially explained by the luminance sensitivity reduction while the structural changes of the RNFL do not have any significant association with it. The cellular structures, which are responsible for the lateral antagonism, are probably vulnerable in the disease of DM. It would be probably one of the new areas to study for the early changes in diabetic human retina.

In order to further investigate the function of the middle to inner retinal layers, Experiment C was carried out. This experiment examined antagonistic processes by means of a "long-duration" mfERG paradigm. The "long-duration" mfERG measurement was carried out using blue and white stimuli. The "long-duration" mfERG minimizes the overlap of the on- and off-pathway responses as compared to the conventional mfERG paradigm. With the insertion of a blue colour filter, the stimulus changes from a white (broad-band spectral stimulation) to blue (narrow-band spectral stimulation), and there is a decreased involvement of lateral antagonism. The larger amplitude of the on-response component (N2) in the diabetic patients suggested an imbalance of lateral antagonism in the diabetic

retina at the early stage (with no or mild NPDR) of the disease. This situation seems unlikely be solely explained by the changes of ganglion cells, the on- or off-pathways. It is hypothesized that the decreased percentage change of the N2 amplitude in the diabetic group may further indicate an impairment of the interaction at the middle retinal level.

Novel findings from the above experiments were, firstly, it demonstrated the linear and non-linear properties of the DC and IC responses through repeated measures experimental design of the MOFO mfERG paradigm. The optimal luminance combination of MOFO mfERG measurement was also obtained. Secondly, by means of MOFO mfERG, it showed that the functional deterioration exists at the middle and /or inner retina even before the visible DR lesions. Thirdly, the amplitudes of the DC and IC responses have better diagnostic power in screening out the diabetic retina than the implicit time. Fourthly, MOFO mfERG paradigm is superior to two other common clinical devices (automated perimetry and OCT) in differentiating the "No DR" retina from the "DR" retina. Furthermore the functional deterioration in the diabetic retina can only be partially explained by the luminance sensitivity reduction, while the structural changes of RNFL do not have any significant association with it. Fifthly, the cellular structures, which are responsible for the lateral antagonism, are vulnerable in the disease of DM. It would be probably one of the new areas to study for the early changes in diabetic human retina.

The objective mfERG findings of the above experiments agree with previous studies (as mentioned in Ch. 4.3), that functional deterioration exists early, becoming apparent before the clinically visible vascular changes. The MOFO

mfERG indicates that the functional deterioration exists before the visible vascular lesions in the human diabetic retina. With the comparison among mfERG, automated perimetry and OCT RNFL thickness measurement, it further provides evidence that the functional deterioration comes earlier than the structural damage in humans. Together with the imbalance of the lateral antagonism for those with no or only mild NPDR lesions from the above experiments, it proposes that the functional damage may exist earlier than the structural damage in the diabetic retina. Applying similar experimental setup to study the retinal functional changes in the type I diabetic patients who are newly diagnosed would have been useful for providing further support on this hypothesis. As the functional deterioration of the type I diabetic patients can be investigated before the development of any vascular damage which was proposed not to exist in the first month of the onset of DM.

The mfERG paradigm shows a greater power to differentiate the "No DR" retina from the "DR" retina than two other common clinical devices. The results from this study can help to develop a method for early detection in preventing or delaying the progression of the sight-threatening visual loss in the diabetic patients, for use in daily clinical operation. We hope this would relieve the social economic burden on this public health issue by reducing the number of DR cases at advance stage in terms of early detection and prompt treatment at the early stage. Moreover, with the application of the modified mfERG paradigms and with different stimulus colours, it is proposed that the middle retinal components may indicate the potential retinal sites vulnerable at the early stages of DM. These techniques will help to provide target retinal components to assess experimental therapeutic treatment(s) in DR, to assist in retaining the retinal

function before irreversible retinopathy occurs.

9.2 Limitations of in this study

Due to the upper luminance limitation of the mfERG display unit, the luminance combination in Experiment A1 reached only a maximum value of 400 cd/m^2. The optimal luminance for MOFO mfERG may be beyond this limited range, but the value reached is within the range suggested by the international guideline (Hood et al. 2012).

In the diabetic experiments, the recruited subjects in this study were from the optometric clinic in The Hong Kong Polytechnic University. The medical history of the diabetic patients heavily depended on the hospital medical summary kept by the patients. However, there was a lack of detail about the glycemic control status and the exact onset time of the DM condition. This is a common problem faced in the study of type II DM, as there is always a variable latent period before the condition is diagnosed. Applying similar experimental set-up in type I diabetic patients who are newly diagnosed would have been helpful to study the early functional changes in the human diabetic retina. Moreover, HbA1c of the blood sample would have provided a more reliable plasma glucose level than the on-site fasting spot test. As the HbA1c can reflect the estimation of the averaged plasma glucose level for the past 120 days while the spot test can only reflect the instant plasma glucose level in the capillary which can be fluctuated.

In Experiments A2 to C, the crystalline lenses of the diabetic subjects and their age-matched controls were assessed by the slit-lamp biomicroscopy. Although previous studies (as mentioned in Ch. 4.1.2) found that the crystalline lenses of

the type II diabetic patients were not significantly different from the age-matched healthy controls, performing objective clinical assessments of the crystalline lens by means of ultrasonic or optical methods would have been helpful in a quantitative analysis for showing the non-significant difference in each experiment.

In Experiment C, although the blue stimulation was used, there were still mild middle-wavelength (MW) cone pathway being triggered; if possible, a suppressive amber background would have been helpful in isolating different cone pathway responses in order to further explore the retinal antagonistic interactions at the middle retina.

In terms of the clinical assessments, the major limitations of my study were the absence of fundus fluorescein angiogram (FFA), contrast sensitivity (CS) and colour vision assessments. Performing the FFA would have allowed me to understand the retinal blood circulation and vascular perfusion in a deeper extent. Combining the fundus photodocumentation, biomicroscopy and FFA, the sensitivity and accuracy for classifying DR lesions would have been markedly increased. This would have been useful to improve the grading system of the DR severity in Experiments A2 and B. With the improved grading system, the variation of the experimental data in Experiments A2 and B would be minimized and the "true" diagnostic values of MOFO mfERG would be reflected.

CS and colour vision assessments, as subjective functional tests, were reported to have deterioration in diabetic patients at early stage. Although the accuracy of CS was reported to be low (Ismail & Whitaker 1998) as mentioned in Ch. 4.2.2,

collecting the CS data would have provided a more comprehensive picture of the functional deterioration in the diabetic retina. This would have been helpful to link the objective mfERG functional findings to the subjective visual symptoms of the diabetic patients in their daily life.

Blue-yellow acquired colour deficiency was reported in the diabetic patients (Ismail & Whitaker 1998) as mentioned in Ch. 4.2.3. Collecting the data of the subjective colour vision test would have provided more information for the comparison of the objective mfERG findings from the blue-pathway in Experiment C.

Combining my mfERG findings with the additional clinical data from the FFA, CS and colour vision assessments, it would have provided a more detailed picture of the subjective and objective functional deterioration of the diabetic patients. Variations among the test results might have been useful in further sub-categorizing the diabetic patients into different stages.

9.3 Suggestions for future research

The findings from the human diabetic retina proposed that the impairment of the inhibitory interaction between different retinal pathways may play a key role at the early stage of the disease. In order to further investigate the antagonistic interaction properties, pharmacological dissection studies as suggested by Hood et al. and Chu et al. (Hood et al. 2002; Chu et al. 2008) of the "long-duration" mfERG in an animal model (such as pig or primate) will help to isolate the cellular component contributing to N2. Studying the "long-duration" mfERG component N2, which was found to be affected in the diabetic retina, in both

control and diabetic models will be useful in order to explore further aspects of the cellular or physiological changes in the diabetic retina.

Moreover, applying different chromatic stimuli with suppressive background may help to further understand this property. As in the current study, it was hypothesized that the middle retina might be a potential site early affected in the diabetic patients, although the blue stimuli was used, there were still mild MW cone pathway being triggered; if possible, a suppressive amber background will be helpful in isolating different cone pathway responses in order to further explore the retinal antagonistic interactions at the middle retina.

A more systematic recruitment of the subjects with clear onset time and known glycemic control condition on both types I and II diabetic patients will give a better understanding of the difference of these two types of DM. Measurement of HbA1c rather than the instant capillary plasma glucose level is suggested in order to obtain a more reliable plasma glucose level reading. Further subcategories of diabetic patients in term of medical intervention and glycemic control will give more details of the nature of the disease. Those with glucose intolerance will also be an interesting group for investigation, in the period before they deteriorate to become diabetic.

References

Agardh E, Stjernquist H, Heijl A & Bengtsson B (2006): Visual acuity and perimetry as measures of visual function in diabetic macular oedema. Diabetologia 49: 200-6.

Aiello LP, Gardner TW, King GL, Blankenship G, Cavallerano JD, Ferris III FL & Klein R (1998): Diabetic retinopathy. Diabetes Care 21: 143-56.

Alberti KG & Zimmet PZ (1998): Definition, diagnosis and classification of diabetes mellitus and its complications. Part 1: diagnosis and classification of diabetes mellitus provisional report of a WHO consultation. Diabet Med 15: 539-53.

Alder VA, Cringle SJ & Constable IJ (1983): The retinal oxygen profile in cats. Invest Ophthalmol Vis Sci 24: 30-6.

Aldington SJ, Kohner EM, Meuer S, Klein R & Sjolie AK (1995): Methodology for Retinal Photography and Assessment of Diabetic-Retinopathy - the Eurodiab IDDM Complications Study. Diabetologia 38: 437-444.

Arden GB & Constable PA (2006): The electro-oculogram. Prog Retin Eye Res 25: 207-48.

Arden GB, Gunduz MK, Kurtenbach A, Volker M, Zrenner E, Gunduz SB, Kamis U, Ozturk BT & Okudan S (2010): A preliminary trial to determine whether prevention of dark adaptation affects the course of early diabetic retinopathy. Eye 24: 1149-55.

Arden GB, Wolf JE & Tsang Y (1998): Does dark adaptation exacerbate diabetic retinopathy? Evidence and a linking hypothesis. Vision Res 38: 1723-9.

Asano E, Mochizuki K, Sawada A, Nagasaka E, Kondo Y & Yamamoto T (2007): Decreased nasal-temporal asymmetry of the second-order kernel response of multifocal electroretinograms in eyes with normal-tension glaucoma. Jpn J Ophthalmol 51: 379-89.

Bandello F, Lattanzio R, Zucchiatti I & Del Turco C (2013): Pathophysiology and treatment of diabetic retinopathy. Acta Diabetol 50: 1-20.

Barber AJ (2003): A new view of diabetic retinopathy: a neurodegenerative disease of the eye. Prog Neuropsychopharmacol Biol Psychiatry 27: 283-90.

Barber AJ, Gardner TW & Abcouwer SF (2011): The significance of vascular and neural apoptosis to the pathology of diabetic retinopathy. Invest Ophthalmol Vis Sci 52: 1156-63.

Barber AJ, Lieth E, Khin SA, Antonetti DA, Buchanan AG & Gardner TW (1998): Neural apoptosis in the retina during experimental and human diabetes. Early onset and effect of insulin. J Clin Invest 102: 783-91.

Bearse MA Jr, Adams AJ, Han Y, Schneck ME, Ng J, Bronson-Castain K & Barez S (2006): A multifocal electroretinogram model predicting the development of diabetic retinopathy. Prog Retin Eye Res 25: 425-48.

Bearse MA Jr, Han Y, Schneck ME & Adams A (2003): Enhancement and mapping of inner retinal contributions to the human multifocal electroretinogram (mfERG). Invest Ophthalmol Vis Sci 44: ARVO E-abstract 2696.

Bearse MA Jr, Han Y, Schneck ME & Adams AJ (2004): Retinal function in normal and diabetic eyes mapped with the slow flash multifocal electroretinogram. Invest Ophthalmol Vis Sci 45: 296-304.

Bearse MA Jr, Han Y, Schneck ME, Barez S, Jacobsen C & Adams AJ (2004): Local multifocal oscillatory potential abnormalities in diabetes and early diabetic retinopathy. Invest Ophthalmol Vis Sci 45: 3259-65.

Bearse MA Jr & Sutter EE (1999): Contrast dependence of multifocal ERG components. Vision Science and Its Applications, OSA Technical Digest Series 1: 24-27.

Bek T & Lund-Andersen H (1990): Localised blood-retinal barrier leakage and retinal light sensitivity in diabetic retinopathy. Br J Ophthalmol 74: 388-92.

Bengtsson B, Heijl A & Agardh E (2005): Visual fields correlate better than visual acuity to severity of diabetic retinopathy. Diabetologia 48: 2494-500.

Bengtsson B, Hellgren KJ & Agardh E (2008): Test-retest variability for standard automated perimetry and short-wavelength automated perimetry in diabetic patients. Acta Ophthalmol 86: 170-6.

Biallosterski C, Van Velthoven ME, Michels RP, Schlingemann RO, DeVries JH & Verbraak FD (2007): Decreased optical coherence tomography-measured pericentral retinal thickness in patients with diabetes mellitus type 1 with minimal diabetic retinopathy. Br J Ophthalmol 91: 1135-8.

Bloomgarden ZT (2008): Diabetic retinopathy. Diabetes Care 31: 1080-3.

Bresnick GH, Condit RS, Palta M, Korth K, Groo A & Syrjala S (1985): Association of hue discrimination loss and diabetic retinopathy. Arch Ophthalmol 103: 1317-24.

Bressler NM, Edwards AR, Antoszyk AN, Beck RW, Browning DJ, Ciardella AP, Danis RP, Elman MJ, Friedman SM, Glassman AR, Gross JG, Li HK, Murtha TJ, Stone TW & Sun JK (2008): Retinal thickness on Stratus optical coherence tomography in people with diabetes and minimal or no

diabetic retinopathy. Am J Ophthalmol 145: 894-901.

Brinchmann-Hansen O, Dahl-Jorgensen K, Hanssen KF & Sandvik L (1992): Oscillatory potentials, retinopathy, and long-term glucose control in insulin-dependent diabetes. Acta Ophthalmol (Copenh) 70: 705-12.

Bronson-Castain KW, Bearse MA Jr, Neuville J, Jonasdottir S, King-Hooper B, Barez S, Schneck ME & Adams AJ (2009): Adolescents with type 2 diabetes early indications of focal retinal neuropathy, retinal thinning, and venular dilation. Retina 29: 618-26.

Browning DJ, Fraser CM & Clark S (2008): The relationship of macular thickness to clinically graded diabetic retinopathy severity in eyes without clinically detected diabetic macular edema. Ophthalmology 115: 533-9.

Camera A, Hopps E & Caimi G (2007): Diabetic microangiopathy: physiopathological, clinical and therapeutic aspects. Minerva Endocrinol 32: 209-29.

Carmichael TR, Carp GI, Welsh ND & Kalk WJ (2005): Effective and accurate screening for diabetic retinopathy using a 60 degree mydriatic fundus camera. S Afr Med J 95: 57-61.

Chan HH & Brown B (2000): Pilot study of the multifocal electroretinogram in ocular hypertension. Br J Ophthalmol 84: 1147-53.

Chan HH, Ng YF & Chu PH (2011): Applications of the multifocal electroretinogram in the detection of glaucoma. Clin Exp Optom 94: 247-58.

Chan HL & Brown B (1998): Investigation of retinitis pigmentosa using the multifocal electroretinogram. Ophthalmic Physiol Opt 18: 335-50.

Chan HL & Brown B (1999): Multifocal ERG changes in glaucoma. Ophthalmic Physiol Opt 19: 306-16.

Chen H, Zhang M, Huang S & Wu D (2008): The photopic negative response of flash ERG in nonproliferative diabetic retinopathy. Doc Ophthalmol 117: 129-35.

Chylack LT Jr, Wolfe JK, Singer DM, Leske MC, Bullimore MA, Bailey IL, Friend J, McCarthy D & Wu SY (1993): The Lens Opacities Classification System III. The longitudinal study of cataract study group. Arch Ophthalmol 111: 831-36.

Cho HY, Lee DH, Chung SE & Kang SW (2010): Diabetic retinopathy and peripapillary retinal thickness. Korean J Ophthalmol 24: 16-22.

Chu PH, Chan HH & Brown B (2006): Glaucoma detection is facilitated by luminance modulation of the global flash multifocal electroretinogram.

Invest Ophthalmol Vis Sci 47: 929-37.

Chu PH, Chan HH & Brown B (2007): Luminance-modulated adaptation of global flash mfERG: fellow eye losses in asymmetric glaucoma. Invest Ophthalmol Vis Sci 48: 2626-33.

Chu PH, Chan HH, Ng YF, Brown B, Siu AW, Beale BA, Gilger BC & Wong F (2008): Porcine global flash multifocal electroretinogram: possible mechanisms for the glaucomatous changes in contrast response function. Vision Res 48: 1726-34.

Clark M (2004): Understanding diabetes. Chichester ; John Wiley and Sons Ltd: pp.1-3.

Cunha-Vaz J (2007): Characterization and relevance of different diabetic retinopathy phenotypes. Dev Ophthalmol 39: 13-30.

DeBuc DC & Somfai GM (2010): Early detection of retinal thickness changes in diabetes using OCT. Med Sci Monit 16: 15-21.

Dersu I & Wiggins MN (2006): Understanding visual fields, Part II: Humphrey visual fields. Journal of Ophthalmic Medical Technology 2.

Diabetes Division, Hong Kong Society for Endocrinology, Metabolism and Reproduction (2000): A statement for health care professionals on type 2 diabetes mellitus in Hong Kong. Hong Kong Med J 6: 105-7.

Early Treatment Diabetic Retinopathy Study Research Group (1991): Fundus photographic risk factors for progression of diabetic retinopathy. ETDRS report number 12. Ophthalmology 98: 823-33.

Early Treatment Diabetic Retinopathy Study Research Group (1991): Grading diabetic retinopathy from stereoscopic color fundus photographs--an extension of the modified Airlie House classification. ETDRS report number 10. Ophthalmology 98: 786-806.

Elner SG, Elner VM, Field MG, Park S, Heckenlively JR & Petty HR (2008): Retinal flavoprotein autofluorescence as a measure of retinal health. Trans Am Ophthalmol Soc 106: 215-24.

Feitosa-Santana C, Oiwa NN, Paramei GV, Bimler D, Costa MF, Lago M, Nishi M & Ventura DF (2006): Color space distortions in patients with type 2 diabetes mellitus. Vis Neurosci 23: 663-8.

Fong DS, Aiello L, Gardner TW, King GL, Blankenship G, Cavallerano JD, Ferris III FL & Klein R (2003): Diabetic retinopathy. Diabetes Care 26: 226-9.

Fortune B, Schneck ME & Adams AJ (1999): Multifocal electroretinogram delays reveal local retinal dysfunction in early diabetic retinopathy. Invest Ophthalmol Vis Sci 40: 2638-51.

Friberg TR, Lace J, Rosenstock J & Raskin P (1987): Retinal microaneurysm counts in diabetic retinopathy: colour photography versus fluorescein angiography. Can J Ophthalmol 22: 226-9.

Garg S & Davis RM (2009): Diabetic retinopathy screening update. Clinical diabetes 27: 140-5.

Garway-Heath DF, Holder GE, Fitzke FW & Hitchings RA (2002): Relationship between electrophysiological, psychophysical, and anatomical measurements in glaucoma. Invest Ophthalmol Vis Sci 43: 2213-20.

Garway-Heath DF, Poinoosawmy D, Fitzke FW & Hitchings RA (2000): Mapping the visual field to the optic disc in normal tension glaucoma eyes. Ophthalmology 107: 1809-15.

Gerth C (2009): The role of the ERG in the diagnosis and treatment of Age-Related Macular Degeneration. Doc Ophthalmol 118: 63-8.

Ghirlanda G, Di Leo MA, Caputo S, Cercone S & Greco AV (1997): From functional to microvascular abnormalities in early diabetic retinopathy. Diabetes Metab Rev 13: 15-35.

Greenstein VC, Hood DC, Ritch R, Steinberger D & Carr RE (1989): S (blue) cone pathway vulnerability in retinitis pigmentosa, diabetes and glaucoma. Invest Ophthalmol Vis Sci 30: 1732-7.

Han Y, Adams AJ, Bearse MA Jr & Schneck ME (2004): Multifocal electroretinogram and short-wavelength automated perimetry measures in diabetic eyes with little or no retinopathy. Arch Ophthalmol 122: 1809-15.

Han Y, Bearse MA Jr, Schneck ME, Barez S, Jacobsen C & Adams AJ (2004): Towards optimal filtering of "standard" multifocal electroretinogram (mfERG) recordings: findings in normal and diabetic subjects. Br J Ophthalmol 88: 543-50.

Han Y, Bearse MA Jr, Schneck ME, Barez S, Jacobsen CH & Adams AJ (2004): Multifocal electroretinogram delays predict sites of subsequent diabetic retinopathy. Invest Ophthalmol Vis Sci 45: 948-54.

Hanover JA (2001): Glycan-dependent signaling: O-linked N-acetylglucosamine. FASEB J 15: 1865-76.

Harding SP, Broadbent DM, Neoh C, White MC & Vora J (1995): Sensitivity and specificity of photography and direct ophthalmoscopy in screening for sight threatening eye disease: the Liverpool Diabetic Eye Study. BMJ 311: 1131-5.

Harrison WW, Bearse MA Jr, Ng JS, Jewell NP, Barez S, Burger D, Schneck ME & Adams AJ (2011): Multifocal electroretinograms predict onset of

diabetic retinopathy in adult patients with diabetes. Invest Ophthalmol Vis Sci 52: 772-7.

Heijl A & Patella VM (2002): Essential perimetry: The field analyzer primer. Germany; Carl Zeiss Meditec Inc.: pp. 44-70.

Heintz E, Wirehn AB, Peebo BB, Rosenqvist U & Levin LA (2010): Prevalence and healthcare costs of diabetic retinopathy: a population-based register study in Sweden. Diabetologia 53: 2147-54.

Hellstedt T, Vesti E & Immonen I (1996): Identification of individual microaneurysms: a comparison between fluorescein angiograms and red-free and colour photographs. Graefes Arch Clin Exp Ophthalmol 234 Suppl 1: S13-7.

Heng LZ, Comyn O, Peto T, Tadros C, Ng E, Sivaprasad S & Hykin PG (2013): Diabetic retinopathy: pathogenesis, clinical grading, management and future developments. Diabet Med 30: 640-50.

Henson DB & North RV (1979): Dark adaptation in diabetes mellitus. Br J Ophthalmol 63: 539-41.

Holopigian K, Greenstein VC, Seiple W, Hood DC & Carr RE (1997): Evidence for photoreceptor changes in patients with diabetic retinopathy. Invest Ophthalmol Vis Sci 38: 2355-65.

Holopigian K, Seiple W, Lorenzo M & Carr R (1992): A comparison of photopic and scotopic electroretinographic changes in early diabetic retinopathy. Invest Ophthalmol Vis Sci 33: 2773-80.

Holt RI (2004): Diagnosis, epidemiology and pathogenesis of diabetes mellitus: an update for psychiatrists. Br J Psychiatry Suppl 47: S55-63.

Hood DC (2003): Objective measurement of visual function in glaucoma. Curr Opin Ophthalmol 14: 78-82.

Hood DC, Bach M, Brigell M, Keating D, Kondo M, Lyons JS, Marmor MF, McCulloch DL & Palmowski-Wolfe AM (2012): ISCEV standard for clinical multifocal electroretinography (mfERG) (2011 edition). Doc Ophthalmol 124: 1-13.

Hood DC, Bach M, Brigell M, Keating D, Kondo M, Lyons JS & Palmowski-Wolfe AM (2008): ISCEV guidelines for clinical multifocal electroretinography (2007 edition). Doc Ophthalmol 116: 1-11.

Hood DC, Frishman LJ, Saszik S & Viswanathan S (2002): Retinal origins of the primate multifocal ERG: implications for the human response. Invest Ophthalmol Vis Sci 43: 1673-85.

Hood DC, Greenstein V, Frishman L, Holopigian K, Viswanathan S, Seiple W, Ahmed J & Robson JG (1999): Identifying inner retinal contributions to

the human multifocal ERG. Vision Res 39: 2285-91.

Hood DC, Seiple W, Holopigian K & Greenstein V (1997): A comparison of the components of the multifocal and full-field ERGs. Vis Neurosci 14: 533-44.

Ismail GM & Whitaker D (1998): Early detection of changes in visual function in diabetes mellitus. Ophthalmic Physiol Opt 18: 3-12.

Jeppesen P, Knudsen ST, Poulsen PL, Mogensen CE, Schmitz O & Bek T (2007): Response of retinal arteriole diameter to increased blood pressure during acute hyperglycaemia. Acta Ophthalmol Scand 85: 280-6.

Kaneko M, Sugawara T & Tazawa Y (2000): Electrical responses from the inner retina of rats with streptozotocin-induced early diabetes mellitus. J Jpn Ophthalmol Soc 101: 775-8.

Kempen JH, O'Colmain BJ, Leske MC, Haffner SM, Klein R, Moss SE, Taylor HR & Hamman RF (2004): The prevalence of diabetic retinopathy among adults in the United States. Arch Ophthalmol 122: 552-63.

Kern TS & Barber AJ (2008): Retinal ganglion cells in diabetes. J Physiol 586: 4401-8.

Kern TS & Engerman RL (1995): Vascular lesions in diabetes are distributed non-uniformly within the retina. Exp Eye Res 60: 545-9.

Khalaf SS, Al-Bdour MD & Al-Till MI (2007): Clinical biomicroscopy versus fluorescein angiography: effectiveness and sensitivity in detecting diabetic retinopathy. Eur J Ophthalmol 17: 84-8.

Khan ZA & Chakrabarti S (2007): Cellular signaling and potential new treatment targets in diabetic retinopathy. Exp Diabetes Res 2007: 31867.

Kim SH, Lee SH, Bae JY, Cho JH & Kang YS (1997): Electroretinographic evaluation in adult diabetics. Doc Ophthalmol 94: 201-13.

Kizawa J, Machida S, Kobayashi T, Gotoh Y & Kurosaka D (2006): Changes of oscillatory potentials and photopic negative response in patients with early diabetic retinopathy. Jpn J Ophthalmol 50: 367-73.

Klein R, Klein BE, Moss SE, Davis MD & DeMets DL (1984): The Wisconsin epidemiologic study of diabetic retinopathy. II. Prevalence and risk of diabetic retinopathy when age at diagnosis is less than 30 years. Arch Ophthalmol 102: 520-6.

Klein R, Klein BE, Moss SE, Davis MD & DeMets DL (1984): The Wisconsin epidemiologic study of diabetic retinopathy. III. Prevalence and risk of diabetic retinopathy when age at diagnosis is 30 or more years. Arch Ophthalmol 102: 527-32.

Klemp K, Larsen M, Sander B, Vaag A, Brockhoff PB & Lund-Andersen H

(2004): Effect of short-term hyperglycemia on multifocal electroretinogram in diabetic patients without retinopathy. Invest Ophthalmol Vis Sci 45: 3812-9.

Kondo M & Miyake Y (2000): Assessment of local cone on- and off-pathway function using multifocal ERG technique. Doc Ophthalmol 100: 139-54.

Kondo M, Miyake Y, Horiguchi M, Suzuki S & Tanikawa A (1998): Recording multifocal electroretinogram on and off responses in humans. Invest Ophthalmol Vis Sci 39: 574-80.

Kowluru RA & Abbas SN (2003): Diabetes-induced mitochondrial dysfunction in the retina. Invest Ophthalmol Vis Sci 44: 5327-34.

Kowluru RA & Chan PS (2007): Oxidative stress and diabetic retinopathy. Exp Diabetes Res 2007: 43603-14.

Kretschmann U, Bock M, Gockeln R & Zrenner E (2000): Clinical applications of multifocal electroretinography. Doc Ophthalmol 100: 99-113.

Kurtenbach A, Flogel W & Erb C (2002): Anomaloscope matches in patients with diabetes mellitus. Graefes Arch Clin Exp Ophthalmol 240: 79-84.

Kurtenbach A, Langrova H & Zrenner E (2000): Multifocal oscillatory potentials in type 1 diabetes without retinopathy. Invest Ophthalmol Vis Sci 41: 3234-41.

Lai TY, Chan WM, Lai RY, Ngai JW, Li H & Lam DS (2007): The clinical applications of multifocal electroretinography: a systematic review. Surv Ophthalmol 52: 61-96.

Lam BL (2005): Electrophysiology of vision: clinical testing and applications. London; Taylor & Francis: pp. 1-83; 105-18.

Laron M, Bearse MA Jr, Bronson-Castain K, Jonasdottir S, King-Hooper B, Barez S, Schneck ME & Adams AJ (2011): Interocular symmetry of abnormal multifocal electroretinograms in adolescents with diabetes and no retinopathy. Invest Ophthalmol Vis Sci 53: 316-21.

LeRoith D, Taylor SI & Olefsky JM (2004): Diabetes mellitus - a fundamental and clinical text. Philadelphia; Lippincott Williams and Wilkins: pp. 458-9; 1441-54.

Li PS, Wong TH, Tang WW & Lai JS (2004): Diabetic retinopathy. Hong Kong Pract 26: 346-53.

Lieth E, Barber AJ, Xu B, Dice C, Ratz MJ, Tanase D & Strother JM (1998): Glial reactivity and impaired glutamate metabolism in short-term experimental diabetic retinopathy. Penn State Retina Research Group. Diabetes 47: 815-20.

Linsenmeier RA (1986): Effects of light and darkness on oxygen distribution and

consumption in the cat retina. J Gen Physiol 88: 521-42.

Linsenmeier RA, Braun RD, McRipley MA, Padnick LB, Ahmed J, Hatchell DL, McLeod DS & Lutty GA (1998): Retinal hypoxia in long-term diabetic cats. Invest Ophthalmol Vis Sci 39: 1647-57.

Liu DP, Molyneaux L, Chua E, Wang YZ, Wu CR, Jing H, Hu LN, Liu YJ, Xu ZR & Yue DK (2002): Retinopathy in a Chinese population with type 2 diabetes: factors affecting the presence of this complication at diagnosis of diabetes. Diabetes Res Clin Pract 56: 125-31.

Lopes de Faria JM, Russ H & Costa VP (2002): Retinal nerve fibre layer loss in patients with type 1 diabetes mellitus without retinopathy. Br J Ophthalmol 86: 725-8.

Lung JC & Chan HH (2010): Effects of luminance combinations on the characteristics of the global flash multifocal electroretinogram (mfERG). Graefes Arch Clin Exp Ophthalmol 248: 1117-25.

Lung JC, Swann PG & Chan HH (2012): Early local functional changes in the human diabetic retina: a global flash multifocal electroretinogram study. Graefes Arch Clin Exp Ophthalmol 250: 1745-54.

Lung JC, Swann PG, Wong DS & Chan HH (2012): Global flash multifocal electroretinogram: early detection of local functional changes and its correlations with optical coherence tomography and visual field tests in diabetic eyes. Doc Ophthalmol 125: 123-35.

Luo X, Patel NB, Harwerth RS & Frishman LJ (2011): Loss of the low-frequency component of the global-flash multifocal electroretinogram in primate eyes with experimental glaucoma. Invest Ophthalmol Vis Sci 52: 3792-804.

Luu CD, Koh AH & Ling Y (2005): The ON/OFF-response in retinopathy of prematurity subjects with myopia. Doc Ophthalmol 110: 155-61.

Luu CD, Szental JA, Lee SY, Lavanya R & Wong TY (2010): Correlation between retinal oscillatory potentials and retinal vascular caliber in type 2 diabetes. Invest Ophthalmol Vis Sci 51: 482-6.

Marmor MF, Tan F, Sutter EE & Bearse MA Jr (1999): Topography of cone electrophysiology in the enhanced S cone syndrome. Invest Ophthalmol Vis Sci 40: 1866-73.

Masland RH (2001): Neuronal diversity in the retina. Curr Opin Neurobiol 11: 431-6.

McFarlane M, Wright T, Stephens D, Nilsson J & Westall CA (2012): Blue Flash ERG PhNR Changes Associated with Poor Long-Term Glycemic Control in Adolescents with Type 1 Diabetes. Invest Ophthalmol Vis Sci 53:

741-8.

Miyake Y, Yagasaki K, Horiguchi M & Kawase Y (1987): On- and off-responses in photopic electroretinogram in complete and incomplete types of congenital stationary night blindness. Jpn J Ophthalmol 31: 81-7.

Mizutani M, Gerhardinger C & Lorenzi M (1998): Muller cell changes in human diabetic retinopathy. Diabetes 47: 445-9.

Nagy D, Schonfisch B, Zrenner E & Jagle H (2008): Long-term follow-up of retinitis pigmentosa patients with multifocal electroretinography. Invest Ophthalmol Vis Sci 49: 4664-71.

Ng JS, Bearse MA Jr, Schneck ME, Barez S & Adams AJ (2008): Local diabetic retinopathy prediction by multifocal ERG delays over 3 years. Invest Ophthalmol Vis Sci 49: 1622-8.

Ng YF, Chan HH, Chu PH, Siu AW, To CH, Beale BA, Gilger BC & Wong F (2008): Pharmacologically defined components of the normal porcine multifocal ERG. Doc Ophthalmol 116: 165-76.

Nilsson M, Von Wendt G, Wanger P & Martin L (2007): Early detection of macular changes in patients with diabetes using Rarebit Fovea Test and optical coherence tomography. Br J Ophthalmol 91: 1596-8.

Nitta K, Saito Y, Kobayashi A & Sugiyama K (2006): Influence of clinical factors on blue-on-yellow perimetry for diabetic patients without retinopathy: comparison with white-on-white perimetry. Retina 26: 797-802.

Ong GL, Ripley LG, Newsom RS, Cooper M & Casswell AG (2004): Screening for sight-threatening diabetic retinopathy: comparison of fundus photography with automated color contrast threshold test. Am J Ophthalmol 137: 445-52.

Onozu H & Yamamoto S (2003): Oscillatory potentials of multifocal electroretinogram in diabetic retinopathy. Doc Ophthalmol 106: 327-32.

Oshitari T, Hanawa K & Adachi-Usami E (2009): Changes of macular and RNFL thicknesses measured by Stratus OCT in patients with early stage diabetes. Eye 23: 884-9.

Ozawa L & Itoh M (2003): Cathode ray tube phosphors. Chem Rev 103: 3835-56.

Ozdek S, Lonneville YH, Onol M, Yetkin I & Hasanreisoglu BB (2002): Assessment of nerve fiber layer in diabetic patients with scanning laser polarimetry. Eye 16: 761-5.

Palmowski-Wolfe AM, Allgayer RJ, Vernaleken B, Schotzau A & Ruprecht KW (2006): Slow-stimulated multifocal ERG in high- and normal-tension

glaucoma. Doc Ophthalmol 112: 157-68.

Palmowski-Wolfe AM, Todorova MG, Orguel S, Flammer J & Brigell M (2007): The 'two global flash' mfERG in high and normal tension primary open-angle glaucoma. Doc Ophthalmol 114: 9-19.

Palmowski AM, Sutter EE, Bearse MA Jr & Fung W (1997): Mapping of retinal function in diabetic retinopathy using the multifocal electroretinogram. Invest Ophthalmol Vis Sci 38: 2586-96.

Parisi V & Uccioli L (2001): Visual electrophysiological responses in persons with type 1 diabetes. Diabetes Metab Res Rev 17: 12-8.

Parravano M, Oddone F, Mineo D, Centofanti M, Borboni P, Lauro R, Tanga L & Manni G (2008): The role of Humphrey Matrix testing in the early diagnosis of retinopathy in type 1 diabetes. Br J Ophthalmol 92: 1656-60.

Poloschek CM & Sutter EE (2002): The fine structure of multifocal ERG topographies. J Vis 2: 577-87.

Porta M & Bandello F (2002): Diabetic retinopathy - A clinical update. Diabetologia 45: 1617-34.

Raitelaitiene R, Paunksnis A, Ivanov L & Kurapkiene S (2005): Ultrasonic and biochemical evaluation of human diabetic lens. Medicina (Kaunas) 41: 641-8.

Rangaswamy NV, Shirato S, Kaneko M, Digby BI, Robson JG & Frishman LJ (2007): Effects of Spectral Characteristics of Ganzfeld Stimuli on the Photopic Negative Response (PhNR) of the ERG. Invest Ophthalmol Vis Sci 48: 4818-28.

Remky A, Weber A, Hendricks S, Lichtenberg K & Arend O (2003): Short-wavelength automated perimetry in patients with diabetes mellitus without macular edema. Graefes Arch Clin Exp Ophthalmol 241: 468-71.

Resnikoff S, Pascolini D, Etya'ale D, Kocur I, Pararajasegaram R, Pokharel GP & Mariotti SP (2004): Global data on visual impairment in the year 2002. Bull World Health Organ 82: 844-51.

Rosenbloom AL, Joe JR, Young RS & Winter WE (1999): Emerging epidemic of type 2 diabetes in youth. Diabetes Care 22: 345-54.

Rudnicka AR & Birch J (2000): Diabetic eye disease - identification and co-management. Oxford; Butterworth-Heinemann: pp. 85-89.

Saeki M & Gouras P (1996): Cone ERGs to flash trains: the antagonism of a later flash. Vision Res 36: 3229-35.

Sato S, Hirooka K, Baba T, Yano I & Shiraga F (2008): Correlation between retinal nerve fibre layer thickness and retinal sensitivity. Acta Ophthalmol 86: 609-13.

Scanlon PH, Malhotra R, Greenwood RH, Aldington SJ, Foy C, Flatman M & Downes S (2003): Comparison of two reference standards in validating two field mydriatic digital photography as a method of screening for diabetic retinopathy. Br J Ophthalmol 87: 1258-63.

Schmier JK, Covert DW, Lau EC & Matthews GP (2009): Medicare expenditures associated with diabetes and diabetic retinopathy. Retina 29: 199-206.

Schmitz-Valckenberg S, Holz FG, Bird AC & Spaide RF (2008): Fundus autofluorescence imaging: review and perspectives. Retina 28: 385-409.

Schneck ME, Bearse MA Jr, Han Y, Barez S, Jacobsen C & Adams AJ (2004): Comparison of mfERG waveform components and implicit time measurement techniques for detecting functional change in early diabetic eye disease. Doc Ophthalmol 108: 223-30.

Schneck ME, Shupenko L & Adams AJ (2008): The fast oscillation of the EOG in diabetes with and without mild retinopathy. Doc Ophthalmol 116: 231-6.

Scott IU, Flynn HW & Smiddy WE (2010): Diabetes and ocular disease: past, present, and future therapies. Oxford; Oxford University Press: 13-24; 321-338.

Sharma KK & Santhoshkumar P (2009): Lens aging: effects of crystallins. Biochim Biophys Acta 1790: 1095-108.

Shiba T, Yamamoto T, Seki U, Utsugi N, Fujita K, Sato Y, Terada H, Sekihara H & Hagura R (2002): Screening and follow-up of diabetic retinopathy using a new mosaic 9-field fundus photography system. Diabetes Res Clin Pract 55: 49-59.

Shimada Y, Bearse MA Jr & Sutter EE (2005): Multifocal electroretinograms combined with periodic flashes: direct responses and induced components. Graefes Arch Clin Exp Ophthalmol 243: 132-41.

Shimada Y, Li Y, Bearse MA Jr, Sutter EE & Fung W (2001): Assessment of early retinal changes in diabetes using a new multifocal ERG protocol. Br J Ophthalmol 85: 414-9.

Shinoda K, Rejdak R, Schuettauf F, Blatsios G, Volker M, Tanimoto N, Olcay T, Gekeler F, Lehaci C, Naskar R, Zagorski Z & Zrenner E (2007): Early electroretinographic features of streptozotocin-induced diabetic retinopathy. Clin Experiment Ophthalmol 35: 847-54.

Shirao Y & Kawasaki K (1998): Electrical responses from diabetic retina. Prog Retin Eye Res 17: 59-76.

Sieving PA (1993): Photopic ON- and OFF-pathway abnormalities in retinal dystrophies. Trans Am Ophthalmol Soc 91: 701-73.

Sieving PA, Murayama K & Naarendorp F (1994): Push-pull model of the primate photopic electroretinogram: a role for hyperpolarizing neurons in shaping the b-wave. Vis Neurosci 11: 519-32.

Simo R & Hernandez C (2009): Advances in the medical treatment of diabetic retinopathy. Diabetes Care 32: 1556-62.

Simonsen SE (1980): The value of the oscillatory potential in selecting juvenile diabetics at risk of developing proliferative retinopathy. Acta Ophthalmol 58: 865-78.

Siu SC, Ko TC, Wong KW & Chan WN (1998): Effectiveness of non-mydriatic retinal photography and direct ophthalmoscopy in detecting diabetic retinopathy. Hong Kong Med J 4: 367-70.

Soliman W, Hasler P, Sander B & Larsen M (2010): Local retinal sensitivity in relation to specific retinopathy lesions in diabetic macular oedema. Acta Ophthalmol 90: 248-53.

Spaide R (2008): Autofluorescence from the outer retina and subretinal space: hypothesis and review. Retina 28: 5-35.

Sparrow JM, Bron AJ, Phelps Brown NA & Neil HA (1992): Biometry of the crystalline lens in late onset diabetes: the importance of diabetic type. Br J Ophthalmol 76: 428-33.

Speros P & Price J (1981): Oscillatory potentials. History, techniques and potential use in the evaluation of disturbances of retinal circulation. Surv Ophthalmol 25: 237-52.

Sugimoto M, Sasoh M, Ido M, Wakitani Y, Takahashi C & Uji Y (2005): Detection of early diabetic change with optical coherence tomography in type 2 diabetes mellitus patients without retinopathy. Ophthalmologica 219: 379-85.

Sutter EE (2000): The interpretation of multifocal binary kernels. Doc Ophthalmol 100: 49-75.

Sutter EE & Bearse MA Jr (1999): The optic nerve head component of the human ERG. Vision Res 39: 419-36.

Sutter EE, Shimada Y, Li Y & Bearse MA Jr (1999): Mapping inner retinal function through enhancement of adaptation components in the M-ERG. Vision Science and Its Applications, OSA Technical Digest Series 1: 52-5.

Sutter EE & Tran D (1992): The field topography of ERG components in man--I. The photopic luminance response. Vision Res 32: 433-46.

Takahashi H & Chihara E (2008): Impact of diabetic retinopathy on quantitative retinal nerve fiber layer measurement and glaucoma screening. Invest

Ophthalmol Vis Sci 49: 687-92.

Tam TK, Lau CM, Tsang LC, Ng KK, Ho KS & Lai TC (2005): Epidemiological study of diabetic retinopathy in a primary care setting in Hong Kong. Hong Kong Med J 11: 438-44.

Taylor D (2012): Diabetic eye screening revised grading definitions 2012. Gloucester, England; NHS Screening Programmes.

The Diabetes Control and Complications Trial Research Group (1987): Color photography vs fluorescein angiography in the detection of diabetic retinopathy in the diabetes control and complications trial. The Diabetes Control and Complications Trial Research Group. Arch Ophthalmol 105: 1344-51.

Tuch B, Dunlop M & Proietto J (2000): Diabetes research: a guide for postgraduates. Amsterdam; Harwood Academic: pp. 1-3.

Tyrberg M, Ponjavic V & Lovestam-Adrian M (2005): Multifocal electroretinography (mfERG) in insulin dependent diabetics with and without clinically apparent retinopathy. Doc Ophthalmol 110: 137-43.

Tyrberg M, Ponjavic V & Lovestam-Adrian M (2008): Multifocal electroretinogram (mfERG) in patients with diabetes mellitus and an enlarged foveal avascular zone (FAZ). Doc Ophthalmol 117: 185-9.

Tzekov R & Arden GB (1999): The electroretinogram in diabetic retinopathy. Surv Ophthalmol 44: 53-60.

Ueno S, Kondo M, Ueno M, Miyata K, Terasaki H & Miyake Y (2006): Contribution of retinal neurons to d-wave of primate photopic electroretinograms. Vision Res 46: 658-64.

Vadala M, Anastasi M, Lodato G & Cillino S (2002): Electroretinographic oscillatory potentials in insulin-dependent diabetes patients: A long-term follow-up. Acta Ophthalmol Scand 80: 305-9.

Van Bijsterveld OP (2000): Diabetic retinopathy. London; Martin Dunitz Ltd: pp. 2-14, 169-88.

Van Dijk HW, Kok PH, Garvin M, Sonka M, Devries JH, Michels RP, Van Velthoven ME, Schlingemann RO, Verbraak FD & Abramoff MD (2009): Selective loss of inner retinal layer thickness in type 1 diabetic patients with minimal diabetic retinopathy. Invest Ophthalmol Vis Sci 50: 3404-9.

Van Dijk HW, Verbraak FD, Kok PH, Garvin MK, Sonka M, Lee K, Devries JH, Michels RP, Van Velthoven ME, Schlingemann RO & Abramoff MD (2010): Decreased retinal ganglion cell layer thickness in patients with type 1 diabetes. Invest Ophthalmol Vis Sci 51: 3660-5.

Veldman BA & Vervoort G (2002): Pathogenesis of renal microvascular

complications in diabetes mellitus. Neth J Med 60: 390-6.

Verma A, Rani PK, Raman R, Pal SS, Laxmi G, Gupta M, Sahu C, Vaitheeswaran K & Sharma T (2009): Is neuronal dysfunction an early sign of diabetic retinopathy? Microperimetry and spectral domain optical coherence tomography (SD-OCT) study in individuals with diabetes, but no diabetic retinopathy. Eye 23: 1824-30.

Vujosevic S, Benetti E, Massignan F, Pilotto E, Varano M, Cavarzeran F, Avogaro A & Midena E (2009): Screening for diabetic retinopathy: 1 and 3 nonmydriatic 45-degree digital fundus photographs vs 7 standard early treatment diabetic retinopathy study fields. Am J Ophthalmol 148: 111-8.

Wallis MG, Smith ME, Kolka CM, Zhang L, Richards SM, Rattigan S & Clark MG (2005): Acute glucosamine-induced insulin resistance in muscle in vivo is associated with impaired capillary recruitment. Diabetologia 48: 2131-9.

Wang WQ, Ip TP & Lam KS (1998): Changing prevalence of retinopathy in newly diagnosed non-insulin dependent diabetes mellitus patients in Hong Kong. Diabetes Res Clin Pract 39: 185-91.

Wangsa-Wirawan ND & Linsenmeier RA (2003): Retinal oxygen: fundamental and clinical aspects. Arch Ophthalmol 121: 547-57.

Warrian KJ, Lorenzana LL, Lankaranian D, Dugar J, Wizov SS & Spaeth GL (2010): The assessment of disability related to vision performance-based measure in diabetic retinopathy. Am J Ophthalmol 149: 852-60.

Westall CA (2005): Detecting ocular-visual function changes in diabetes. Br J Ophthalmol 89: 1392-3.

WHO (2008): The global burden of disease 2004 update. Geneva, Switzerland; World Health Organization.

WHO (2009): Global health risks: mortality and burden of disease attributable to selected major risk. Geneva, Switzerland; World Health Organization.

WHO (2010): WHO non-communicable disease 2010. Geneva, Switzerland; World Health Organization. pp. 9-31.

WHO (2011): Use of glycated haemoglobin (HbA1c) in the diagnosis of diabetes mellitus: abbreviated report of a WHO consultation 2011. Geneva, Switzerland; World Health Organization.

WHO (2012): World health statistics 2012. Geneva, Switzerland; World Health Organization.

Wiemer NG, Dubbelman M, Hermans EA, Ringens PJ & Polak BC (2008): Changes in the internal structure of the human crystalline lens with diabetes mellitus type 1 and type 2. Ophthalmology 115: 2017-23.

Wild S, Roglic G, Green A, Sicree R & King H (2004): Global prevalence of diabetes: estimates for the year 2000 and projections for 2030. Diabetes Care 27: 1047-53.

Wilkinson CP, Ferris III FL, Klein RE, Lee PP, Agardh CD, Davis M, Dills D, Kampik A, Pararajasegaram R & Verdaguer JT (2003): Proposed international clinical diabetic retinopathy and diabetic macular edema disease severity scales. Ophthalmology 110: 1677-82.

Williams GA, Scott IU, Haller JA, Maguire AM, Marcus D & McDonald HR (2004): Single-field fundus photography for diabetic retinopathy screening: a report by the American Academy of Ophthalmology. Ophthalmology 111: 1055-62.

Wolsley CJ, Silvestri G, O'Neill J, Saunders KJ & Anderson RS (2009): The association between multifocal electroretinograms and OCT retinal thickness in retinitis pigmentosa patients with good visual acuity. Eye 23: 1524-31.

Wong TY & Hyman L (2008): Population-based studies in ophthalmology. Am J Ophthalmol 146: 656-63.

Woodcock A, Bradley C, Plowright R, Ffytche T, Kennedy-Martin T & Hirsch A (2004): The influence of diabetic retinopathy on quality of life: interviews to guide the design of a condition-specific, individualised questionnaire: the RetDQoL. Patient Educ Couns 53: 365-83.

Wu S & Sutter EE (1995): A topographic study of oscillatory potentials in man. Vis Neurosci 12: 1013-25.

Yam JC & Kwok AK (2007): Update on the treatment of diabetic retinopathy. Hong Kong Med J 13: 46-60.

Yamamoto S, Kamiyama M, Nitta K, Yamada T & Hayasaka S (1996): Selective reduction of the S cone electroretinogram in diabetes. Br J Ophthalmol 80: 973-5.

Yamamoto S, Takeuchi S & Kamiyama M (1997): The short wavelength-sensitive cone electroretinogram in diabetes: relationship to systemic factors. Doc Ophthalmol 94: 193-200.

Yau JW, Rogers SL, Kawasaki R, Lamoureux EL, Kowalski JW, Bek T, Chen SJ, Dekker JM, Fletcher A, Grauslund J, Haffner S, Hamman RF, Ikram MK, Kayama T, Klein BE, Klein R, Krishnaiah S, Mayurasakorn K, O'Hare JP, Orchard TJ, Porta M, Rema M, Roy MS, Sharma T, Shaw J, Taylor H, Tielsch JM, Varma R, Wang JJ, Wang N, West S, Xu L, Yasuda M, Zhang X, Mitchell P & Wong TY (2012): Global prevalence and major risk factors of diabetic retinopathy. Diabetes Care 35: 556-64.

Yokoi M, Yamagishi SI, Takeuchi M, Ohgami K, Okamoto T, Saito W, Muramatsu M, Imaizumi T & Ohno S (2005): Elevations of AGE and vascular endothelial growth factor with decreased total antioxidant status in the vitreous fluid of diabetic patients with retinopathy. Br J Ophthalmol 89: 673-5.

Zhang L, Ino-ue M, Dong K & Yamamoto M (2000): Retrograde axonal transport impairment of large- and medium-sized retinal ganglion cells in diabetic rat. Curr Eye Res 20: 131-6.

Zhang P, Zhang X, Brown J, Vistisen D, Sicree R, Shaw J & Nichols G (2010): Global healthcare expenditure on diabetes for 2010 and 2030. Diabetes Res Clin Pract 87: 293-301.

Zhou W, Rangaswamy N, Ktonas P & Frishman LJ (2007): Oscillatory potentials of the slow-sequence multifocal ERG in primates extracted using the Matching Pursuit method. Vision Res 47: 2021-36.